

© Copyright 2016

Andreia S. Costa

Characterization of the role of viral sensing and migratory capacity in regulatory T cells after  
neurotropic viral infection

Andreia S. Costa

A dissertation

submitted in partial fulfillment of the  
requirements for the degree of

Doctor of Philosophy

University of Washington

2016

Reading Committee:

Jennifer Lund Friesen, Chair

Martin Prlic

Michael Gale, Jr.

Program Authorized to Offer Degree:

Pathobiology

University of Washington

**Abstract**

Characterization of the role of viral sensing and migratory capacity in regulatory T cells after neurotropic viral infection

Andreia S. Costa

Chair of the Supervisory Committee:  
Dr. Jennifer Lund Friesen  
Department of Global Health

Regulatory T cells (Tregs) are recognized as suppressors of autoimmunity, yet Tregs also play an important although variable role in the development of an immune response to infection. The mechanism of Treg sensing of infection and migration to immune activation sites during viral infections is not yet clearly defined. Furthermore, given the rapid spread of flaviviruses such as West Nile virus (WNV) and Zika virus, it is critical that we develop a thorough and complete understanding of the key mediators of an effective anti-flaviviral response.

One key family of viral sensors, the RIG-I-like receptors, are known to signal through the adaptor protein mitochondrial antiviral-signaling protein or MAVS. MAVS-null mouse models experimentally infected with WNV display signs of grossly dysregulated immunity, elevated

viral titers, and death that correlate with a failure of Treg expansion following infection. Thus, we sought to determine if intrinsic MAVS signaling is required for participation of Tregs in anti-WNV immunity. Despite evidence of increased Treg cell division indicated by Ki67 expression, FoxP3 expression was down-regulated after WNV infection in MAVS-deficient mice.

Additionally, we observed the successful generation of an effective anti-WNV immune response in both the secondary lymphoid organs as well as the central nervous system when Tregs lacked MAVS, thereby demonstrating that Treg detection of the presence of WNV through the RIG-I like receptor/MAVS signaling pathway is not required for the generation of effective immunity. Together, these data suggest that while MAVS signaling has a considerable impact on Treg identity, this effect is not mediated by intrinsic MAVS signaling but rather is likely an effect of the overproduction of pro-inflammatory cytokines generated in MAVS- deficient mice after WNV infection.

We also investigated the effect of Treg migratory marker expression both at steady state and on the development of an effective WNV-directed immune response. We utilized an ITGb1<sup>Flox</sup> x FoxP3<sup>Cre</sup> conditional knockout mouse (CKO) model to generate Tregs that lack the ability to express  $\beta$ 1-integrin, a transmembrane protein reported to be necessary for migration to sites of inflammation and the central nervous system. Through flow cytometric analyses, we found that wild type (WT) Treg expression of  $\beta$ 1-integrin correlated with an activated, migratory phenotype as indicated by increased surface expression of CD44, CXCR3, and CCR5. In addition, we found that when the balance of  $\beta$ 1-integrin +/- Tregs is altered, the expression of suppressive proteins such as CD73 and CTLA4 is significantly altered. Analysis of the CD8+ T cell compartment within the CKO revealed that a greater percentage of CD8+ T cells displayed signs of activation including increased CD44, CXCR3 and Ly6C expression at steady state as compared to WT

controls. When these mice were infected with WNV, CKOs and WT controls generated similar frequencies of WNV-specific CD8<sup>+</sup> T cells in response, both at peak of the infection in the spleen and when assessed at an early memory time point. However after a second exposure to WNV, expansion of CKO-derived WNV-specific CD8<sup>+</sup> T cells was greatly diminished despite significant proliferation of non-WNV-specific CKO-derived CD8<sup>+</sup> T cells in the same mouse. In sum, these data suggest that Treg migratory capability is critical for the maintenance and development of a functional CD8<sup>+</sup> T cell response both at steady state and after an infectious challenge.

Through our investigations of Treg function, both in viral sensing and migratory function, we sought to further the understanding of Tregs as key players in responding to infection and in maintaining homeostasis. Although MAVS signaling was found to be dispensable for Treg function during WNV infection, this finding extends previous work and answers a lingering question in the field. In addition, our work on  $\beta$ 1-integrin on Tregs suggests a potential novel function for an integrin that was previously attributed a minor role in migration. As such, the following report is intended to document these findings and place them within the context of current immunological knowledge.

# TABLE OF CONTENTS

List of Figures .....	v
List of Tables .....	viii
List of Abbreviations .....	ix
Dedication .....	xi
Chapter 1. Regulatory T cells in health and disease .....	1
1.1 Tregs: subsets and functional sub-types .....	2
1.2 Treg function in the context of infection .....	6
Chapter 2. Infection sensing in Regulatory T cells.....	9
2.1 Tregs modulate incidental immunopathology during WNV infection. ....	9
2.2 Intrinsic sensing of West Nile Virus through the RIG-I/MDA5:MAVS axis .....	12
2.3 Tregs can sense the presence of foreign peptides through PRRs. ....	13
2.4 AIM 1: Is intrinsic Treg activation of the viral RNA sensors, RIG-I and MDA5 via the adaptor protein MAVS, necessary for Treg expansion and function during WNV infection? 15	
2.4.1 FoxP3 expression is down regulated in Tregs following WNV infection of MAVS <sup>-/-</sup> mice. ....	15
2.4.2 Intrinsic MAVS signaling is not required for Treg proliferation or suppressive function in vitro.....	20
2.4.3 Treg expression of MAVS does not affect WNV disease in vivo. ....	22

2.4.4	Intrinsic MAVS signaling is dispensable for Treg expansion and function following WNV infection in vivo.....	25
2.4.5	Immunity to WNV is not compromised in the absence of Tregs expressing MAVS.....	27
2.4.6	Discussion.....	29
2.4.7	Limitations and unanswered questions.....	31
Chapter 3. Regulatory T cell migration and tissue-specific function.....		33
3.1	The integrin as a therapeutic target and their effects on the immune response.....	33
3.2	AIM 2: What is the function of $\beta 1$ integrin expression in Tregs?.....	35
3.2.1	Tregs differentially express integrin $\beta 1$ at steady state.....	35
3.2.2	Integrin $\beta 1$ expression correlates with effector Treg phenotype.....	36
3.2.3	Treg specific deletion of integrin $\beta 1$ leads to increased frequency and enhancement of effector Treg population.....	38
3.2.4	Treg-specific integrin $\beta 1$ deletion leads to upregulation of integrin $\beta 7$ and increased frequency of Tregs in gut-associated lymphoid tissues.....	42
3.2.5	CD8 <sup>+</sup> T cells in integrin $\beta 1$ CKOs have dysregulated expression of activation and migration markers.....	44
3.2.6	Hypothesized Mechanism: $\beta 1$ integrin stabilizes TCR:MHC interactions between Tregs and DCs.....	51
3.2.7	CD44 <sup>hi</sup> CD8 <sup>+</sup> T cells from integrin $\beta 1$ CKOs are unlikely to be self-reactive.....	53
3.2.8	Discussion.....	57
3.2.9	Limitations and unanswered questions.....	60
3.2.9.1	<i><math>\beta 1</math> integrin expression and suppressive function</i> .....	61

3.2.9.2	<i>Effects of <math>\beta 7</math> integrin overexpression</i> .....	61
3.2.9.3	<i>Virtual Memory or Innate Memory CD8+ T cells</i> .....	64
Chapter 4.	Materials and Methods .....	67
4.1	AIM I: MAVS is dispensable for Treg function during WNV infection.....	67
	Ethics Statement.....	67
4.1.1	West Nile Virus.....	67
4.1.2	Mice .....	67
4.1.3	90%/10% Mixed bone marrow chimeras.....	68
4.1.4	90%/10% Mixed bone marrow chimeras – Diphtheria toxin administration .....	68
4.1.5	In vivo West Nile Virus infection.....	69
4.1.6	TGF $\beta$ , IL-6 and IL-17 ELISAs .....	70
4.1.7	In vitro Treg suppression assay.....	70
4.1.8	In vitro proliferation assay .....	71
4.1.9	Flow Cytometry .....	72
4.1.10	RNA extraction .....	73
4.1.11	WNV DNA standard for qRT-rtPCR.....	74
4.1.12	qRT-rtPCR for positive strand WNV RNA .....	74
4.2	Aim 2: Integrin $\beta 1$ expression is associated with tissue-specific effector function in Tregs .....	75
4.2.1	Mice .....	75
4.2.2	Virus.....	75
4.2.3	Flow Cytometry .....	75
4.2.4	In vivo viral infection.....	78

4.2.5	Memory time point CD8+ T cell adoptive transfer .....	78
4.2.6	CD8+ T cell in vivo proliferation assay .....	79
4.2.7	CD8+ T cell adoptive transfer after Treg ablation .....	79
Appendix A.....		81
Bibliography .....		94

## LIST OF FIGURES

Figure 1. MAVS <sup>-/-</sup> mice decline rapidly starting day 5 post WNV infection. ....	16
Figure 2. FoxP3 expression is down regulated in Tregs following WNV infection of MAVS <sup>-/-</sup> mice.....	16
Figure 3. Treg suppressive molecule expression increased in MAVS <sup>-/-</sup> mice after WNV infection. ....	17
Figure 4 Activation profile of MAVS <sup>-/-</sup> Tregs is comparable to WT after WNV infection. ....	18
Figure 5. FoxP3 is down regulated in ROR $\gamma$ T co-expressing cells in the spleen and mesenteric lymph nodes.....	19
Figure 6. FoxP3 down regulation occurs in the presence of T <sub>H</sub> 17 polarizing conditions.....	20
Figure 7. Intrinsic MAVS signaling is not required for Treg proliferation <i>in vitro</i> .....	21
Figure 8. Intrinsic MAVS signaling is not required for Treg suppressive function <i>in vitro</i> . ....	22
Figure 9. Schematic of hematopoietic stem cell transfer and WNV infection schedule. ....	23
Figure 10. Visceral phase of infection was analyzed during early and late periods. ....	24
Figure 11. Weight loss and WNV cerebellum titers are comparable between MAVS <sup>-/-</sup> Treg chimeras and WT controls.....	25
Figure 12. Expansion and suppressive function of Tregs is comparable between MAVS <sup>-/-</sup> Treg chimeras and WT controls during early visceral phase of WNV infection.....	26
Figure 13. Treg infiltration/expansion of the brain is comparable between groups regardless of infection stage after WNV infection.....	27
Figure 14. T cell frequencies including WNV specific CD8 <sup>+</sup> T cells in spleen and brain were comparable between groups during early phase of WNV infection. ....	28
Figure 15. T cell frequencies including WNV specific CD8 <sup>+</sup> T cells in spleen and brain were comparable between groups during late phase of WNV infection .....	29
Figure 16. $\beta$ 1 integrin is constitutively expressed in a subset of Tregs that correlates with	

effector Treg description.....	36
Figure 17. $\beta$ 1+ Tregs express higher levels of proteins associated with suppression, activation and migration. ....	37
Figure 18. Schematic of ITGb1 conditional knockout.Recreated and adapted from Harno, E. et al. <i>Cell Metab.</i> 18, 21–28 (2013) <sup>76</sup> .....	38
Figure 19. Deletion of ITGb1 leads to increased frequency and enhancement of eTreg population.....	39
Figure 20. Activated phenotype in $\beta$ 1 integrin CKO Tregs surpasses that of WT controls. ....	41
Figure 21. CKO Tregs express higher levels of CXCR3, CD103 and KLRG1 – markers of terminal differentiation. ....	42
Figure 22. Deletion of ITGb1 leads to increased trafficking of Tregs to gut associated lymphoid organs.....	44
Figure 23. Treg specific ITGb1 deletion leads to increased CD44 expression in CD8+ T cells at steady state. ....	46
Figure 24. CKO derived CD8+ T cells have an activated and mobile profile as compared to WT controls. ....	47
Figure 25. Mortality rates and frequency of WNV-specific CD8+ T are comparable after infection but SLEC/MPEC ratios are skewed. ....	48
Figure 26. CD8+ T cell memory recall is impaired after development in ITGb1 CKO environment. ....	50
Figure 27. Unstable interactions between CKO Tregs and DCs could lead to enrichment of incidentally activated self-reactive CD8+ T cells.....	52
Figure 28. CKO derived CD8+ T cells express comparable levels of CD5 as WT controls. ....	54
Figure 29. Proliferation of CKO derived CD8+ T cells is comparable to WT in lymphopenic conditions. ....	55
Figure 30. Weight loss after Treg depletion is not accelerated or exacerbated, despite the addition of CKO-derived CD8+ T cells.....	57
Figure 31. Donor Tregs (Ly5.2+) supplant endogenous Tregs 4 days after initiation	

of DT treatment .....	69
Figure 32. Small intestine collected from uninfected WT and <i>T. muris</i> infected ITGb1 CKO mice in cell culture media.....	83
Figure 33. Weights were not significantly different between male or female CKO and WT mice despite <i>T. muris</i> infection.....	84
Figure 34. Protozoal trophozoites can be seen in the lumen of colon taken from infected CKO mice but is absent in WT controls. ....	85
Figure 35. <i>T. foetus/T. muris</i> 18s ribosomal sequence alignment.....	86
Figure 36. Master mix composition and primer sequence for <i>T. muris</i> detection assay. ....	86
Figure 37. PCR denaturation, annealing and extension schedule for <i>T. muris</i> detection assay .....	87
Figure 38. <i>T. muris</i> infection is easily transmitted but can evade detection by sentinel mice. ....	88
Figure 39. <i>T. muris</i> spread was most evident while animals were housed in breeding racks. ....	89
Figure 40. Schematic depicts the combination Metronidazole and fostering strategy used to clear CKO mice of <i>T. muris</i> infection. ....	91
Figure 41. CKO foster pup fecal samples are free of <i>T. muris</i> DNA after metronidazole treatment.....	92

## LIST OF TABLES

Table 1. Summary of the effects of Tregs during select infections .....	8
Table 2: Antibodies used in Flow cytometric analyses .....	77

## LIST OF ABBREVIATIONS

1. APC = Antigen presenting cell
2. BBB = Blood brain barrier
3. CKO = Conditional knock out
4. CNS = Central nervous system
5. CTL = Cytotoxic T lymphocyte
6. cTreg = Central Regulatory T cell
7. DC = Dendritic cell
8. DT = Diphtheria toxin
9. DTR = Diphtheria toxin receptor
10. eTreg = Effector Regulatory T cell
11. FoxP3 = Forkhead box P3
12. GPR15 = G-protein coupled receptor 15
13. HSV-1/2 = Herpes Simple Virus 1/2
14. iNKT cell = Invariant natural killer T cell
15. IS = Immune synapse
16. ISG = Interferon stimulated gene
17. ITGb1 = Integrin beta 1
18. LCMV = Lymphocytic choriomeningitis
19. LFA-1 = Lymphocyte function-associated antigen 1
20. LGP2 = Laboratory of genetics and physiology 2
21. MAVS = Mitochondrial antiviral-signaling protein (aka IPS-1, Cardif or VISA)
22. MDA5 = Melanoma differentiation – associated antigen 5
23. MFI = Median fluorescence intensity
24. mLN = Mesenteric lymph node
25. MPEC = Memory Precursor Effector Cell
26. p-SMAC = Peripheral supramolecular activation cluster
27. PAMP = Pathogen associated molecular pattern
28. pDC = Plasmacytoid dendritic cell
29. PML = Progressive multifocal encephalopathy
30. PP = Peyer's patch
31. PRR = Pattern recognition receptors
32. pTreg = peripherally-derived regulatory T cell
33. qRT-rtPCR = Quantitative reverse transcription – real time polymerase chain reaction
34. RA = Retinoic acid
35. RIG-I = Retinoic acid-inducible gene 1
36. RLRs = RIG-I like receptors
37. SLEC = Short Lived Effector Cell
38. SLO = Secondary lymphoid organs
39. *T. mobilensis* = *Tritrichomonas mobilensis*
40. *T. muris* = *Tritrichomonas muris*
41. T1D = Type 1 diabetes
42. Treg = Regulatory T cell
43. tTreg = thymus-derived regulatory T cell
44. VCAM-1 = Vascular cell adhesion molecule 1
45. VLA-4 = Very late antigen 4
46. VM = Virtual memory (CD8+ T cells)
47. WNV = West Nile Virus

## ACKNOWLEDGEMENTS

It is with deepest gratitude that I thank Dr. Jennifer Lund for her support, both of my Dissertation work and for her encouragement of scientific inquiry wherever it led. Jenny provided an environment that was rich with possibility and allowed me to pursue even the wildest of hypotheses; if not to satisfy my scientific curiosity then to expand the boundaries of my thinking. Beyond her grounded scientific advice, she facilitated and actively participated in my career aspirations and for that I will always be in her debt.

In addition I would like to acknowledge my lab mates, including Dr. Andrew Soerens who challenged my ideas at every turn and helped further my research with every paper he suggested. I would like to thank Esteban Garza for his patience, optimism and industriousness during experiments whether day or night, weekday or weekend and all while preparing for his own journey into medical school. Dr. Jessica Graham and Jessica Swarts provided invaluable support and instruction in all things related to West Nile Virus and did so with ebullience. The entire Lund Lab helped create the kind of supportive and collaborative environment that fosters scientific success and I am thankful for each of their contributions. Dr. Kylie Quinn, although not a member of the Lund lab, provided invaluable advice when setbacks seemed insurmountable and has been a guiding force both scientifically and personally for nearly a decade.

Finally, I would like to acknowledge my committee members for their time, consideration and thoughtful analysis of my work as it has developed over the years. They have asked the questions that have shaped my thinking and pushed me to focus my efforts when it was most necessary.

## **DEDICATION**

To my parents Jose and Maria, who taught me that hard work is the currency of success.

To my brother Michael, who inspires me to persevere.

To Nor and Der, who taught me how to enjoy life.

To my love David, who provides the solid foundation on which I build my dreams.

## Chapter 1. REGULATORY T CELLS IN HEALTH AND DISEASE

The immune system has traditionally been described as operating in two modes, active and reactive. The ongoing surveillance function is an active process in which dedicated “sampling” cells such as dendritic cells, ingest their micro-environment and regurgitate pieces of it for display on their surfaces. Although antigen presenting cells (APCs) do not fully represent the surveillance function of the immune system, they represent the main feature of the “change-detection” apparatus employed<sup>1</sup>. Other “change-detection” mechanisms including the detection of missing “self” by NK cells for example detect differences mediated by loss of expression rather than gain. The second mode, reaction, arises as a result of triggering of alarm features in the surveillance mechanisms. Reactive cells have a panoply of functions that can be categorized roughly into 3 areas: soluble chemical release (e.g. cytokine, chemokine and antibody production), cell:cell modulation (follicular helper T cell [T<sub>FH</sub>] interactions with B cells and the formation of germinal centers for example) and direct cell killing (e.g. CTL killing through perforin). With this level of complexity a tightly regulated balance must be maintained to ensure that aberrant activation is avoided yet homeostatic conditions are preserved.

G rard Eberl described an equilibrium model of immunity in which four different types of immune responses, ranging from Type 1, targeting intracellular pathogens, Type 2, targeting helminthes and other multicellular parasites, Type 3, targeting extracellular pathogens and Type 4, maintaining the exclusion of commensal/opportunistic microbes, are constantly in flux<sup>2</sup>. This dynamic model introduces a third operational mode for the immune system, one that is proactive. The proactive mode requires that the system never truly be at rest but instead be constantly retuning the balance amongst the different developing responses to maintain equilibrium. This

tuning function relies heavily on immune suppressive cell types of which regulatory T cells are critical members.

Although the concept of a suppressor lymphocyte first gained traction in the early 1970s<sup>3</sup> it was not until the transcription factor FoxP3 was found to confer suppressive identity that the modern Treg as a CD4+ T cell subset was defined<sup>4,5</sup>. Using a FoxP3 directed human diphtheria toxin receptor (DTR) knock-in mouse model, Kim *et al* found that after diphtheria toxin (DT) mediated deletion of Tregs, mice quickly developed a characteristic form of autoimmunity that included splenomegaly, lymphadenopathy and the spontaneous development of colitis culminating in a wasting disease<sup>6</sup>. The ability to specifically investigate Tregs by analysis of FoxP3 expression has led to an explosion of research into this critical cell type. In the intervening years, a variety of functions outside of the necessary prevention of autoimmunity have been attributed to Tregs both in the context of infection and in the maintenance of homeostasis.

## 1.1 TREGS: SUBSETS AND FUNCTIONAL SUB-TYPES

Nowhere is the burgeoning study of Treg multi-functionality better illustrated than in the continued discovery of new Treg subsets. Tregs are currently classified into two main classes based on their developmental origin. Thymus-derived Tregs or tTregs (formerly called natural Tregs<sup>7</sup>) develop in the thymus where tTreg pre-cursor cells are believed to undergo a similar positive selection process as other T cells. The leading hypothesis suggests that Tregs are then generated based on a seeming subversion of the negative-selection process, surviving despite an increased TCR affinity for self-antigen<sup>8</sup>. Furthermore, a recent study suggests that tTregs can be operationally targeted for a specific organ if presented with organ-specific antigen by DCs during development in the thymus<sup>9</sup>. The question of whether tTregs remain Tregs after leaving

the thymus has generated conflicting reports; while fate-mapping studies indicate that tTregs retain particularly stable FoxP3 expression even in the context of inflammation<sup>10</sup>. Other groups have utilized FoxP3-GFP-Cre x Rosa26-loxP-stop-loxP-YFP mouse models (these mice are GFP+YFP+ if FoxP3 is expressed and become GFP-YFP+ if FoxP3 was expressed and then lost) to identify tTregs that have lost FoxP3 expression (“exFoxP3 T cells”) after exposure to inflammatory conditions such as those found during autoimmunity<sup>11</sup>. It is possible that the discordance in these findings is in part due to alterations in the interactions of key proteins with FoxP3 caused by the introduction of the GFP fusion protein at FoxP3’s N-terminus. The placement of the GFP insert has been shown to affect the suppressive capacity of Tregs during some forms of autoimmune inflammation as well as disrupting the cooperative function of PPAR $\gamma$  and FoxP3 in visceral adipose tissue (VAT) Tregs<sup>12,13,14</sup>. Continuing investigations of Treg function in different tissue micro-environments have indicated that the heterogeneity within FoxP3 expressing cells (whether transient or stable expression) is quite large. As such it is likely that Tregs, as a broadly defined T cell class, can have an identity that is both stable and phenotypically plastic<sup>15</sup>.

The second major Treg class, peripherally-derived Tregs (pTregs), leave the thymus as CD4+FoxP3- T cells and are induced to express FoxP3 by cues encountered in the periphery. (The definition of a potential third subtype, induced-Tregs [*in vitro*-induced Tregs] or iTregs remains contentious<sup>7,16</sup>. Some investigators consider iTregs generated *in vitro* through exposure of CD4+FoxP3- T cells to IL-2 and TGF- $\beta$  and pTregs to be equivalent however this distinction remains controversial. For the purposes of this review, we will consider pTregs as CD4+ T cells that acquired FoxP3 expression *in vivo* but outside of the thymus). The generation of pTregs from CD4+FoxP3- T cells is thought to occur via TCR stimulation with self-antigen and IL-2

exposure in the periphery, although interactions with specialized APCs and cytokines such as TGF $\beta$ , vitamin metabolites such as retinoic acid and microbial byproducts<sup>17</sup> are also thought to be important depending on the tissue type<sup>18</sup>. What the quantitative contribution of each of these subtypes is to Treg suppressive function within an organism remains an open question. Although expression of the transcription factor Helios<sup>19</sup> and the surface marker Neuropilin-1<sup>20</sup> have been suggested as distinguishing features of tTregs, broader acceptance of these defining markers has remained slow because of a lack of consistency in reported labeling of tTregs vs. pTregs<sup>21,22</sup>.

Regardless of their origin, Tregs mediating self-tolerance can also be classified based on their predilection to migrate to the periphery vs. lymphoid organs. Effector Tregs (eTregs) and central Tregs (cTregs) are defined by their differential expression of the migration-associated proteins CD44 and CD62L, with eTregs defined as CD44<sup>hi</sup>, CD62L<sup>lo</sup> Tregs and hence remaining in peripheral circulation and secondary-lymphoid-organ-homing cTregs defined via CD44<sup>lo</sup>, CD62L<sup>hi</sup>, CCR7<sup>+</sup> expression<sup>23</sup>. These designations share many common features with the central and effector memory T cell descriptions from which they are derived<sup>24</sup>, including an activated phenotype, an immune profile indicative of terminal differentiation, including KLRG-1 and CD103 expression<sup>25</sup> and a higher turnover characterizing eTregs. Conversely, cTregs are longer lived and can convert into eTregs based on an inverse relationship to Ly6C expression within an IL-2 replete environment<sup>26</sup>, suggesting that these cells retain the ability to further differentiate. Investigation of the nuances of the functional and phenotypic characteristics of eTregs and cTregs is ongoing (see Chapter 3.1.2) and the contributing factors that give rise to the layers of heterogeneity amongst Tregs will continue to be revealed.

Tregs have a wealth of tools with which they mediate suppressive function including trans-endocytosis of stimulatory proteins on APC cell surfaces and competition for CD28 binding

through expression of CTLA-4<sup>27</sup>, de-phosphorylation of pro-inflammatory ATP through surface expression of CD39 and CD73<sup>28</sup> and production of anti-inflammatory cytokines that do not rely on cell-to-cell contact such as IL-10<sup>29</sup>, TGF $\beta$ <sup>30</sup> and IL-35<sup>31</sup> to name a few. Selectively employing different suppressive mechanisms allows Tregs to effectively target specific effector cell populations based on the inflammatory cues present. Tregs have been found to up regulate expression of the same or a complimentary transcription factor as the effector cell type they are suppressing<sup>32</sup>. For example, much like T<sub>H1</sub> T cells, T<sub>H1</sub>-suppressing Tregs can up regulate the transcription factor T-bet in response to IFN $\gamma$ , leading to surface expression of migratory proteins including CXCR3. This mirrored expression might serve to allow Tregs to efficiently track their targeted effector population. The importance of Treg expression of T-bet in suppressing T<sub>H1</sub>-mediated inflammation was illustrated in a Treg adoptive transfer experiment in which T-bet-deficient Tregs were introduced into a FoxP3-germline mutation model of autoimmunity known as the *scurfy* mouse<sup>33</sup>. *Scurfy* mice infused with T-bet deficient Tregs failed to prevent the expansion of activated IFN $\gamma$ -producing CD4<sup>+</sup> T cells as effectively as transferred T-bet-sufficient Tregs<sup>33</sup> indicating that T-bet expression is required in Tregs in the specific control of T<sub>H1</sub>-mediated inflammation. Similar pairings between Tregs and other effector T cell types have been found including the transcription factor ROR $\gamma$ T (STAT3) for T<sub>H17</sub> cells<sup>34</sup> and GATA3 (IRF4) in the control of T<sub>H2</sub> cells<sup>35</sup>.

With the advent of more detailed and thorough gene expression assays, the number of discovered Treg “flavors” is sure to continue growing. Beyond their role in preventing autoimmunity in its many forms however, Tregs use many of the same suppressive tools to ensure the successful generation of anti-pathogen immune responses whilst limiting potential tissue damage in the process.

## 1.2 TREG FUNCTION IN THE CONTEXT OF INFECTION

Treg-depletion, used in tandem with the panoply of different infection models available, has highlighted the role of Tregs in ensuring the proper development of effector responses while mitigating the collateral damage resulting from pathogen clearance. Given the diversity of immunologic challenges presented by different pathogen classes including bacterial, viral and eukaryotic invaders, it is not surprising that it is difficult to predict the function of Tregs in developing a pathogen-specific response. Likely because Tregs play such a pivotal role in the mediation of a developing immune response, some pathogens such as *Mycobacterium tuberculosis* have evolved strategies that co-opt the suppressive function of Tregs to ensure the pathogen's success.

In a murine model of *M.tb.* infection, Shafiani *et al* investigated the TCR specificity of Tregs given that the thymic-selection of Tregs is thought to be based on TCR recognition of self. Using a *M.tb.*-specific MHC-II tetramer, they found that indeed, during infection Tregs expanded in response to *M.tb.* antigens but not to an irrelevant bacterial antigen, suggesting that at least in the context of *M.tb.* infection, responding Tregs are specific to the pathogen<sup>36</sup>. However, this finding does not negate the possibility of concomitant cross-reactivity to self. Furthermore, adoptively transferring *M.tb.*-specific Tregs into *M.tb.* infected mice increased the bacterial burden and delayed the arrival of critical IFN $\gamma$ -producing T<sub>H</sub>1 cells<sup>37</sup>. These data suggest that *M.tb.* may be manipulating Tregs in order to hinder or delay the arrival of an effector response, thereby maintaining a timeline that better suits its metabolic needs<sup>38</sup>.

Experimental infection models in which Treg depletion results in more robust effector responses (See Table 1) seem to favor the theory that Tregs serve to constrain a response and hence reducing their effect would be globally beneficial to the infected host. However, Tregs can

play an unexpected role in the off-target effects of over-exuberant pathogen clearance. In particular, Type 1 diabetes (T1D) develops as a result of immune-mediated destruction of insulin producing cells in the pancreas and infection with certain viruses (including LCMV) has been shown to prevent or delay the development of T1D in a diabetes predisposed mouse model (NOD) despite eliciting a robust and inflammatory response in the pancreas<sup>39</sup>. Diana *et al* investigated the mechanism of this unique correlation and found that, through the cooperation of iNKT cells and pDCs, the frequency of Tregs with an activated phenotype increased significantly in the pancreatic islets after LCMV infection in mice<sup>40</sup>. Furthermore, through the production of TGF $\beta$ , these Tregs were able to inhibit antiviral-CD8+ T cells that would otherwise damage islet cells, thereby preventing the development of T1D<sup>40</sup>. This example underscores one of the potential benefits of maintaining the delicate balance between the development of an effective effector response and containing the inherent damage that this response can cause.

Multi-cellular eukaryotic parasites represent a class of highly complex pathogens with the added immune hurdle of genetic similarity to a eukaryotic host's own cells. Increased pathogen complexity appears to correlate with a more complex role for Tregs, as the evasion strategies and co-opting opportunities utilized by these pathogens likewise increases. Developing an effective immune response to parasites is often further complicated by the skewed elicitation of a more suppressive T<sub>H</sub>2 response, often leading to chronicity instead of clearance of a pathogen. Although this elicitation of a T<sub>H</sub>2-weighted response has been thoroughly characterized in helminth infections<sup>41</sup>, protozoan infections caused by *Leishmania* species share many of the same immune characteristics and further highlight the role of Tregs within a developing response. Using a *Leishmania* species capable of infecting and producing chronic disease in both mouse and human hosts, *Leishmania (Viannia) panamensis*, Ehrlich *et al* investigated the role of

Tregs in the course of this disease<sup>42</sup>. In particular, they found that Tregs from *L.V. panamensis* mice showed reduced suppressive function as compared to naïve controls in an *ex vivo* T cell suppression assay. Despite this finding, Treg ablation using a DERE model similar to a FoxP3-DTR model, exacerbated disease. In support of this finding, transfer of Tregs into a chronically infected mouse reduced lesion size, suggesting that Tregs may be simultaneously supporting and restraining disease by both preventing the development of an effector response sufficiently robust to clear infection and consequently limiting tissue damage associated with this response<sup>42</sup>. Although there are many more examples of the variable role of Tregs during infection (Table 1), even the few described above highlight the difficulty in generalizing the role of Tregs during different infections<sup>43,44</sup>.

Table 1. Summary of the effects of Tregs during select infections

<i>Pathogen</i>	<i>Effected Tissues (Mouse)</i>	<i>Treg response</i>
Influenza Virus	Lung	Treg depletion improved Flu-specific CD8+ T cell responses <sup>45</sup>
<i>M. tuberculosis</i>	Lung	<i>M. tb</i> -specific Tregs prevent the establishment of an effective effector response <sup>36,37</sup>
West Nile Virus	Spleen and CNS	Treg-depletion leads to increased morbidity and mortality <sup>46</sup>
HSV-2	Female reproductive tract	Treg-depletion leads to ineffective HSV-2 specific CD4+ T cell priming and increased morbidity <sup>47,48</sup>
LCMV	Systemic	Treg expansion helps prevent the development of T1D in NOD mice after infection <sup>40</sup>
<i>Leishmania sps.</i>	Skin	Treg production of IL-10 leads to chronicity <sup>49,42</sup>
HSV-1	Eye/Skin	Tregs limit effector infiltration of the eye preventing damage <sup>44</sup> /Treg-depletion during skin infection improves HSV-1 specific CD4+ and CD8+ T cell responses <sup>50</sup>
<i>Listeria monocytogenes</i>	Gastrointestinal tract	Treg depletion led to the generation of reduced affinity <i>L.m.</i> -specific CD8+ T cells <sup>51</sup>
<i>Schistosoma mansoni</i>	Systemic	Antigens associated with <i>S. mansoni</i> eggs induce pTreg formation that aids in the prevention of T1D development in NOD mice <sup>52</sup>

The critical suppressive function of Tregs is also vital in maintaining homeostasis and establishing tolerance in many forms, including at the fetal-maternal boundary<sup>53</sup>, in response to food antigens introduced through the gut in the form of oral tolerance<sup>54</sup> and in maintaining immunological quiescence at the boundaries between the microbiome and self<sup>55,56</sup>. As with pathogens, growing cancers can also co-opt the tolerance-inducing capability of Tregs. Solid tumors actively recruit Tregs by inducing chemokine production in surrounding cells and the utilizing the sequestered Tregs to form a quiescent boundary that reduces the ability of effector cells to form an effective anti-tumor immune response<sup>57</sup>.

The examples provided of the functional role of Tregs in both health and disease only begin to describe the importance of this cell type. The discovery of the Treg-defining transcription factor FoxP3 led to the rapid development of tools and mouse models with which to probe the inner workings of this critical cell type. In the work described in this dissertation, we have manipulated Tregs through the specific deletion of key proteins in sensing and migration pathways. By probing these models with viral infections, we hoped to broaden our understanding of the mechanism of action of Tregs, and by extension, our understanding of the interconnectedness of the immune system.

## Chapter 2. INFECTION SENSING IN REGULATORY T CELLS

### 2.1 TREGS MODULATE INCIDENTAL IMMUNOPATHOLOGY DURING WNV INFECTION.

As discussed above, due to the multi-functionality of Tregs, it is often difficult to predict their role in an emerging response to infection. As such, it is imperative that Treg function within the context of particular infections be specifically analyzed. Given the current wave of emerging

tropical diseases including Flaviviruses such as Zika and West Nile Virus (WNV), a clear understanding of both the development of a successful immune response and its potential impediments is of the utmost importance. Beyond the discovery of prophylactic and therapeutic targets, elucidation of the inner workings of a virus-specific adaptive response has the potential to inform future treatments of yet undiscovered viruses within the same family.

West Nile Virus was first isolated in Uganda in 1937 and although sporadic outbreaks were common in the Middle East, it was not until its introduction to the United States (New York) in 1999<sup>6</sup> that in-depth investigation of WNV pathogenesis began. Since making landfall, WNV has spread to all 48 contiguous states with over 16,000 documented cases of human neuroinvasive disease as of 2012<sup>58</sup>. Although humans are incidental hosts, statistical extrapolation from reported neuroinvasive cases suggest that in the 10 years since its introduction to the U.S., over 3 million people may have been infected<sup>59</sup>, underscoring the need for both treatment options and a greater understanding of the immunological consequences of the disease.

Currently, WNV pathogenesis is thought to proceed through three distinct phases. The initial transmission phase, termed the early phase, encompasses the transfer of WNV from the bite of the mosquito into the skin where keratinocytes and skin-associated sentinel cells such as Langerhans cells become infected<sup>60</sup>. As the virus replicates, infected DCs migrate to draining LNs where it infects other DCs as well as macrophages and neutrophils. Dissemination to the spleen and other tissues, including potentially the kidney<sup>61</sup>, occurs during this phase, termed the visceral-organ dissemination phase<sup>60</sup>. Finally, although the mechanism of entry is still controversial, in the CNS phase, WNV makes its way across the blood brain barrier (BBB), selectively infecting a variety of different neurons. In humans, particularly high viral titers have

been measured in regions associated with motor function including the cerebellum, the brain stem and the spinal chord<sup>62</sup>.

As nearly all WNV related fatalities result from neuroinvasive disease, understanding the mechanisms of disease-associated damage and how to mitigate it is crucial. Although a variety of cell types have been correlated with the development of a protective response against WNV including CD4+ T cells<sup>63</sup>, B cells<sup>64</sup> and monocytes<sup>65</sup>, CD8+ T cells in particular have been implicated in both helping to clear WNV-infected cells and exacerbating collateral immunopathology<sup>66</sup>. Tregs are particularly adept at restraining these over-zealous effector responses. Through the use of FoxP3-DTR mice, our lab has shown that in the absence of Tregs, WNV-infected mice show increased rates of morbidity and mortality, where nearly 100% of mice succumb after Treg depletion as compared to ~30-50% in WT controls<sup>46</sup>. A similar, albeit less dramatic, correlation was found in humans. Confirmed WNV+ blood donors that were symptomatic had lower Treg frequencies than asymptomatic WNV+ counterparts<sup>46</sup>. In addition, other groups have found that Treg expression of CTLA-4 is altered in patients with neuroinvasive disease, reinforcing the importance of a functional Treg response post WNV infection<sup>67</sup>. After further investigation of the role of Tregs in shaping the WNV specific CD8+ T cell response, we found that Treg depletion resulted in increased CD4+ and CD8+ T cell infiltration of the brain. These cells also expressed higher levels of activation markers and greater cytokine production in response to WNV stimulation<sup>68</sup>. Those mice that survived WNV infection after Treg ablation showed a significant deficit in the formation and retention of resident memory CD8+ T cells<sup>68</sup>. These data indicate that Tregs not only constrain a developing WNV specific response but also help ensure proper memory development after clearance.

## 2.2 INTRINSIC SENSING OF WEST NILE VIRUS THROUGH THE RIG-I/MDA5:MAVS AXIS

Because the viral peak of CNS infection is reached in as little as 7-8 days post the initial WNV transmission event<sup>60</sup>, understanding the early mechanisms by which cells detect infection and begin to mount a response is of critical importance. Additionally, elucidating these pathways often has the added benefit of revealing the tactics through which viruses subvert the system. One of the early detection mechanisms ubiquitously expressed by nearly all WNV susceptible cell types are the single stranded/double stranded viral RNA sensors known as RIG-I-like receptors, of which RIG-I, MDA5 and LGP2 are putative members. After binding to viral RNA, these sensors set off a signaling cascade mediated by the mitochondrial membrane associated adaptor protein MAVS. Subsequently, MAVS activation leads to a variety of downstream effects including Type I IFN production, nuclear translocation of NF- $\kappa$ B leading to pro-inflammatory cytokine production and the transcription of numerous ISGs<sup>69</sup>.

MAVS signaling has been shown to be critical for early control of WNV replication. In particular, MAVS deleted mice (in which MAVS expression has been ablated in all cells) show dramatically accelerated mortality preceded by acute lymphadenopathy, splenomegaly and symptoms of pro-inflammatory cytokine overproduction<sup>70</sup>. Extending this work, other groups have drilled down to investigate the effect of MAVS deletion on particular cell subsets including a broad focus on CD45+ hematopoietic cells<sup>71</sup> confirming the immune dysregulation that follows WNV infection. Given the stated importance of MAVS signaling, the Treg response in modulating inflammation and activation after infection and the reduced frequencies of Tregs found in MAVS<sup>-/-</sup> mouse models after infection<sup>70</sup>, it follows that the effect of MAVS signaling in Tregs should be investigated.

### 2.3 TREGS CAN SENSE THE PRESENCE OF FOREIGN PEPTIDES THROUGH PRRS.

As previously described, the immune response is tightly regulated to maximize potential anti-microbial responses such that infections can be cleared, leaving behind life-long, protective memory responses, while at the same time sparing host tissues and preventing extensive autoimmunity and immunopathology. One method by which the immune system achieves this balance is through self/non-self discrimination, or recognition of pathogen-associated molecular patterns (PAMPs) through pattern recognition receptors (PRRs). While this level of recognition has traditionally been characterized within antigen-presenting cells (APCs), recent studies have examined the potential for T cells to sense the presence of foreign products through PRRs<sup>72</sup>. In particular, T cells express various Toll-like receptors (TLRs), and T cells were first reported to respond to direct TLR stimulation when it was observed that in an APC-free cell culture, TCR-triggered T cells could be further stimulated to produce IL-2 and to proliferate by the TLR9 agonist CpG<sup>73</sup>. Since that initial finding, CD4+ and CD8+ T cell stimulation through various TLRs has been shown to promote antigen-specific proliferation, cell survival, homeostatic proliferation of memory cells, and cytokine expression<sup>74,75,76,77,78,79</sup>.

In addition Tregs were shown to express TLR8, ligation of which inhibited their suppressive function in humans<sup>80</sup>. Human studies of TLR2 expression in Tregs have found that binding of TLR2 ligand also reduces Treg suppressive function and this abrogation of function may contribute to the formation of pro-inflammatory T<sub>H</sub>17 cells by enhancing IL-6 and IL-17 production<sup>81</sup>. Conversely, it has been reported that LPS stimulation of Tregs induces proliferation and enhanced suppressive capacity in the murine system<sup>82</sup>. Using an RLR knock out mouse model of MDA5, Anz *et al* demonstrated that exposure to viral RNA through infection with encephalomyocarditis virus resulted in a loss of Treg function, an effect that was dependent

on the intrinsic expression of MDA5 in Tregs<sup>83</sup>. Given this finding, the lack of Treg expansion seen the MAVS-deleted WNV infection mouse model<sup>70</sup> and the critical role that PRRs have been shown to play in Treg function, we propose to further investigate the necessary of intrinsic MAVS expression in the development of a productive WNV-specific immune response.

## 2.4 AIM 1: IS INTRINSIC TREG ACTIVATION OF THE VIRAL RNA SENSORS, RIG-I AND MDA5 VIA THE ADAPTOR PROTEIN MAVS, NECESSARY FOR TREG EXPANSION AND FUNCTION DURING WNV INFECTION?

### 2.4.1 *FoxP3 expression is down regulated in Tregs following WNV infection of MAVS<sup>-/-</sup> mice.*

Our previous work suggested that Tregs in MAVS<sup>-/-</sup> mice failed to proliferate in response to WNV infection as compared to WT controls<sup>70</sup>. Therefore, we further investigated this finding in order to fully characterize the Treg response in the complete absence of MAVS signaling. In particular, we examined the frequency and phenotype of Tregs within MAVS<sup>-/-</sup> mice during WNV infection to determine if the expression of key suppressive molecules was altered in this system. We found that in addition to the previously described secondary lymphoid organ enlargement<sup>70</sup>, WNV-infected MAVS<sup>-/-</sup> mice rapidly declined beginning at day 5 p.i., exhibiting dramatic weight loss (Figure 1) and symptoms such as ruffled fur, lethargy and diarrhea. On day 6 p.i. we noted inflammation in intestinal tissues, discoloration in the liver, blackened gall bladders and enlarged mesenteric lymph nodes in MAVS<sup>-/-</sup> but not MAVS-sufficient groups (data not shown). These symptoms indicate that WNV infection in MAVS<sup>-/-</sup> mice leads to the development of a grossly dysregulated systemic inflammatory response with gut involvement similar to that seen in DSS colitis models in MAVS<sup>-/-</sup> mice<sup>84</sup>.

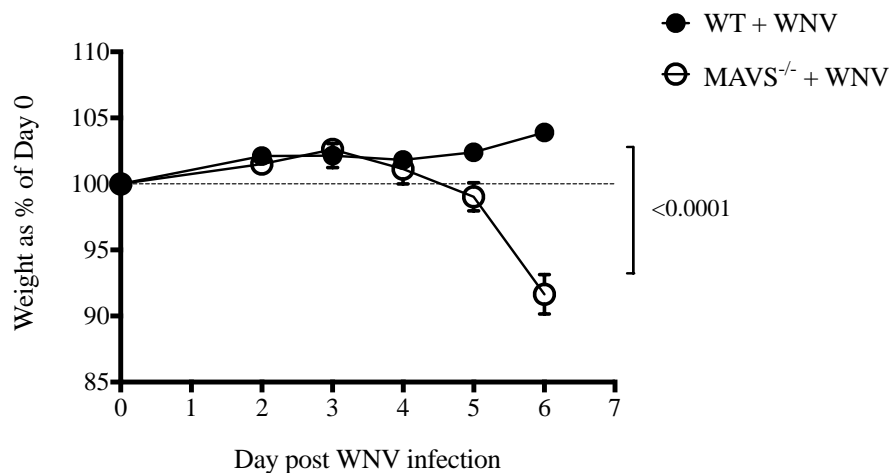


Figure 1. MAVS<sup>-/-</sup> mice decline rapidly starting day 5 post WNV infection.

When we examined the frequency of CD4<sup>+</sup>FoxP3<sup>+</sup> Tregs, we found that in contrast to pre – infection, Treg frequency was significantly reduced in MAVS<sup>-/-</sup> mice after WNV infection as compared to WT controls. However, upon per cell analysis of FoxP3 expression through median fluorescence intensity (MFI) measurement, we found a downshift in FoxP3 fluorescence (Figure 2).

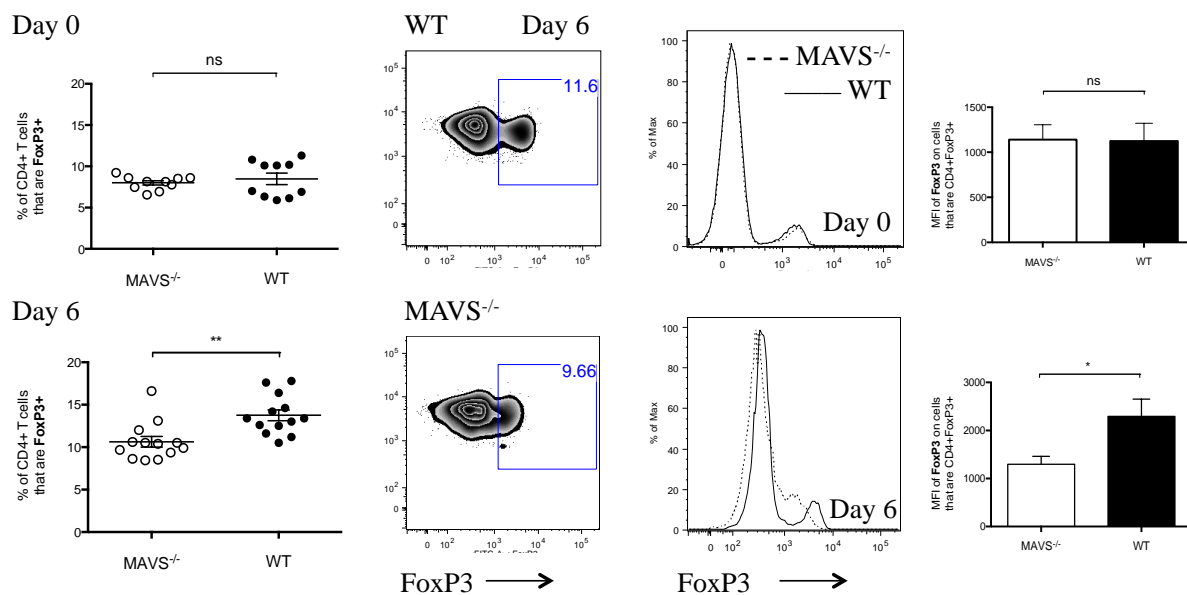


Figure 2. FoxP3 expression is down regulated in Tregs following WNV infection of MAVS<sup>-/-</sup> mice.

The degree of FoxP3 expression has been shown to be directly associated with Treg suppressive capability in both FoxP3 attenuation models<sup>85</sup> and ex vivo allograft transplantation models<sup>86</sup>, where decreased expression leads to the development of scurfy-like autoimmunity. Thus, we assessed the frequency of Treg-associated suppressive markers, and unexpectedly found that MAVS<sup>-/-</sup> Tregs have a statistically significant increase in expression of all suppressive molecules measured, including CD73, CTLA-4, and ICOS (Figure 3). This paradoxical decrease in FoxP3 expression and concomitant alteration of suppressive profile may be a reflection of enrichment of less plastic Tregs within the heterogeneous Treg population represented in the spleen<sup>32</sup>.

Suppression:

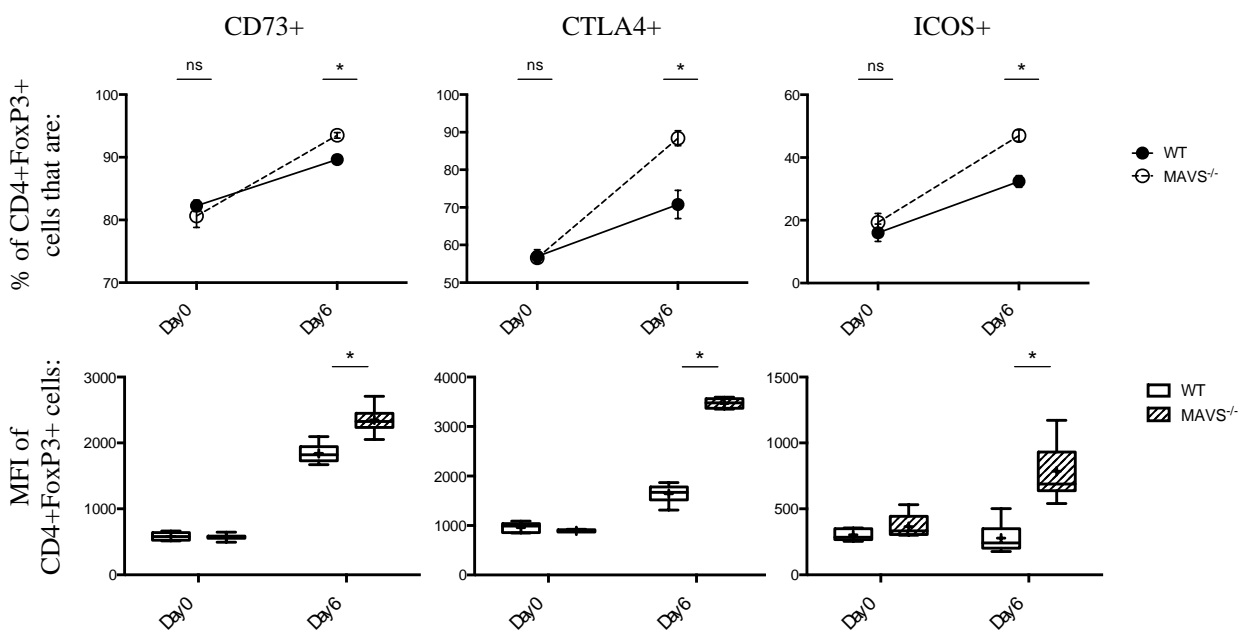


Figure 3. Treg suppressive molecule expression increased in MAVS<sup>-/-</sup> mice after WNV infection.

In addition, the extreme pro-inflammatory environment that develops in the MAVS<sup>-/-</sup> mice after WNV could be contributing to a loss of Treg identity where a subset of Tregs has lost the

ability to express FoxP3 entirely and/or the per cell expression of FoxP3 has dimmed sufficiently that it is no longer discernible. To further characterize MAVS<sup>-/-</sup> Tregs in infected mice, we then examined the activation phenotype of these cells and found that the expression of CD44 and CXCR3 was increased after WNV infection as expected (Figure 4). However, despite the inflammatory conditions in the infected KO mice, MAVS<sup>-/-</sup> Treg expression of CD44, CD25, and CXCR3 was comparable to WT counterparts. To determine Treg functional potential, we assessed the frequency of KLRG1 and CD103, proteins recently associated with terminal differentiation in Tregs<sup>25</sup> (Figure 4), and found that they were similar regardless of MAVS expression. Finally, we found that the cell-cycle progression intracellular protein, Ki67, was significantly increased in MAVS<sup>-/-</sup> Tregs, further suggesting that the decreased Treg frequency measured in MAVS<sup>-/-</sup> mice after WNV infection is more likely due to FoxP3 down regulation rather than a failure of Treg division.

Activation:

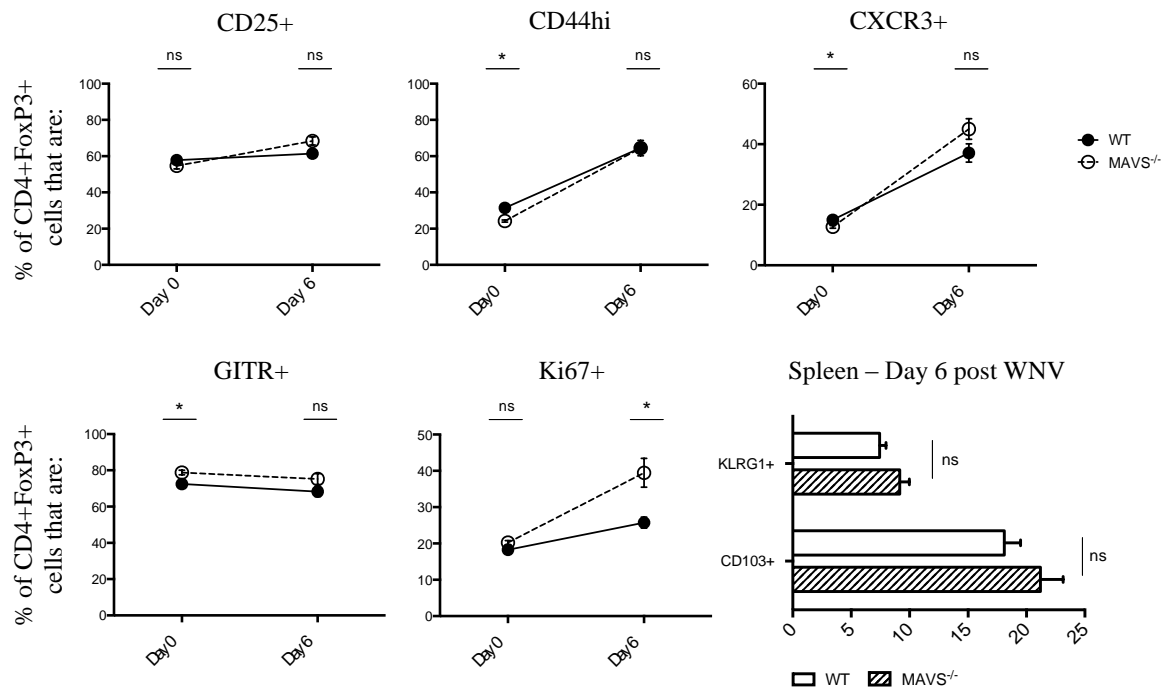


Figure 4 Activation profile of MAVS<sup>-/-</sup> Tregs is comparable to WT after WNV infection.

Since Tregs in MAVS<sup>-/-</sup> mice appeared to be losing expression of FoxP3 following infection with WNV, along with experiencing diarrhea and other signs of gastrointestinal distress, we extended our analysis of Tregs to include the mesenteric lymph nodes (MLN). MAVS<sup>-/-</sup> mice experienced not only profound splenomegaly, but also a significant enlargement of the MLN at day 6 p.i (Figure 5). As an inappropriately regulated T<sub>H</sub>17 response has been previously implicated in gastrointestinal inflammation, we examined the frequency of ROR $\gamma$ T+ CD4 T cells in the spleen and MLN, and while they did not vary significantly regardless of MAVS expression, there were significantly fewer ROR $\gamma$ T+ CD4 T cells expressing FoxP3, based on both frequency and MFI, in the absence of MAVS (Figure 5).

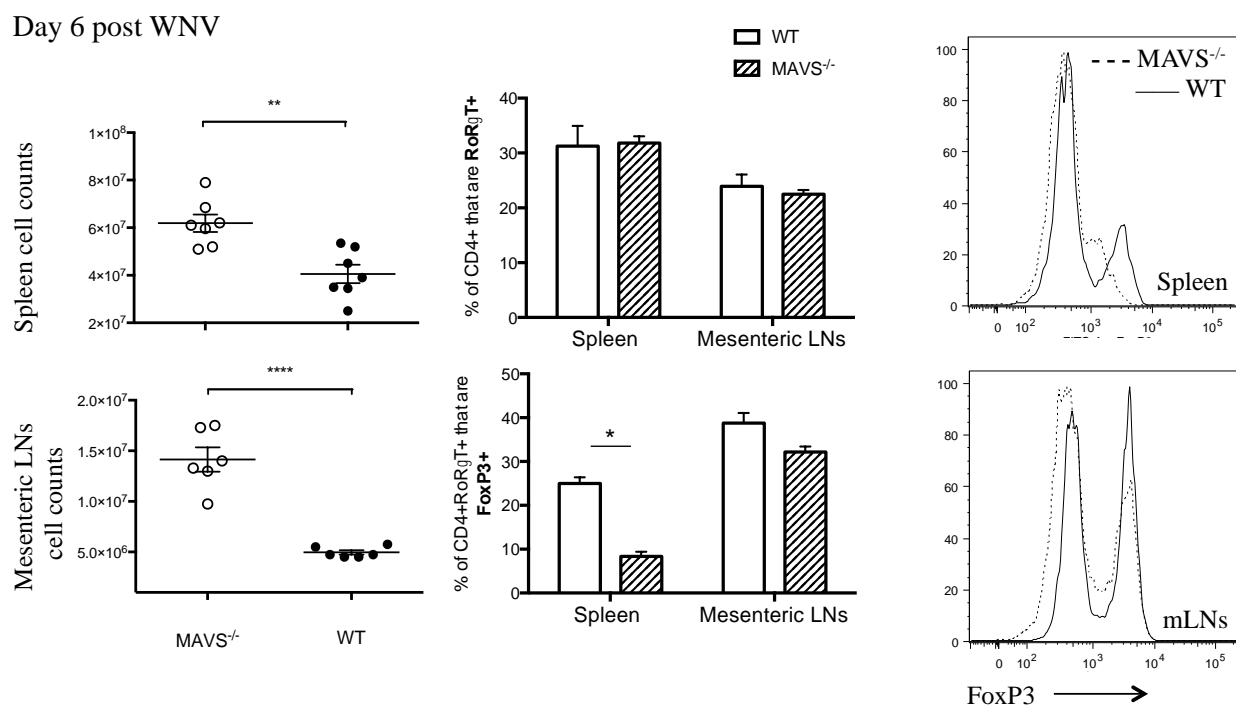


Figure 5. FoxP3 is down regulated in ROR $\gamma$ T co-expressing cells in the spleen and mesenteric lymph nodes.

Similarly, Tregs have been observed to convert from suppressive cells to inflammatory TH17 cells upon treatment with polarizing extrinsic cytokine signals<sup>87,88</sup>. In support of the notion that Tregs require MAVS to maintain FoxP3 expression and thereby stable lineage commitment following WNV infection, MAVS<sup>-/-</sup> mice had significantly elevated serum TGFβ and IL-6 levels following WNV infection (Figure 6). In combination TGFβ and IL-6 are known to support conversion of Tregs to TH17 cells<sup>87,88</sup>, and correspondingly MAVS<sup>-/-</sup> mice had higher serum IL-17 (Figure 6). These results suggest that MAVS is required for Treg stability following WNV infection, though whether or not MAVS is required intrinsically remains uncertain.

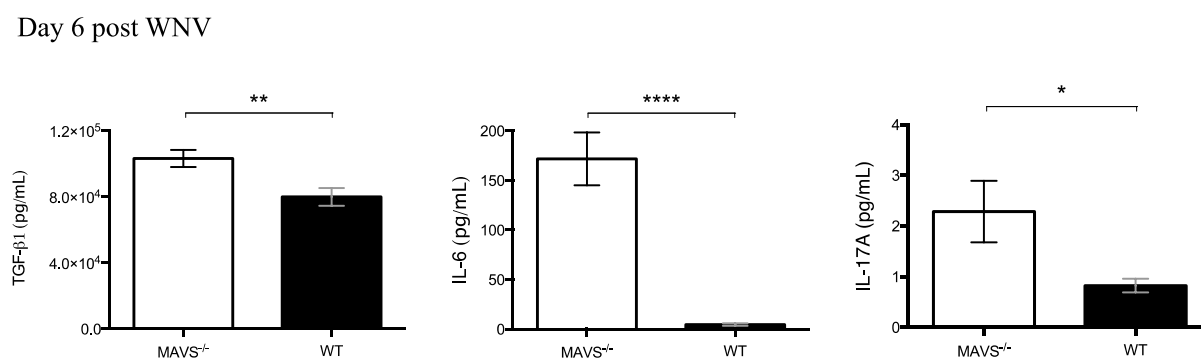


Figure 6. FoxP3 down regulation occurs in the presence of TH17 polarizing conditions.

#### 2.4.2

*Intrinsic MAVS signaling is not required for Treg proliferation or suppressive function in vitro.*

Since our results demonstrated that WNV infection of MAVS<sup>-/-</sup> mice led to decreased expression of FoxP3 (Figure 2), likely account for the deficit of Treg expansion following infection with WNV<sup>70</sup>, we next tested the role of intrinsic MAVS signaling in Treg proliferation *in vitro* using a standard CFSE proliferation assay. Initially, we tested the ability of Tregs to proliferate to a polyclonal TCR stimulus using a crosslinking antibody specific to CD3 and found

that MAVS<sup>-/-</sup> Tregs proliferated as well as WT Tregs. Further, as the frequency of Tregs that proliferated during the period of culture was extremely high, the addition of WNV to the culture was unable to augment proliferation and was again similar regardless of the presence of intrinsic MAVS in Tregs (Figure 7). In order to test the requirement for MAVS in Treg proliferation in response to WNV directly, we cultured Tregs with WNV and WT dendritic cells (DCs) without the addition of anti-CD3 stimulation. WT and MAVS-deficient Tregs were equally able to proliferate under these conditions (Figure 7), suggesting that MAVS is dispensable for Treg proliferation upon TCR stimulation as well as in culture with WT DCs with or without WNV.

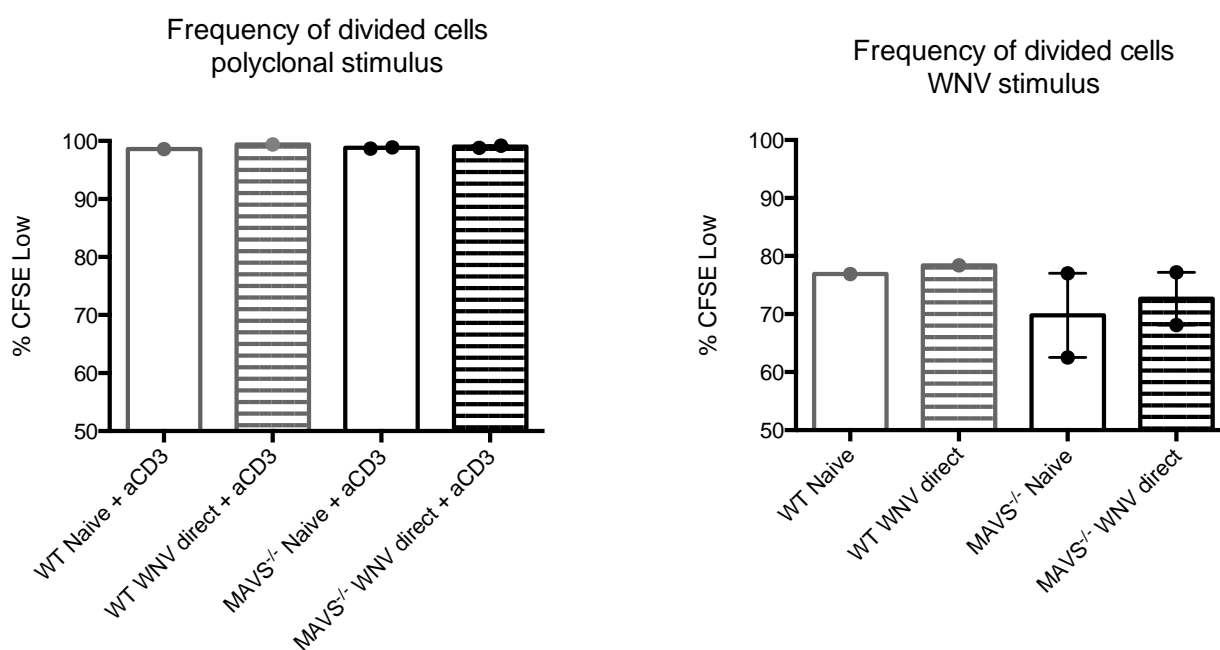


Figure 7. Intrinsic MAVS signaling is not required for Treg proliferation *in vitro*.

Although intrinsic MAVS was not required for Treg proliferation *in vitro*, it remained possible that intrinsic RLR signaling is required for Treg suppressive function, as MAVS<sup>-/-</sup> mice suffered from several hallmarks of mice lacking functional Tregs, including a generally

dysregulated immune response to WNV, enhanced numbers of immune effector cells present in the spleen, and profound splenomegaly<sup>70</sup>. Therefore, we tested the ability of Tregs lacking MAVS to suppress proliferation of conventional T cells using a CFSE-based suppression assay. Following three days of co-culture, WT and MAVS<sup>-/-</sup> Tregs were equally proficient in suppressing T cell proliferation (Figure 8), suggesting that intrinsic MAVS signaling is not required for Treg suppressive function.

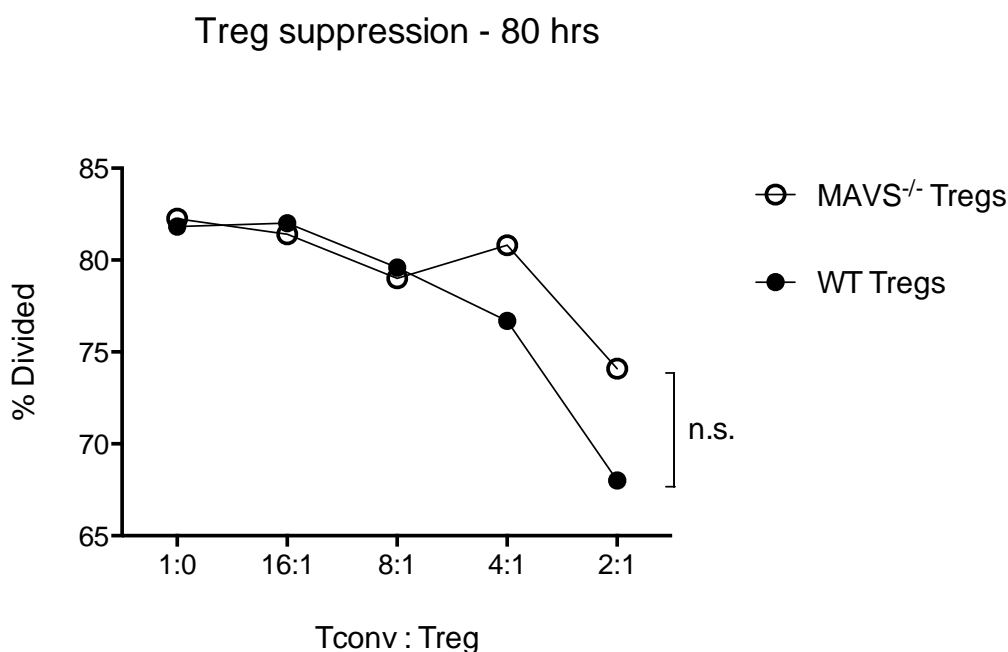


Figure 8. Intrinsic MAVS signaling is not required for Treg suppressive function *in vitro*.

#### 2.4.3

#### *Treg expression of MAVS does not affect WNV disease in vivo.*

Although *in vitro* data did not suggest a role for MAVS signaling in Tregs, given the *in vivo* alteration of FoxP3 expression in MAVS<sup>-/-</sup> mice we further tested the role for this signaling molecule specifically in Tregs in the course of *in vivo* WNV infection. To test the role of MAVS exclusively in Tregs *in vivo*, we used an asymmetric mixed bone marrow chimera mouse model (Figure 9). Briefly, congenically labeled FoxP3<sup>DTR</sup> mice were lethally irradiated and then infused

with a 90% FoxP3<sup>DTR</sup> Ly5.1 + 10% MAVS<sup>-/-</sup> Ly5.2 (or WT Ly5.2) bone marrow mixture. By utilizing a 90/10 ratio we were able to maximize the amount of hematopoietic stem cell precursors available for development of Tregs while simultaneously minimizing the contribution of other MAVS<sup>-/-</sup> or WT cell types that might arise. Following a 3-month recovery time, diphtheria toxin (DT) was administered to deplete all DTR-bearing Tregs, thereby allowing MAVS<sup>-/-</sup> or WT Tregs to expand to fill the compartment in response. Chimeras were then infected subcutaneously in the footpad to mimic the route of vector transmission of WNV.

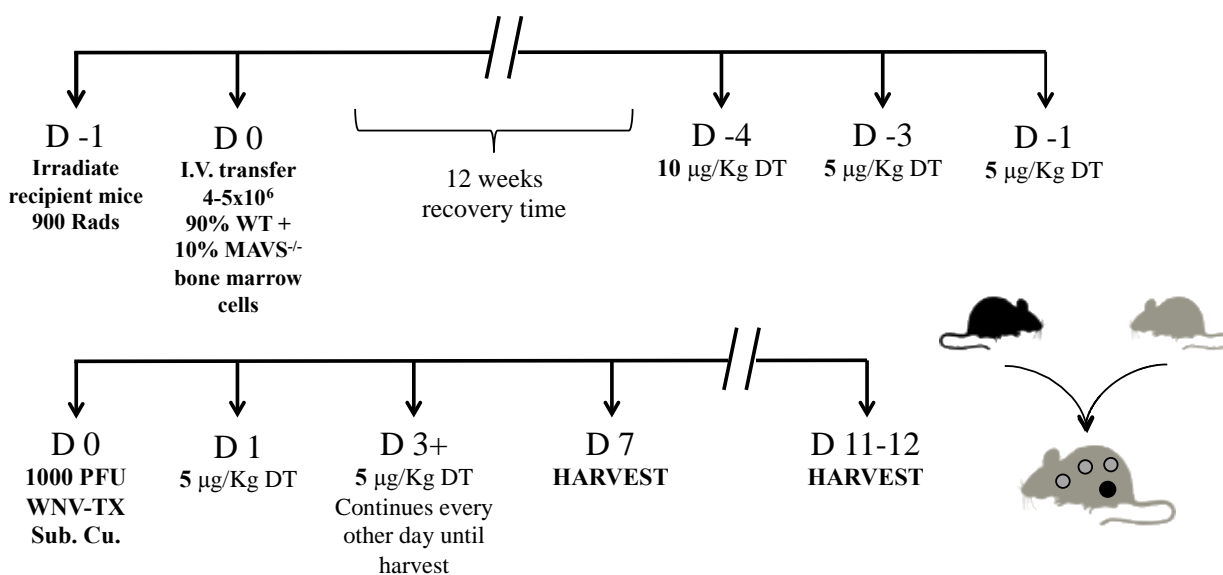


Figure 9. Schematic of hematopoietic stem cell transfer and WNV infection schedule.

In particular, we focused on the visceral phase of WNV infection. This stage of infection can be split into an early phase, at approximately d7 p.i. and a late phase, at approximately d11-12 p.i., in which viral replication begins to wane in secondary lymphoid tissues and has transitioned across the blood brain barrier (Figure 10). Furthermore, WNV-specific CD8<sup>+</sup> T cell responses, as measured by NS4b tetramer binding, track closely with movement of the virus across tissues.

Consequently, Treg expansion has been shown to then temporally follow WNV-specific CD8+ T cell expansion<sup>68</sup>.

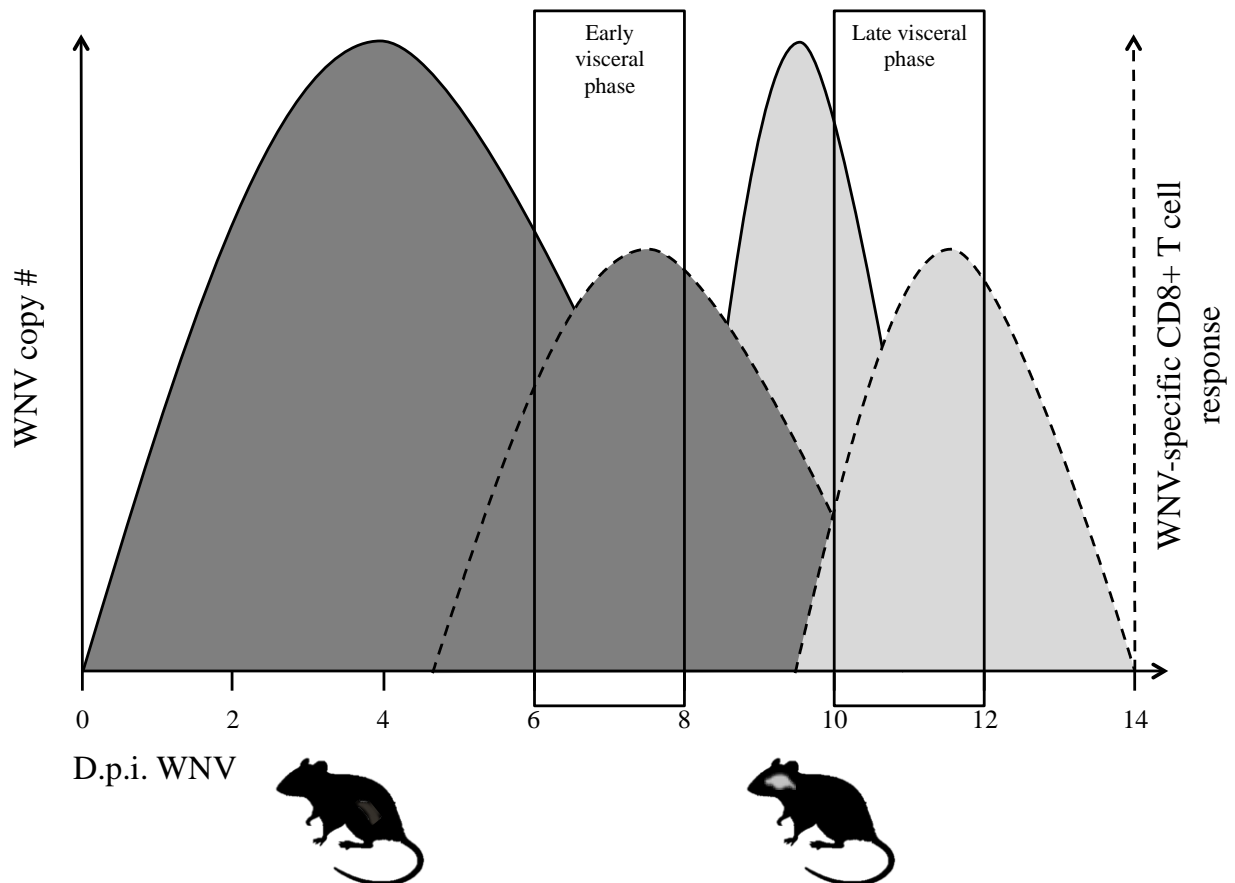


Figure 10. Visceral phase of infection was analyzed during early and late periods.

After infection with WNV, mice were monitored daily for weight loss and clinical manifestations of disease, and mice with MAVS<sup>-/-</sup> Tregs suffered from a nearly identical weight loss (Figure 11A), suggesting that the course of disease was not altered when Tregs lacked MAVS. Additionally, we compared the viral burden in the cerebellum, a CNS substructure known to be especially susceptible to WNV replication<sup>89</sup>, between MAVS<sup>-/-</sup> Treg chimeric mice and WT controls. Quantitative reverse transcription - real-time PCR on cerebellar tissues harvested during the late visceral phase revealed that there was no significant difference in WNV

copy number between groups (Figure 11B). Therefore, we conclude that Treg-intrinsic MAVS does not play a role in disease outcome to WNV *in vivo*.

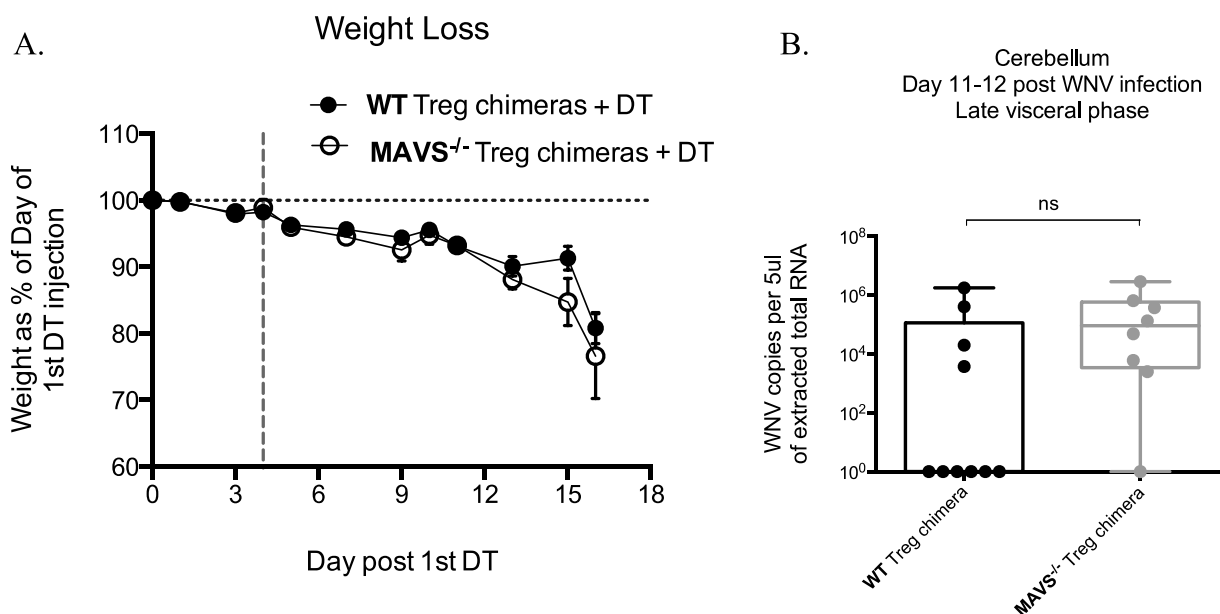


Figure 11. Weight loss and WNV cerebellum titers are comparable between MAVS<sup>-/-</sup> Treg chimeras and WT controls.

#### 2.4.4

#### *Intrinsic MAVS signaling is dispensable for Treg expansion and function following WNV infection in vivo.*

Although we did not observe the increased viral burden and pathogenesis when only Tregs lacked MAVS as compared to the full knockout mouse<sup>70</sup>, it was possible that MAVS signaling in Tregs was required for a subtle element of the immune response to WNV. Therefore, we next examined the extent of Treg expansion following WNV infection. The frequency of Tregs present in the spleen was similar regardless of MAVS expression at the peak of the T cell response (Figure 12A). In addition, we characterized the Treg response during infection by analyzing the frequency of a number of functional and migratory markers associated with suppressive function. CTLA-4 expression by Tregs was compared, as this is a key strategy used

by Tregs to directly suppress antigen presenting cells and therefore the initiation of an immune response. However, splenic Tregs expressed similar levels of CTLA-4 regardless of MAVS expression (Figure 12B).

### Early Visceral phase *Spleen*

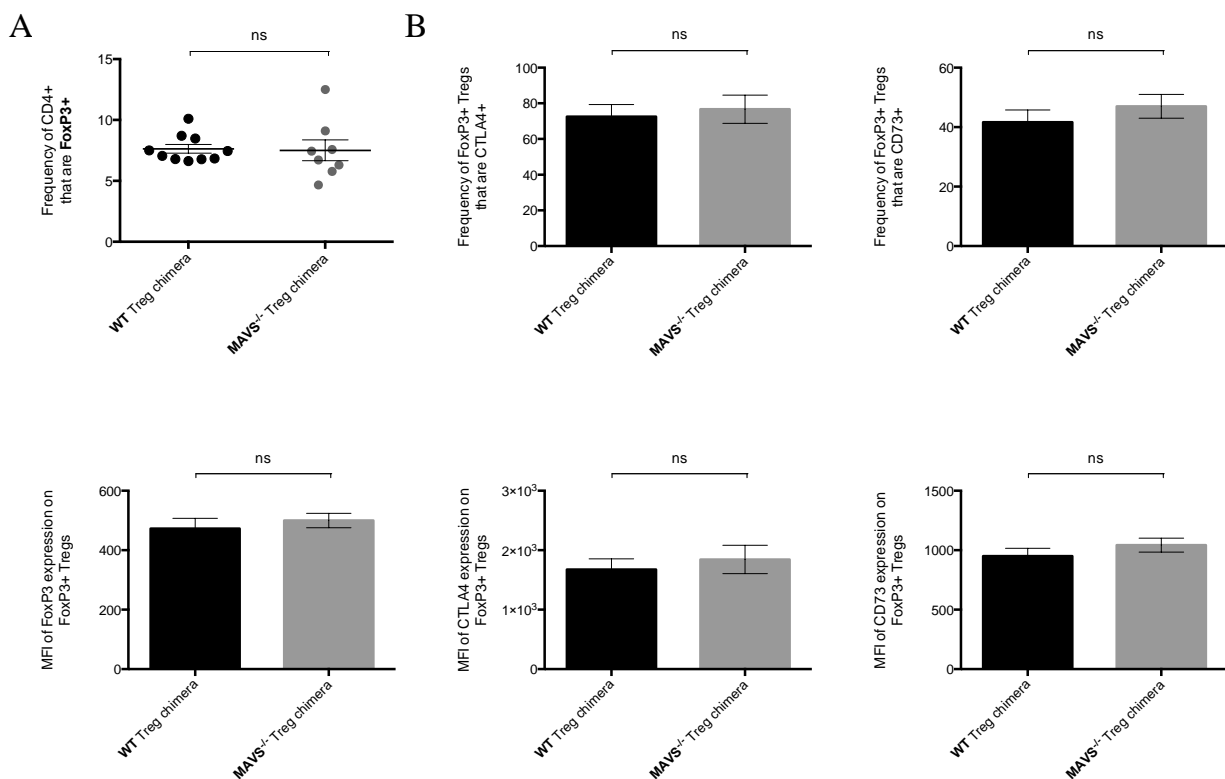


Figure 12. Expansion and suppressive function of Tregs is comparable between MAVS<sup>-/-</sup> Treg chimeras and WT controls during early visceral phase of WNV infection.

Tregs also employ a variety of other suppressive mechanisms including cAMP-mediated inhibition of surrounding effector cells<sup>90</sup>. We found that proteins critical to the function of Tregs such as CD73 and GITR (data not shown) were represented at similar frequencies despite a lack of MAVS expression in Tregs during infection. Furthermore, through median fluorescence intensity (MFI) analysis we found comparable expression of these molecules on a per-cell basis (Figure 12B). Importantly, we found comparable levels of FoxP3 expression between MAVS<sup>-/-</sup>

Treg chimeras and WT controls (Figure 12A), suggesting that intrinsic MAVS signaling is not required for stable expression of FoxP3 by Tregs.

In addition to playing a role in the secondary lymphoid organs, Tregs play a role in the central nervous system, as the T cell response is critical to clearing neuroinvasive WNV infection<sup>91</sup>. Although Treg frequency does increase in the secondary lymphoid organs (SLO) and brain following WNV infection<sup>68</sup> the absence of MAVS within Tregs does not alter this frequency or cell number in the brain (Figure 13).

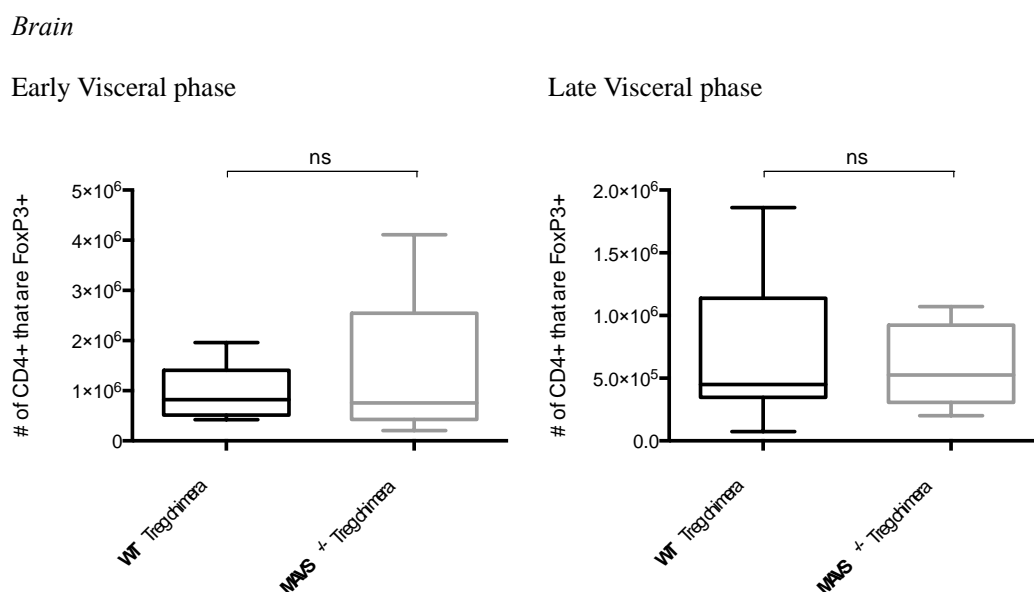


Figure 13. Treg infiltration/expansion of the brain is comparable between groups regardless of infection stage after WNV infection.

Therefore, it appears unlikely that MAVS is required for *in vivo* Treg expansion following WNV infection, or for Treg suppressive function, at least as mediated by CTLA-4, GITR, or CD73.

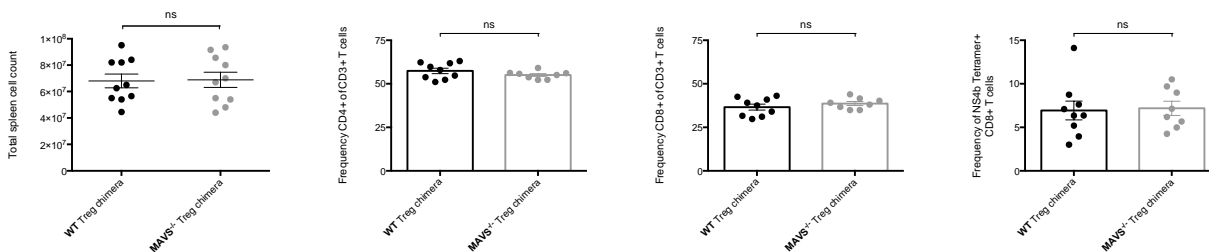
#### 2.4.5 *Immunity to WNV is not compromised in the absence of Tregs expressing MAVS.*

While none of the Treg suppressive marker expression levels examined were altered by the absence of MAVS signaling within Tregs (Figure 12), there are myriad other mechanisms by

which Tregs can suppress T cell responses<sup>92</sup>. Therefore, we next examined the T cell response following WNV infection in the presence or absence of Tregs expressing MAVS. In contrast to full MAVS<sup>-/-</sup> mice, the overall frequency of CD4 and CD8 T cells in both the spleen and brain is nearly identical in MAVS<sup>-/-</sup> Treg chimeric mice as compared to WT controls, indicating that bulk T cell frequency and/or expansion is independent of MAVS expression by Tregs following WNV infection at the early visceral phase (Figure 14).

### Early Visceral phase

#### *Spleen*



#### *Brain*

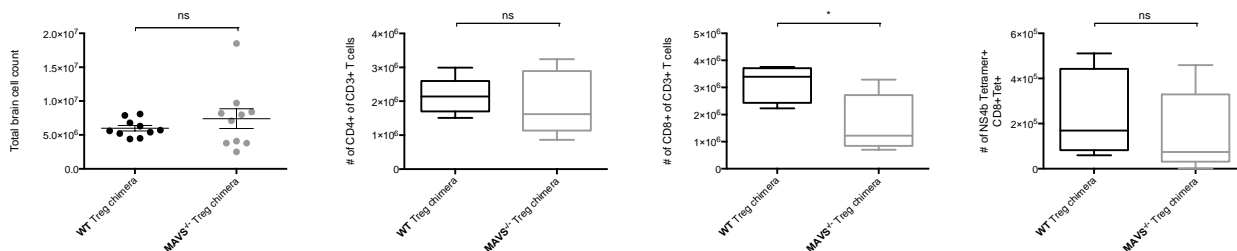


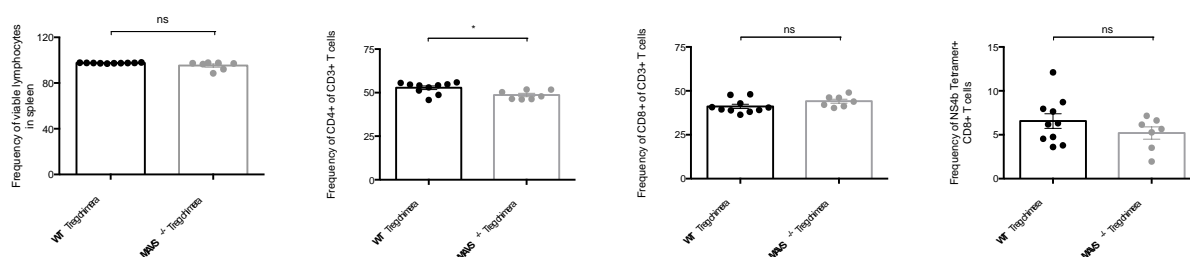
Figure 14. T cell frequencies including WNV specific CD8+ T cells in spleen and brain were comparable between groups during early phase of WNV infection.

In addition, we found that T cell infiltration of the CNS in the late visceral phase was no different between MAVS<sup>-/-</sup> Treg chimeras and controls (Figure 15). When T cells were analyzed for expression of activation and functional markers such as CD44 and CXCR3, we found that both MAVS-deficient or -sufficient Treg groups were comparable (data not shown). Finally, when the WNV-specific CD8 T cell response was examined using MHC class I tetramer staining, similar frequencies of NS4b-specific CD8 T cells were measured in the spleens and

brains of mice independent of Treg expression of MAVS (Figure 14 and Figure 15). In sum, our results indicate that MAVS expression by Tregs is not required for an effective T cell response against WNV infection in vivo.

### Late Visceral phase

#### Spleen



#### Brain

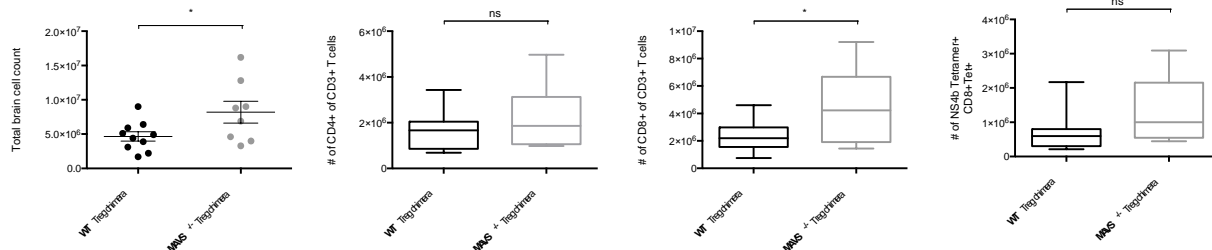


Figure 15. T cell frequencies including WNV specific CD8<sup>+</sup> T cells in spleen and brain were comparable between groups during late phase of WNV infection

### 2.4.6

#### Discussion

Two major paradigms of immunology, clonal selection and pattern recognition, describe mechanistically how cells of the immune system can sense and distinguish foreign invaders that are potentially dangerous to the host. Since it has been shown that Tregs are involved in the immune responses to many distinct pathogens, it appears that this T cell subset must also be able to detect the presence of microbes in order to exert their potential modulatory effects on the ensuing immune response. We reasoned that this could be done via RLR sensing, as our previous study using mice deficient in MAVS showed a lack of Treg expansion following WNV infection, along with uncontrolled inflammation and increased mortality<sup>70</sup>. However, here we show that

rather than a lack of expansion, we see a down regulation of FoxP3 expression in WNV infected MAVS<sup>-/-</sup> mice. In addition, intrinsic MAVS signaling is dispensable for proper control of WNV, and further, it is not required for full Treg functional capacity following infection.

Through our study, we have additionally identified a cell-extrinsic role for MAVS in stable expression of FoxP3 by Tregs. In WNV-infected mice lacking MAVS on all cells, there is a dramatic increase in serum levels of several pro-inflammatory cytokines, including IL-6, which is concurrent with a loss of FoxP3 expression in a large subset of Tregs. Thus, we hypothesize that the pro-inflammatory environment promoted by IL-6 and other cytokines, in addition to uncontrolled virus replication<sup>70</sup>, leads to a change in host strategy away from the suppressive activity of Tregs, perhaps resulting in a more T<sub>H</sub>17-type profile, as suggested by the elevation in serum IL-17 and increased total numbers of ROR $\gamma$ T<sup>+</sup> CD4 T cells that could be considered to be T<sub>H</sub>17 cells. Indeed, it has previously been shown that IL-6 coordinates with IL-1 $\beta$  to block the suppressive effect of Tregs on CD4<sup>+</sup> T cells, at least in part by controlling their responsiveness to IL-2<sup>93</sup>. Interestingly, stimulation of Tregs in the presence of IL-6 was previously reported to result in loss of FoxP3 expression and the acquisition of a T<sub>H</sub>17 phenotype<sup>87,94</sup>, and indeed, IL-6 signaling in psoriasis prevents immune suppression by Tregs<sup>95</sup>. Thus, it appears that under extreme “emergency” conditions, such as during a virus infection when the host lacks a key innate immune sensor, an over-reaction may lead to conversion to a fully inflammatory response, including diminishing the FoxP3 levels in Tregs, which may subsequently result in diminished function given enough time. Importantly, although Treg suppressive marker expression was comparable between groups at day 6 p.i., the time at which MAVS<sup>-/-</sup> mice have diminished FoxP3 expression on Tregs, these mice succumb starting at day 7 post-infection, thus precluding our ability to examine any downstream effects on Treg suppressive capacity in the full knockout.

In sum, our results suggest that Tregs do not sense WNV infection through intrinsic RLR signaling. However, given the appreciated role that Tregs play in anti-WNV immunity<sup>96,68</sup>, it is increasingly vital that we understand how they sense the presence of infection and subsequently initiate their role in the immune response. A thorough characterization of how Tregs detect virus infection is critical if these cells are to be leveraged for therapeutic strategies, as it would be the key to directing these cells toward the type of immune responses required to prevent and/or eliminate infections.

#### 2.4.7

#### *Limitations and unanswered questions*

While our hypothesized candidate for Treg sensing of WNV infection appears dispensable, several other possibilities exist. First, it is well established that activation of T cells is dependent upon signals through the TCR interaction with MHC and cognate peptide antigen, as well as co-stimulatory receptors such as CD28 interacting with B7 molecules on APCs. However, the role for TCR specificity in Treg activation in the course of infection remains controversial, as Tregs are thought to have a relatively high affinity for self-antigens<sup>97</sup>. FoxP3<sup>+</sup> Tregs were first demonstrated to be specific for the microbe *Leishmania major* in a study where they strongly proliferated in response to *Leishmania*-infected DCs, and further, the majority of Tregs in infected tissues were found to be microbe-specific<sup>98</sup>. More recently, *Mycobacterium tuberculosis* (*M.tb.*)-specific Tregs were identified following infection, and these cells were specifically of the thymically-derived, rather than peripherally-induced, lineage<sup>36</sup>, thereby demonstrating that cells exiting the thymus as Tregs can be specific to microbial antigens. Therefore, it is possible that Tregs do express TCRs specific for at least a subset of microbial antigens, though this has not been formally tested in the specific context of WNV infection.

Alternatively, Tregs could sense the presence of infection through Type I IFN signaling or some other type of cytokine signal. Recently, Tregs lacking surface expression of Type I IFN receptor during LCMV infection were shown to impair the development of an effective CD8+ T cell response leading to LCMV chronicity<sup>99</sup>. In a murine model of colitis, it has been demonstrated that Type I IFNs help to maintain FoxP3 on colonic Tregs under inflammatory conditions<sup>100</sup>, and so it is possible that this could occur as well in the context of infection. Because Type I IFN is a key immune effector molecule downstream of RLR recognition of WNV and related viruses<sup>101,102,103</sup>, it is possible that Treg detection of microbial products occurs through RIG-I indirectly via Type I IFN. MAVS signaling was required for WNV-triggered DC production of Type I IFN *in vitro*, though serum levels from mice infected with WNV were similar between WT and MAVS-deficient mice<sup>70</sup>, suggesting that there are multiple redundant pathways capable of triggering the IFN cascade upon WNV infection *in vivo*. Additionally, serum levels of cytokine may not describe IFN levels in various local microenvironments (such as SLO) where Tregs would likely receive signals to promote the response to infection, and so RIG-I-mediated production of type I IFN remains a possibility as a mechanism by which Tregs could sense the presence of WNV infection, though the cellular sources of IFN as well as the timing and location of production remain unresolved.

## Chapter 3. REGULATORY T CELL MIGRATION AND TISSUE-SPECIFIC FUNCTION

### 3.1 THE INTEGRIN AS A THERAPEUTIC TARGET AND THEIR EFFECTS ON THE IMMUNE RESPONSE

Integrin  $\beta 1$  serves as the binding partner for a large array of integrin  $\alpha$ -chains<sup>104</sup> and is nearly ubiquitously expressed by cell types ranging from endothelial cells to immune cells<sup>105</sup>. In addition,  $\alpha\beta$  integrins are known to bind to extracellular matrix components outside of the cell with concomitant intracellular binding to cytoskeletal elements. This transmembrane feature allows for both inside-out signaling resulting from structural cytoskeletal changes initiated through intracellular activation for example, but also outside-in signaling in response to a changing environment.  $\alpha\beta$  integrin functionality has typically been described in terms of their adhesion and migration properties. Although integrin  $\beta 1$  and  $\alpha$ -chain combinations include nearly a dozen varieties, T cells have been shown to express only a small subset. In particular,  $\alpha 4\beta 1$  integrin has been the focus of intense study as a protein that binds to VCAM-4 on endothelial surfaces and allows for T cell access to sites of inflammation and the CNS<sup>106</sup>.

VLA-4 or Very Late Antigen-4 as  $\alpha 4\beta 1$  integrin is commonly known, is the target of the current relapsing remitting multiple sclerosis (MS) treatment, Natalizumab, a monoclonal antibody that binds to  $\alpha 4$  integrin<sup>105</sup>. In 1992, Yednock *et al* found that intraperitoneal administration of anti- $\alpha 4$  integrin prevented the development of paralysis in a majority of EAE mice tested, although the direct effect  $\alpha 4$  integrin on the prevention of circulating lymphocyte entry to the CNS remained speculative<sup>106</sup>. In the intervening years side effects of anti- $\alpha 4$  integrin treatment have come to light including an increased susceptibility to progressive multifocal

encephalopathy (PML) triggered by JC virus infection in addition to reported paradoxical worsening of MS symptoms in some patients<sup>107</sup>. Furthermore, pro-inflammatory T cell types such as T<sub>H</sub>17 cells have been shown to access the CNS regardless of  $\alpha$ 4 integrin blockade<sup>108</sup>. As such, although Natalizumab has shown great clinical success, the as yet unexplained etiology of the side effects underscore the need for a better understanding of the fine points of the effect of  $\alpha$ 4 $\beta$ 1 blockade as they pertain to individual lymphocyte subtypes.

Although it is known that MS severity correlates with poor Treg function and altered distribution<sup>109</sup> few studies have focused on the effect of VLA-4 blockade on Tregs specifically. Stenner *et al* studied human Tregs (defined as: CD4+CD25 (high) CD127 (low) FoxP3+ T cells) and found that Natalizumab blocked Treg transmigration *in vitro* as well as non-Tregs despite both decreased binding of the antibody and expression of  $\alpha$ 4 integrin. Furthermore, Treg frequency in the blood was not altered after treatment nor was functionality restored in MS patients<sup>110</sup>, indicating that perhaps anti- $\alpha$ 4 integrin might affect Tregs differently than other lymphocytes. Conditional knockout mice in which  $\alpha$ 4 integrin is selectively deleted in Tregs while maintaining expression in all other cells types provide a more targeted and “cleaner” experimental tool with which to probe the question of VLA-4 function in Tregs. In fact, in experiments using this model,  $\alpha$ 4 integrin was found to be dispensable for *in vivo* migration of Tregs across the blood brain barrier (BBB) and Tregs instead could use  $\alpha$ L integrin to access the CNS<sup>111</sup>.

As previously mentioned,  $\beta$ 1 integrin is the most promiscuous of the  $\beta$  chains<sup>102</sup>. This promiscuity is likely an indication of gene duplication events resulting in novel  $\alpha$ -integrin binding partnerships. Furthermore, gene duplication events have been implicated as evolutionary drivers<sup>112</sup> of protein moonlighting<sup>113</sup>, in which a protein may serve alternate functions while

retaining its original “purpose”. Given the redundancy of VLA-4 for Treg BBB transmigration this poses the question: does it have an alternate function in Tregs?

### 3.2 AIM 2: WHAT IS THE FUNCTION OF B1 INTEGRIN EXPRESSION IN TREGS?

#### 3.2.1 *Tregs differentially express integrin $\beta 1$ at steady state.*

Glatigny *et al* showed that Treg expression of  $\alpha 4$  integrin is dispensable for migration into the CNS during inflammation<sup>111</sup>. Furthermore this work also showed that selective deletion of  $\alpha 4$  integrin on Tregs did not alter their function, proliferative ability or development at steady state<sup>69</sup>. Therefore, we investigated the role of the second component of VLA-4,  $\beta 1$  integrin, in Tregs to determine if this finding held regardless of the VLA-4 associated integrin analyzed. Upon flow cytometric analysis of  $\beta 1$  integrin distribution on CD4+FoxP3+ T cells, we found that a subset of WT Tregs consistently and constitutively expressed  $\beta 1$  integrin in the spleen at steady state (Figure 16A). Upon closer inspection, we noticed that the 30% frequency of  $\beta 1+$  Tregs was similar to the splenic ratio of the recently described effector Treg (eTregs) subtype<sup>70</sup>. When we applied the eTreg/cTreg (central Tregs) parameters CD44hiCD62L-/low and CD44low/CD62Lhi/+ respectively, to the  $\beta 1$ integrin expressing Tregs we found significant overlap between the eTreg subset and  $\beta 1+$  Tregs (Figure 16B). Although  $\beta 1-$  Tregs have greater representation within the cTreg gate, its exclusivity within that compartment is less obvious. These data suggest that  $\beta 1+$  integrin expression may be a correlate of activation or a surrogate marker for eTregs at steady state.

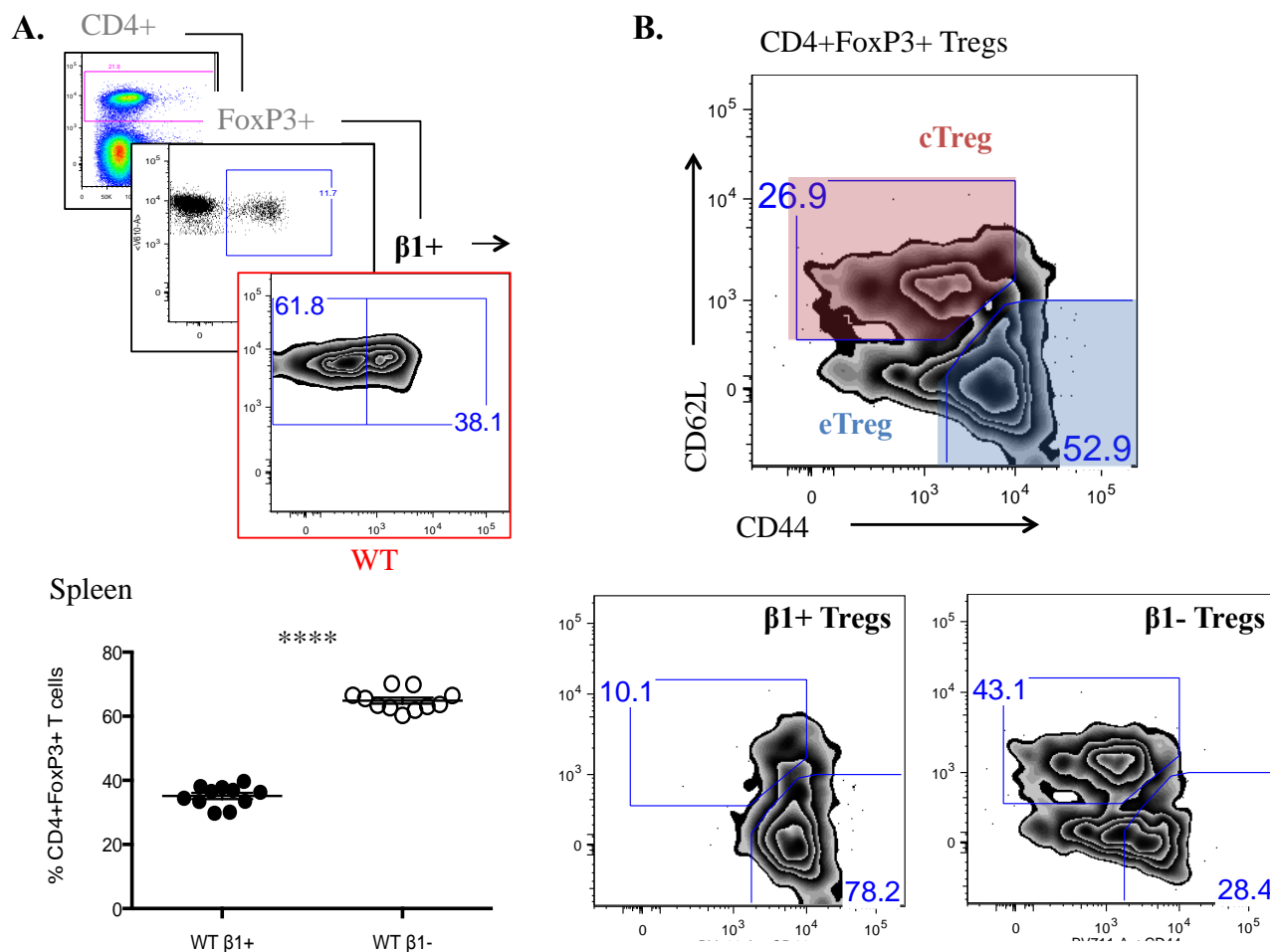


Figure 16.  $\beta 1$  integrin is constitutively expressed in a subset of Tregs that correlates with effector Treg description.

### 3.2.2

#### *Integrin $\beta 1$ expression correlates with effector Treg phenotype.*

Given our finding of a correlation between eTreg and  $\beta 1$  integrin-expressing Tregs, we next assessed whether  $\beta 1+$  Tregs share the distinctively activated phenotype characteristic of eTregs<sup>71</sup>. Indeed, when Tregs were subdivided by  $\beta 1$  integrin expression we found that  $\beta 1+$  Tregs expressed significantly higher levels of activation markers including the previously described CD44 and decreased expression of Ly6C (Figure 17). Down regulation or loss of Ly6C expression has been associated with initial activation in CD8+ T cells with re-expression in

memory, facilitating homing to lymphoid tissues<sup>72</sup>. The function of Ly6C expression in CD4+ T cells has yet to be definitively characterized however data suggests that loss of Ly6C expression also correlates with a memory phenotype at least in the context of a chronic CD4+ T cell-dependent parasite infection<sup>73</sup>. In Tregs, the function of Ly6C is even more nuanced as Ly6C- subsets have been shown to have greater suppressive capacity than their Ly6C+ counterparts as well as a greater propensity to bind to self-antigen<sup>74</sup>.

In line with the reported effect of decreased Ly6C expression, we found that  $\beta 1+$  Tregs correlated with increased expression of both suppressive molecules and migration-associated proteins including the chemokine receptors CXCR3<sup>114</sup> and CCR5 (Figure 17). This activated profile both overlaps with that of eTregs and suggests that  $\beta 1+$  Tregs may represent a subset of Tregs that is highly mobile and poised to act.

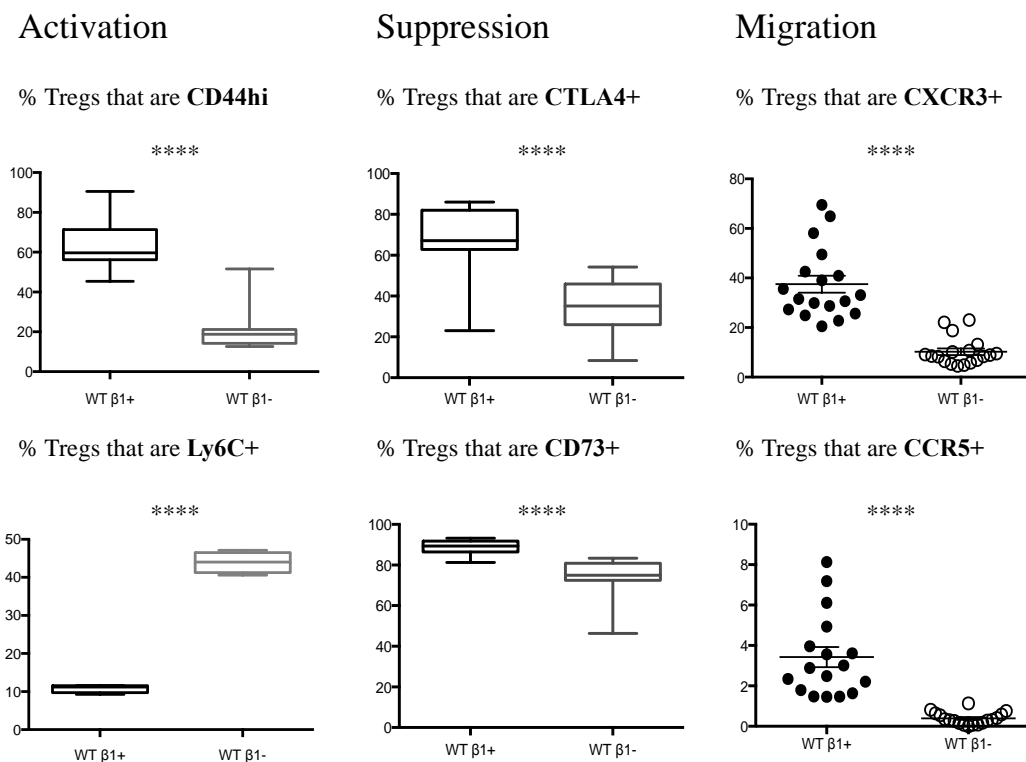


Figure 17.  $\beta 1+$  Tregs express higher levels of proteins associated with suppression, activation and migration.

## 3.2.3

*Treg specific deletion of integrin  $\beta 1$  leads to increased frequency and enhancement of effector Treg population.*

To determine whether  $\beta 1$  integrin expression is merely a correlative marker of eTregs or instead has a functional consequence, we utilized an ITGb1 conditional knockout (CKO) mouse model. These mice contain the ITGb1 gene flanked by LoxP sites and have been crossed to mice expressing Cre recombinase under the control of the FoxP3 promoter to generate Itgb1Flox/Flox x FoxP3eYFP-Cre-ERT2 mice that exclusively lack  $\beta 1$  integrin expression on their Tregs (Figure 18).

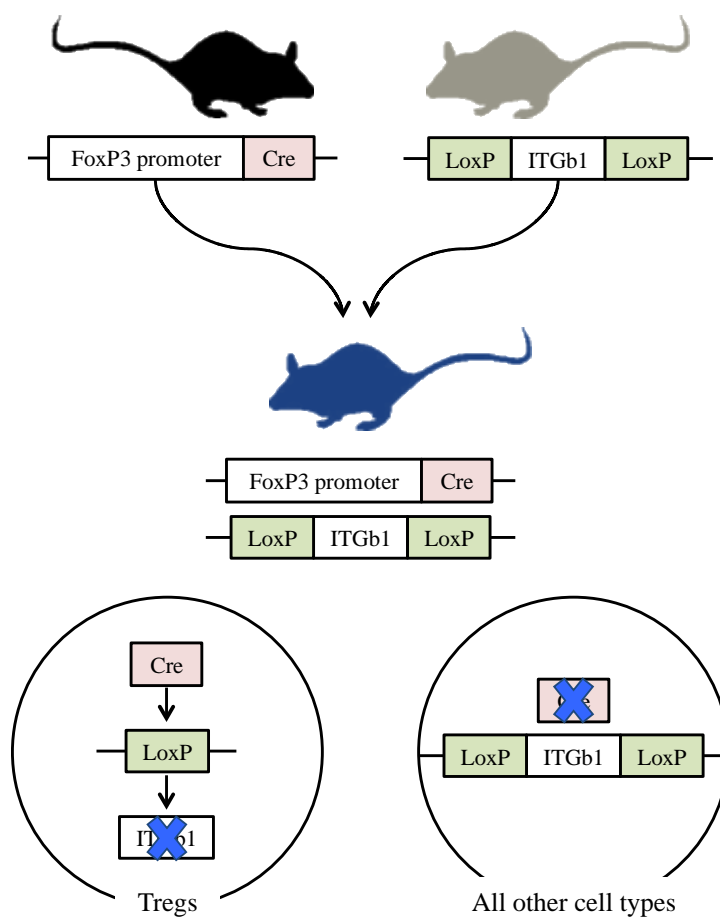


Figure 18. Schematic of ITGb1 conditional knockout. Recreated and adapted from Harno, E. et al. *Cell Metab.* 18, 21–28 (2013)<sup>76</sup>.

We found that in CKO-derived Tregs, as compared to WT controls, the expression of  $\beta 1$  integrin was almost completely abrogated with only a small, but consistent fraction of  $\beta 1^+$  Tregs remaining (Figure 19A). This remaining  $\beta 1^+$  Treg population may be a reflection of Cre recombinase inefficiency or potentially transcription of the excised LoxP flanked ITG $\beta 1$  episome<sup>77</sup>.

When the Treg frequency in CKO mice was assessed we found that the proportion of CD4<sup>+</sup>FoxP3<sup>+</sup> cells in the spleen was comparable to WT controls. However, the frequency of eTregs (CD44<sup>hi</sup>CD62L<sup>low</sup>) was markedly increased in mice lacking  $\beta 1$  integrin specifically in Tregs in addition to a concomitant decrease in the cTreg fraction (CD44<sup>low</sup>CD62L<sup>hi</sup>) (Figure 19B). Together these data suggest that  $\beta 1$  integrin may play some role in the function and development of activated-phenotype Tregs at steady state.

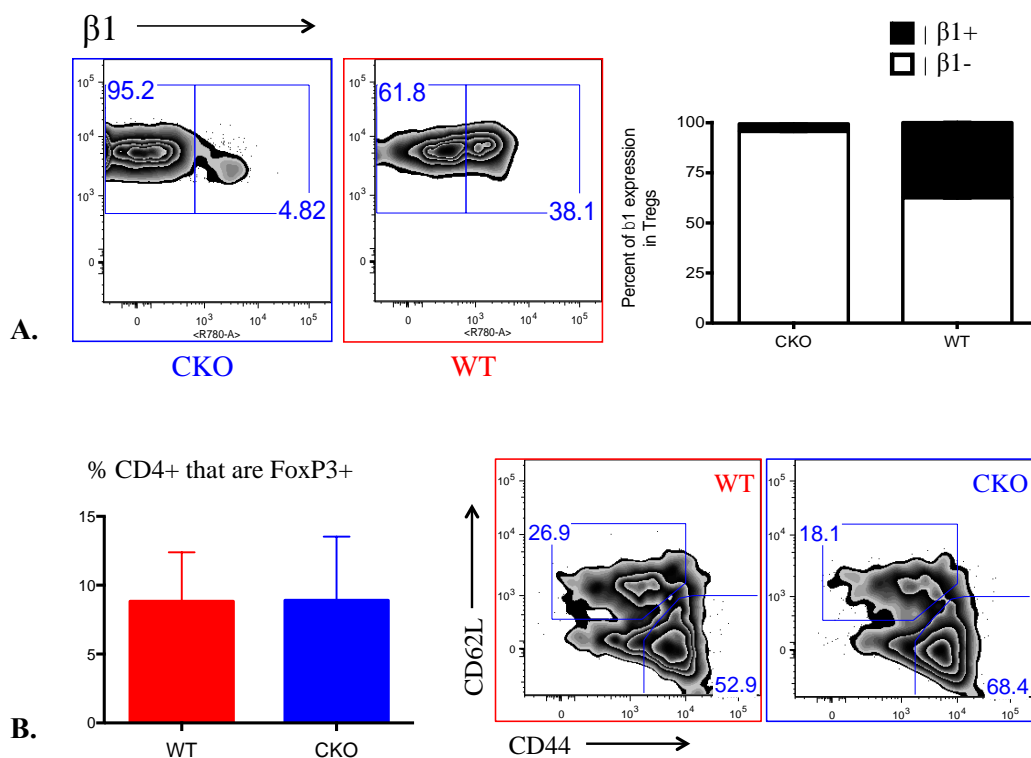


Figure 19. Deletion of ITG $\beta 1$  leads to increased frequency and enhancement of eTreg population.

As such, we next assessed the activation and suppression profile of CKO Tregs to determine if the increased frequency of eTregs in this model was also potentially indicative of altered function. Through antibody staining we found that both the frequency and the per-cell expression of key activation and suppression molecules were altered in  $\beta 1$  integrin CKO Tregs. However, the alteration was not a blanket up regulation of all the proteins investigated but rather included a seemingly paradoxical increase in CTLA4 and a statistically significant decrease in the adenosine modifier CD73. In conjunction with CD39, CD73 serves as a critical suppressive mechanism used to shape the pro-inflammatory purinergic cloud that forms around activated effector cells<sup>78</sup>. Formation of adenosine products via CD73 has also been shown to lead to the generation of peripheral Tregs by abrogating effector cell production of IL-6 and promoting TGF $\beta$  secretion, a cytokine known to enhance FoxP3 expression<sup>79</sup>. The discordance in increased CTLA4 expression and decreased CD73 expression is notably different than the overtly suppressive phenotype attributed to classically described eTregs<sup>80,81</sup> (Figure 20). Furthermore, we noted even higher levels of CD44 expression and a near elimination of Ly6C<sup>+</sup> Tregs in the CKO mice as compared to WT. As previously described, CD44 is associated with activation as is loss or down regulation of Ly6C surface expression<sup>82</sup>. Together these data suggest that the FoxP3-directed elimination of  $\beta 1$  integrin results in the generation of a Treg population that is activated at steady state but functionally differs from eTregs.

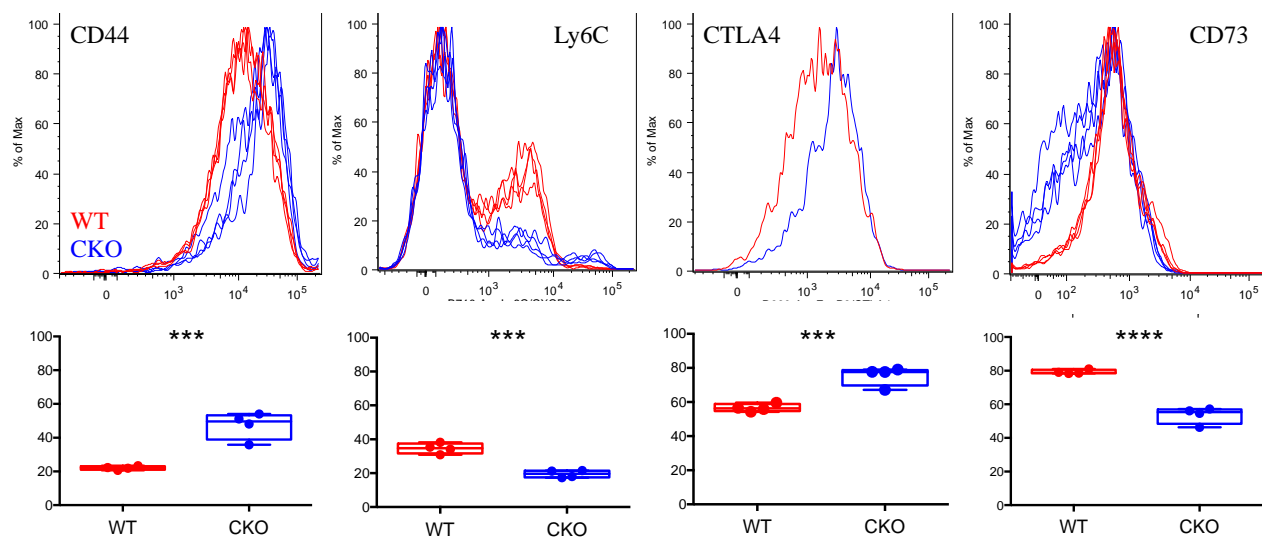


Figure 20. Activated phenotype in  $\beta 1$  integrin CKO Tregs surpasses that of WT controls.

To further characterize the phenotypic changes in CKO Tregs we analyzed other markers associated with activation including CXCR3 and two proteins recently correlated with terminally differentiated Tregs, CD103 and KLRG1<sup>83,84</sup>. We found that all three markers were expressed at significantly higher levels in CKO Tregs as compared to WT (Figure 21). Together, both the altered activation profile and increased expression of differentiation markers indicate that  $\beta 1$  integrin may regulate some aspect of Treg development. Although initial similarities with an eTreg phenotype suggests that deletion of  $\beta 1$  integrin would lead to fewer activated Tregs, unexpectedly the opposite was found. As such, we hypothesized that  $\beta 1$  integrin expression on Tregs may be integral in circumscribing Treg migration or restraining their activation.

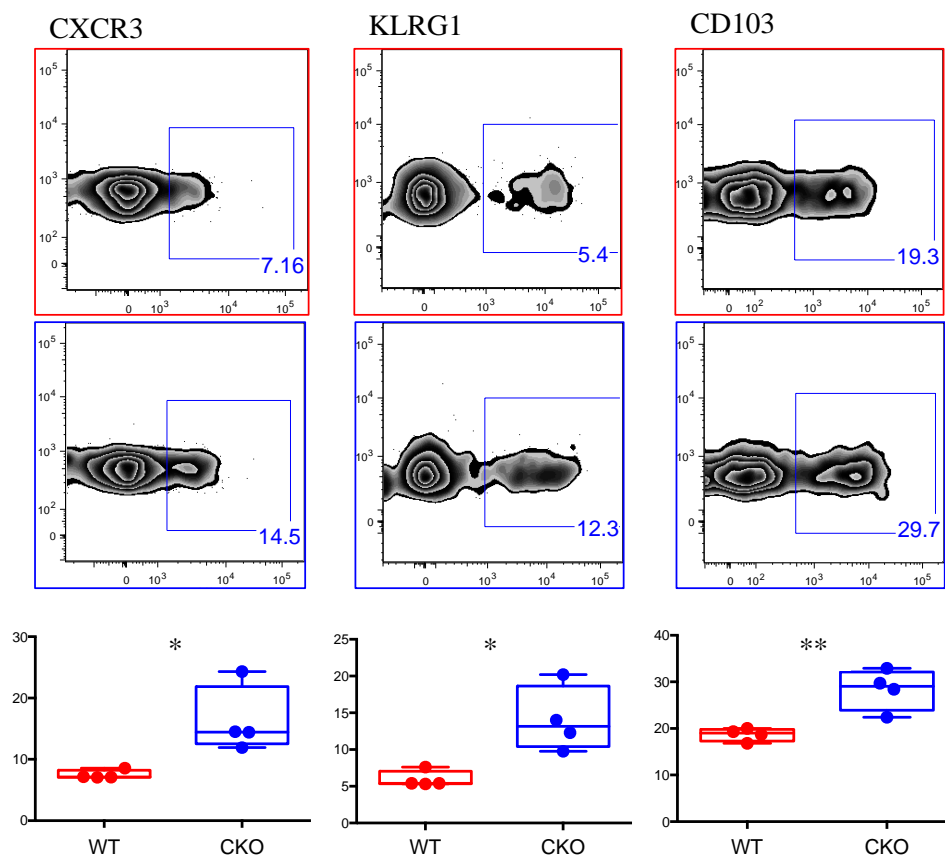


Figure 21. CKO Tregs express higher levels of CXCR3, CD103 and KLRG1 – markers of terminal differentiation.

### 3.2.4

*Treg-specific integrin  $\beta 1$  deletion leads to upregulation of integrin  $\beta 7$  and increased frequency of Tregs in gut-associated lymphoid tissues.*

As previously described,  $\beta 1$  integrin can bind to many different  $\alpha$  integrins, yet  $\alpha 4$  integrin is only known to bind to two different  $\beta$  chains,  $\beta 1$  integrin and  $\beta 7$  integrin<sup>102</sup>. Furthermore, although very few studies have interrogated  $\beta 1$  integrin function in Tregs specifically, DeNucci *et al* utilized ITGb1 CKOs driven by CD4-Cre, thus allowing them to focus on the effects of  $\beta 1$  integrin deletion on CD4<sup>+</sup> T cells. They found that pathogen-specific  $\beta 1$  integrin-null CD4 T cells lost the ability to remain in the bone marrow post-infection<sup>115</sup> and that  $\beta 1$  integrin expression regulated the expression of  $\beta 7$  integrin, although the reverse was not true<sup>116</sup>. As such,

we analyzed the  $\beta 7$  integrin expression on our CKO Tregs and found that, in agreement with the CD4-specific  $\beta 1$  integrin CKOs, it was significantly increased as compared to WT controls (Figure 22).

$\alpha 4\beta 7$  expression has been shown to induce gut-homing in lymphocytes<sup>117</sup>. Extensive loss-of-expression studies of  $\alpha 4\beta 7$ 's gut migratory function have spawned two monoclonal blocking antibodies for treatment of colitis, Etrolizumab<sup>118</sup> and Vedolizumab<sup>119</sup>. Given this homing function and the consequent over-expression of  $\beta 7$  integrin, we analyzed the cellular composition of the gut draining mesenteric lymph nodes (mLNs). We found that although the total cell number in the mLNs was comparable between CKOs and WT mice, the Treg fraction was much larger in the CKOs indicating that  $\beta 1$  integrin deficient Tregs were preferentially trafficking to the mLN (Figure 22).

Additionally, we quantified antigen presenting cell types that are known to reside in the mLN, in particular CD11c+CD11b+ DCs. Although DC frequency was similar between WT and CKOs, the per-cell expression levels of the co-stimulatory molecules CD80 and CD86 were elevated in ITGb1 CKOs (Figure 22). This finding suggests that CKO derived DCs in the mLN may be more activated, which was especially surprising given the increased expression of CTLA-4 in CKO Tregs. One of the proposed mechanisms of CTLA-4 function is the trans-endocytosis of CD80 and CD86 off of the surface of DCs, hampering the ability of DCs to effectively activate effector cells<sup>27</sup>. The increased CD80/CD86 expression we measured in mLN DCs, despite the increased CTLA-4 expression and increased Treg frequency in ITGb1 CKO mice may be an indication that  $\beta 1$  integrin deletion in Tregs impairs their ability to suppress incidentally activated DCs *in vivo* through non-CTLA-4-mediated mechanisms.

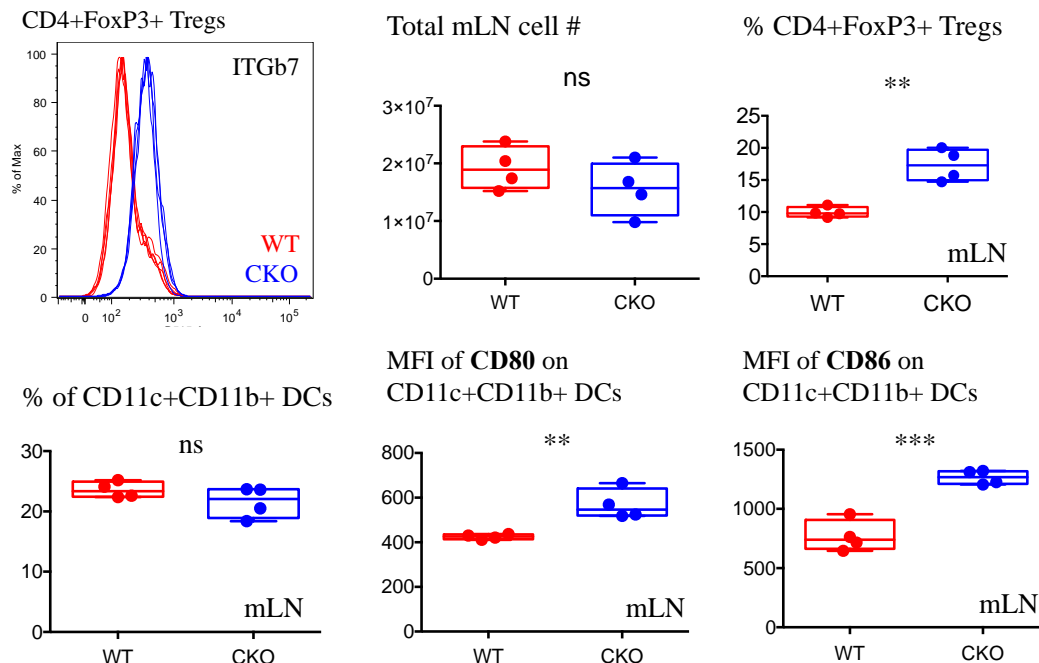


Figure 22. Deletion of ITG $\beta$ 1 leads to increased trafficking of Tregs to gut associated lymphoid organs

### 3.2.5 *CD8<sup>+</sup> T cells in integrin $\beta$ 1 CKOs have dysregulated expression of activation and migration markers*

Next we chose to investigate the impact, if any, Treg-specific  $\beta$ 1 integrin deletion may have on CD8<sup>+</sup> T cells. For example, Tregs have been shown to both directly<sup>120</sup> and indirectly (through effects on DCs) suppress CD8<sup>+</sup> T cell activity<sup>88</sup>. The nuances of Treg:DC:CD8<sup>+</sup> T cell interactions can influence even the avidity of a developing CD8<sup>+</sup> T cell response through a nuanced Treg mediated-regulation of chemokine production<sup>51</sup> and access to DCs<sup>121</sup>. As previously discussed (Chapter 2), the interactions of Tregs and CD8<sup>+</sup> T cells are not limited to maintaining homeostasis and indeed our lab has shown that Tregs can impact the formation of CD8<sup>+</sup> T cell memory during West Nile Virus<sup>68</sup> as well as the priming of other effector cell types during HSV-2 infection<sup>48</sup>.

As such, we first analyzed the expression pattern of the activation marker CD44 on CD8<sup>+</sup> T cells in CKO and WT naïve mice. Traditionally, flow cytometric staining of CD8<sup>+</sup> T cells in naïve mice reveals a small frequency of CD44<sup>hi</sup> cells in conjunction with a “smeared”-like pattern of expression representing CD44<sup>int</sup> and CD44<sup>low</sup> cells. We found that in our WT naïve mice, as expected, there are proportionally many fewer CD44<sup>hi</sup> CD8<sup>+</sup> T cells as compared to those cells with lower expression levels (Figure 23, Two representative mice are shown and CD44<sup>hi</sup> population is circled in red). This differential expression pattern presumably reflects the lack of foreign antigen exposure in naïve WT mice, which are housed in specific-pathogen free (SPF) conditions. Conversely in more antigen-experienced mice, such as the recently described “dirty mice” that are exposed to a long list of non-SPF pathogens in a short period, the CD44<sup>hi</sup> population is greatly enlarged and remains stable for the life of the mouse<sup>122</sup>. Unexpectedly we found that CD8<sup>+</sup> T cells from the  $\beta$ 1 integrin CKO mice had a dramatic expansion of the CD44<sup>hi</sup> compartment. Furthermore, rather than the smeared or transitional appearance of CD44<sup>int</sup>/low expression in WT mice, CKO mice had a more binary expression of CD44, with the most notable difference in the CD44<sup>int</sup> proportion (Figure 23, circled in blue and further illustrated in CD44 histogram and quantified in the associated plot).

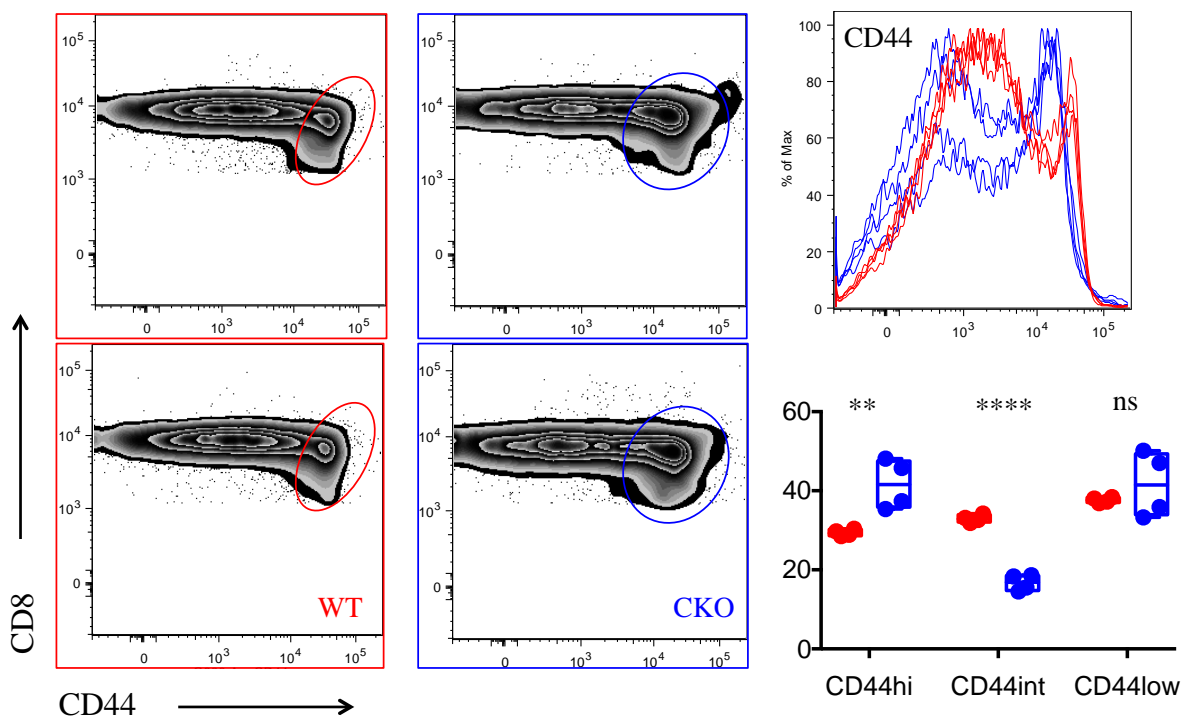


Figure 23. Treg specific ITGb1 deletion leads to increased CD44 expression in CD8+ T cells at steady state.

Given the surprisingly enhanced CD44<sup>hi</sup> expression in  $\beta$ 1 integrin CKO-derived CD8+ T cells, we investigated other canonical activation-associated markers to determine the extent of the phenotypic differences elicited by development in this environment. We found that in contrast to the decreased Ly6C expression in CKO Tregs (Figure 20), Ly6C expression in CD8+ T cells in these mice is significantly increased. This is likely a reflection of the different roles that Ly6C plays in each of these cell types. As previously described, down regulation of Ly6C is associated with increased suppressive capacity in Tregs<sup>123</sup>, and conversely up regulation of Ly6C is correlated with increased CD44 expression<sup>124</sup> and memory formation in CD8+ T cells<sup>125</sup>. It remains to be determined whether as in Tregs, Ly6C<sup>-/low</sup> cells are enriched for self-reactivity as compared to Ly6C<sup>+/hi</sup> cells. Given that the overwhelming majority of CD8+ T cells in a naive WT mouse are Ly6C low, a self-reactive profile in these cells is unlikely. In addition to increased

Ly6C expression, CD8<sup>+</sup> T cells in naive CKOs also displayed increased CXCR3 expression (Figure 24). This activated profile was found in the spleen and mesenteric LNs.

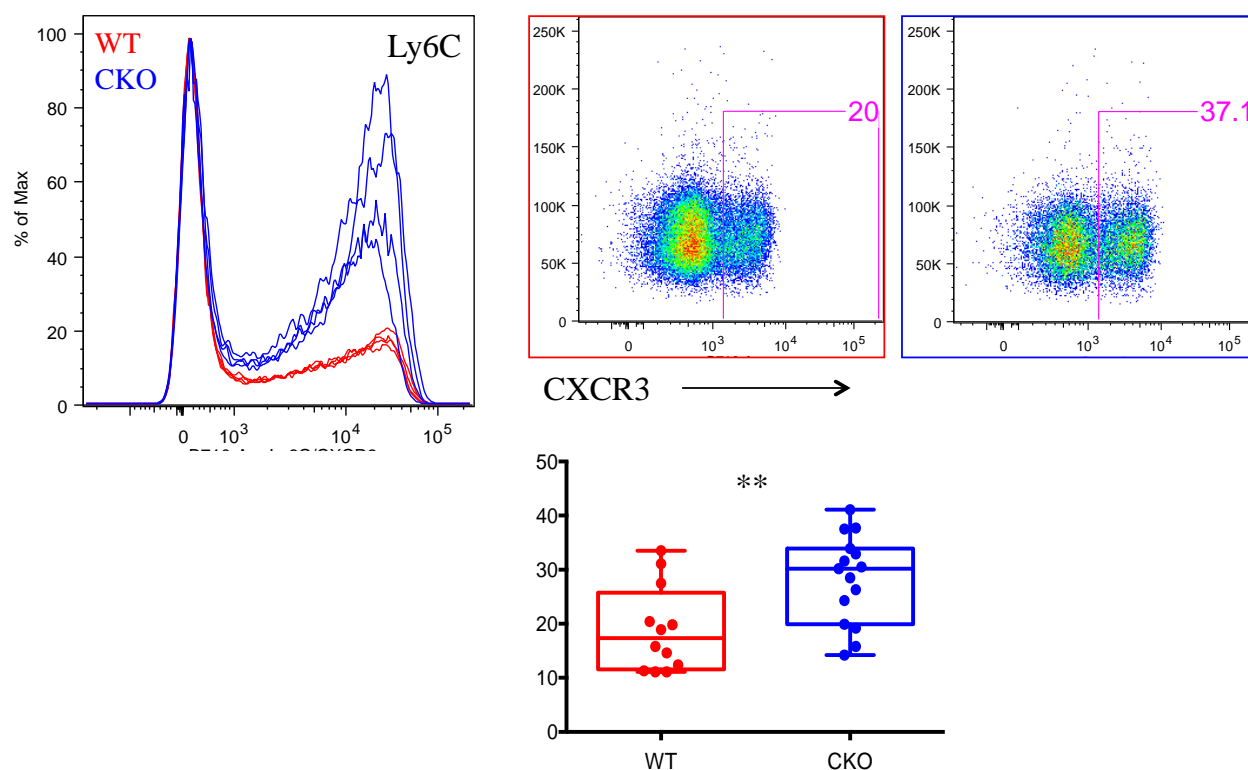


Figure 24. CKO derived CD8<sup>+</sup> T cells have an activated and mobile profile as compared to WT controls.

Because the activated phenotype of naive  $\beta 1$  integrin CKO derived CD8<sup>+</sup> T cells was intriguing, we decided to further probe the system by overlaying an infection model known to require both optimal Treg and CD8<sup>+</sup> T cell functions for an effective protective response, WNV<sup>68</sup>. Thus, we infected CKOs and age matched WT controls with 1000 PFU WNV-Tx subcutaneously to mimic the natural route of infection and monitored mice for weight loss and survival. Although the CKO-derived Treg and CD8<sup>+</sup> T cell activation profiles significantly differ from that of WT controls, survival rates were comparable between both groups (Figure 25A). Both groups were also able to generate similar frequencies of WNV-specific CD8<sup>+</sup> T cells as measured through binding to an NS4b (the immunodominant WNV peptide<sup>126</sup>) tetramer (Figure

25B). In addition, contraction of antigen-specific CD8<sup>+</sup> T cells appeared to occur at similar rates as shown by analysis at day 21-post infection (Figure 25B). Interestingly, when we delved further into the WNV-specific CD8<sup>+</sup> T cell populations of CKOs vs. WT mice we found that the proportion of short-lived effector cells (SLECs) was dramatically enlarged, seemingly at the cost of the memory precursor (MPECs)<sup>127</sup> population (Figure 25C). This finding mirrors the skewed SLEC/MPEC ratio found after WNV infection in Treg-depleted mice<sup>68</sup>, suggesting that despite the sufficient Treg frequency, enhanced CTLA-4 expression and activated phenotype of  $\beta$ 1 integrin-null Tregs in CKO mice CD8<sup>+</sup> T cell memory development is still compromised.

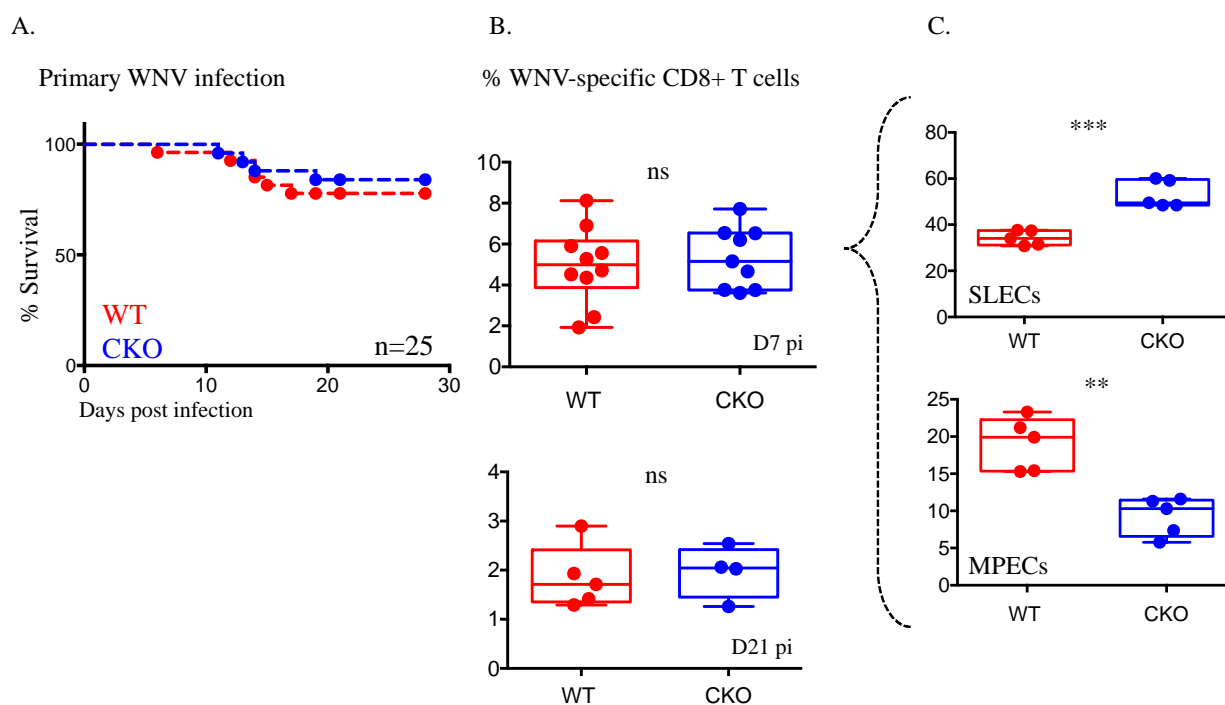


Figure 25. Mortality rates and frequency of WNV-specific CD8<sup>+</sup> T are comparable after infection but SLEC/MPEC ratios are skewed.

The increased SLEC proportion that arises in WNV-infected CKO mice suggests that the development of memory CD8<sup>+</sup> T cells may be hampered, yet the lack of increased mortality and morbidity suggests that despite this potential handicap, a protective primary response is sufficiently generated. One potential outcome of this abnormal enrichment of SLECs is a deficit

in recall ability such that the response to a primary infection initially appears adequate, but the developmental impairment reveals itself after a second exposure. This phenomenon has been particularly well characterized in instances of memory CD8<sup>+</sup> T cells development in the absence of CD4<sup>+</sup> T cell help. Using MHC II<sup>-/-</sup> mice, hence mice that lacked the ability to specifically prime CD4<sup>+</sup> T cells during infection, Sun and Bevan showed that these mice were able to generate comparable numbers of antigen-specific CD8<sup>+</sup> T cells and clear an introduced *Listeria monocytogenes* infection in the same timeframe as wild type controls<sup>128</sup>. However, upon re-challenge with *L. monocytogenes* at a memory time point, the antigen-specific CD8<sup>+</sup> T cell fraction failed to expand and subsequently the bacterial load was significantly higher in the KOs<sup>128</sup>. These data indicate that the original development of the pathogen-specific response was compromised due to a lack of CD4<sup>+</sup> T cell help, but the consequence of that hindered development was not obvious during a primary infection.

Given the described precedent and our finding of skewed SLEC/MPEC WNV-specific CD8<sup>+</sup> T cell ratios in CKOs after primary infection, we sought to assess the potential effects on the recall response. We first infected  $\beta$ 1 integrin CKOs and WT controls as above (1000 PFU WNV-Tx sub.cu.) and monitored these mice until a suitable memory time point (d50+ post-infection). Spleens and lymph nodes (including mLNs) were collected and bulk CD8<sup>+</sup> T cells isolated from either CKOs or WT mice. 3-5x10<sup>6</sup> isolated CD8<sup>+</sup> T cells from this preparation were then intravenously introduced to Ly5.1 congenically marked recipient mice. Recipient mice were subsequently infected with WNV (1000 PFU WNV-Tx) such that the WNV-specific subset of transferred CD8<sup>+</sup> T cells were exposed to WNV for a second time and endogenous recipient CD8<sup>+</sup> T cells would be exposed for the first time. Recipients were euthanized and spleens collected 8-9 days post infection and the CD8<sup>+</sup> T cell compartment (both donor and endogenous)

analyzed (Figure 26A). We found that the total frequency of CD8<sup>+</sup> T cells was comparable between those mice that had received cells from either CKOs or WT mice (Figure 26A). Unexpectedly, when we assessed the contribution of donor versus endogenous CD8<sup>+</sup> T cells within the compartment we found that despite receiving equal numbers of cells 9-10 days prior, the CKO-derived CD8<sup>+</sup> T cells expanded roughly 3-fold more than their WT counterparts (Figure 26B). Using an NS4b-specific tetramer, we then analyzed the contribution of WNV-specific (immundominant peptide only) CD8<sup>+</sup> T cells within the transferred population. We found that despite the significant expansion of the CKO-derived transferred memory CD8<sup>+</sup> T cells, the WNV-specific fraction was nearly 6X smaller as compared to that in WT recipients (Figure 26B).

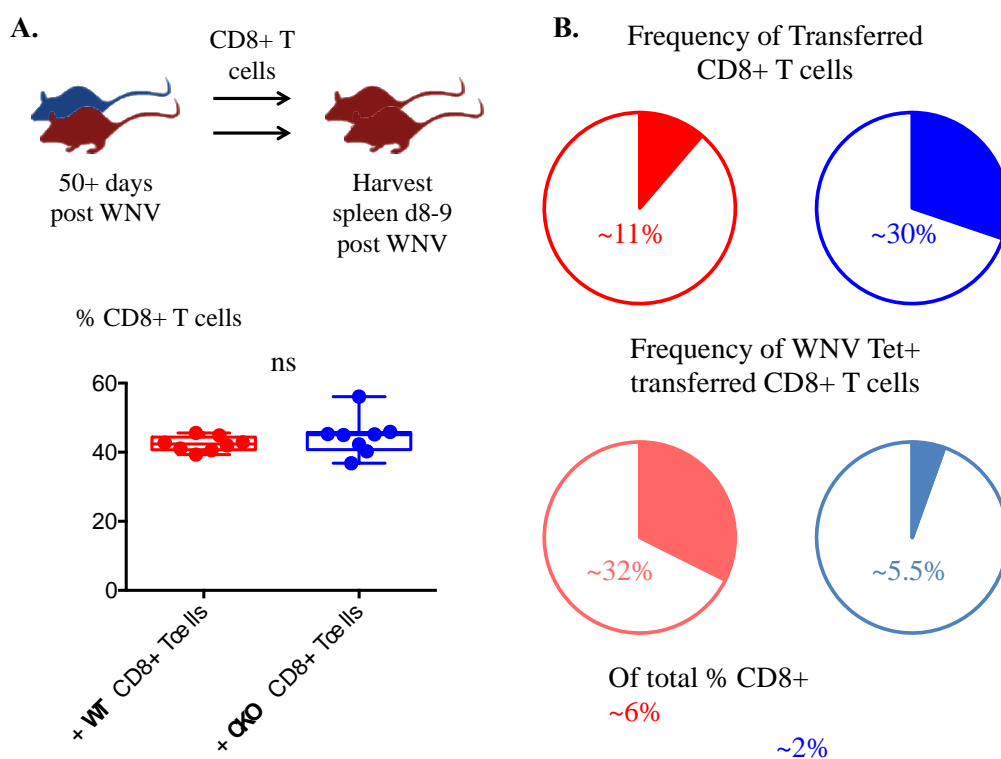


Figure 26. CD8<sup>+</sup> T cell memory recall is impaired after development in ITGb1 CKO environment.

Together these data suggest that  $\beta 1$  integrin deletion on Tregs has a profound effect not only on Treg function but also plays a role in DC activation as well as in the maintenance of CD8+ T cells at steady state and in their response to the introduction of a foreign peptide. To begin to parse out a potential mechanism that adequately addresses the varied and consequential effects of the loss of  $\beta 1$  integrin expression in Tregs we again reviewed the literature on  $\beta 1$  integrin function. Mittelbrunn *et al* analyzed the dynamics of VLA-4 binding within the immune synapse and found that, when analyzed independently, both T cell expressed  $\alpha 4$  and  $\beta 1$  migrated to the contact surface in a co-culture of T cells and APCs in the presence of a polyclonal stimulatory superantigen<sup>129</sup>. In addition they found that both  $\alpha 4$  and  $\beta 1$  integrin concentrated at the peripheral ring (known as the p-SMAC) that surrounds the TCR:MHC and CD3 central cluster within the immune synapse during T cell-APC interactions<sup>129</sup>. In combination with the phenotypic alterations in Tregs, DCs and CD8+ T cells catalogued in our data, these data introduce the possibility that  $\beta 1$  integrin may play an indirect role in the activation of effector cells via Treg interactions with APCs.

### 3.2.6 *Hypothesized Mechanism: $\beta 1$ integrin stabilizes TCR:MHC interactions between Tregs and DCs.*

The functional consequence of integrin clustering within a developing immune synapse has been well characterized for another integrin,  $\alpha L\beta 2$  also known as LFA-1 (lymphocyte function-associated antigen 1). LFA-1 is has been shown to cluster in the p-SMAC and was originally thought to enhance the contact between effector cells and APCs via its adhesive properties<sup>130</sup>, but further investigations found that LFA-1 plays a distinct and necessary role in productive TCR stimulation and cellular activation mediated by signaling through its  $\beta 2$  integrin cytoplasmic tail<sup>131</sup>. Furthermore, Onishi *et al* showed that LFA-1 expression on Tregs in particular mediates

their clustering around DCs in the spleen and that in conjunction with CTLA-4, LFA-1 mediated the down regulation of CD80/CD86 on splenic DCs<sup>132</sup>.

Given the similarities in the p-SMAC localization of  $\beta 1$  integrin and LFA-1, as well as the alterations in the activation state of Tregs, DCs and CD8<sup>+</sup> T cells described above in our  $\beta 1$  integrin CKO mouse model, we contend that  $\beta 1$  integrin expression on Tregs, perhaps within the context of VLA-4, aids in the stabilization of Treg/DC interactions. Given the observation of a CD8<sup>+</sup> T cell activated phenotype at steady state, we further propose that this supportive function ensures that antigen that is presented to CD8<sup>+</sup> T cells by DCs in the absence of inflammation does not result in aberrant activation of either cell type (Figure 27A). As such we propose that in the absence of  $\beta 1$  integrin, Treg suppression of activated DCs that are incidentally presenting self-antigen, is less productive and hence these DCs become refractory to Treg cell contact-dependent forms of regulation.

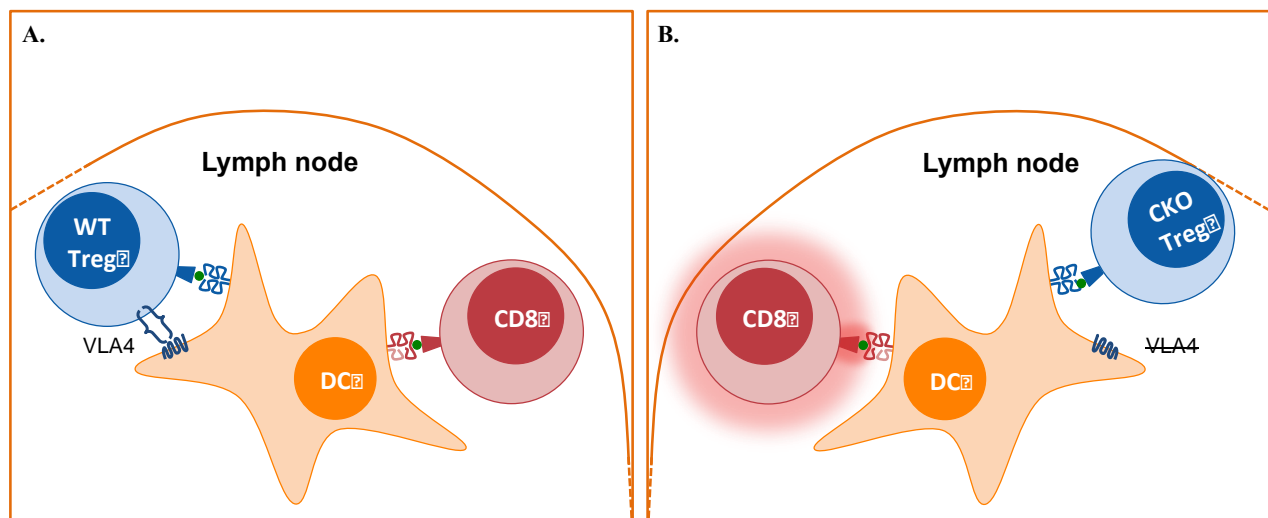


Figure 27. Unstable interactions between CKO Tregs and DCs could lead to enrichment of incidentally activated self-reactive CD8<sup>+</sup> T cells.

To this end, Thauland *et al* have shown that the levels of CD80/CD86 expressed on the DC surface can alter Treg motility, wherein higher costimulatory molecule concentrations leads to

reduced Treg motility<sup>133</sup>. Given the elevated expression of CD80/CD86 by DCs in our CKOs, a feedback cycle of Treg sequestration in LNs (as we found in mLNs [Figure 22]) could be a potential consequence of our proposed mechanism. In addition, self-cross reactive CD8+ T cells (perhaps those that escaped the rigors of thymic selection) could potentially interact with these activated DCs, leading to up regulation of CD44 as well as the other characteristic signs of activation that we have noted (Figure 27B). Although the  $\beta 1$  integrin CKO model does not display any overt signs of autoimmune disease that might be associated with an accumulation of self-reactive CD8+ T cells, the expansion of transferred CKO-derived CD8+ T cells (Figure 26B) that are not pathogen-specific in the context of inflammation may be an indicative of this population. As such, there may be an enrichment of self-reactive CD8+ T cells that remain quiescent in the absence of inflammatory cues and in conjunction with the presence of the phenotypically hyper-active CKO Tregs, only becoming fully active after transfer when in the inflammatory setting of an infection. Given this hypothesis we next sought to investigate the potential self-reactive activity, if any, of  $\beta 1$  integrin CKO derived CD8+ T cells.

### 3.2.7 *CD44<sup>hi</sup> CD8+ T cells from integrin $\beta 1$ CKOs are unlikely to be self-reactive.*

The decreased frequency of WNV-specific CD8+ T cells within the expanded transferred CKO derived population (Figure 26B) may be due to aberrant priming to self-antigens and enrichment of self-reactive CD8+ T cells in the CKO environment. To test the hypothesis that CKO derived CD8+ T cells may have a TCR repertoire more attuned to self-recognition, we first analyzed the CD5 expression levels within the CD8+ T cell compartment of CKOs vs. WT mice. CD5 is first expressed in lymphocytes as they undergo selection in the thymus and is correlated with increased TCR sensitivity to self-antigen<sup>134, 135</sup>. After flow cytometric comparison of CD5

expression on CKO derived or WT CD8<sup>+</sup> T cells, we found similar expression levels, both in frequency and on a per-cell basis between groups (Figure 28). CD5 expression levels remained comparable even after analyzing the CD44<sup>hi</sup> CD8<sup>+</sup> T cell subset as well (data not shown).

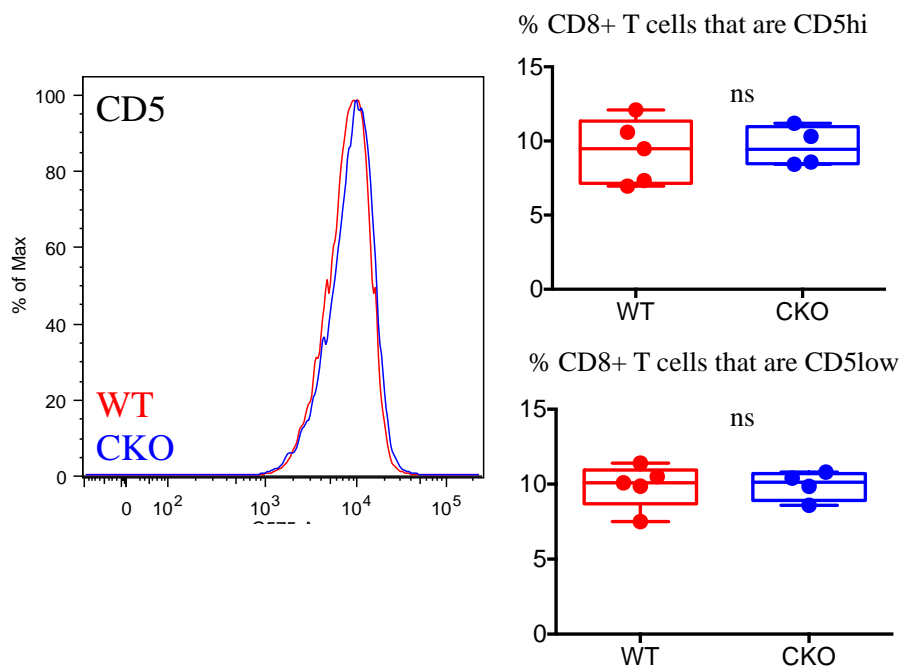


Figure 28. CKO derived CD8<sup>+</sup> T cells express comparable levels of CD5 as WT controls.

Although we did not find a difference in CD5 expression between CD8<sup>+</sup> T cells from CKO vs. WT mice, we recognize that CD5 expression differences can be very subtle and it is possible that we were simply unable to properly distinguish nuances between groups. As such, we next utilized an induced lymphopenic mouse model to help elucidate any potential self-antigen preference in CKO derived CD8<sup>+</sup> T cells.

Briefly, recipient mice were sub-lethally irradiated (900 rads) to eliminate hematopoietic cells and their progenitors, thereby creating a lymphopenic environment that would both encourage proliferation of transferred T cells but also create pro-inflammatory conditions in the presence of released self-antigens from dead/dying cells<sup>136</sup>. Twenty four hours later, recipient mice were intravenously infused with a 50/50 mixture of congenically and proliferation dye

labeled WT and CKO derived CD8<sup>+</sup> T cells from naïve mice (Figure 29). We hypothesized that if CKO derived CD8<sup>+</sup> T cells were enriched for self-reactive clones, then exposing these cells to a lymphopenic environment with an abundance of self-antigens present would lead to a proliferative advantage over their WT counterparts. Splensens were collected at day 3 post cell transfer and proliferation dye dilution quantified. We found that both WT and CKO derived CD8<sup>+</sup> T cells underwent at least 4 divisions as measured by the number of calculated generations (Figure 29). Although there was no difference between groups in number of divisions, the cell number within each generation was significantly different with fewer CKO derived CD8<sup>+</sup> T cells represented in the most divided group (generation 4) and the most cells represented in the undivided and single division groups, generation 0 and 1 respectively. Rather than a proliferative advantage, these results may indicate that CKO derived CD8<sup>+</sup> T cells have a proliferative disadvantage in this setting or perhaps a metabolic deficiency.

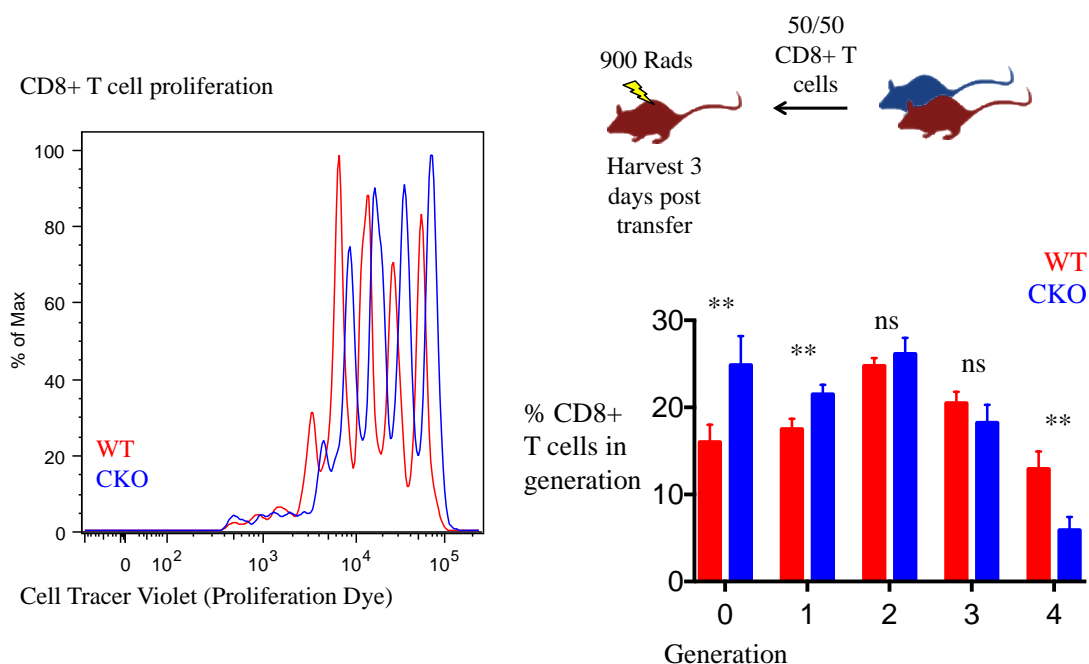


Figure 29. Proliferation of CKO derived CD8<sup>+</sup> T cells is comparable to WT in lymphopenic conditions.

Finally, we also hypothesized that if CKO-derived CD8<sup>+</sup> T cells were enriched for self-reactivity, then exposure to inflammation, serving as signal 2<sup>137</sup>, (in this case during WNV infection) might lead to full activation of these cells and the potential formation of self-reactive memory CD8<sup>+</sup> T cells. As such, in an environment depleted of the suppressive regulation of Tregs, these CD8<sup>+</sup> T cells would be expected to accelerate the development of autoimmunity earlier and more aggressively than Treg depletion alone. To test this hypothesis we again intravenously transferred 3-5x10<sup>6</sup> CKO-derived bulk CD8<sup>+</sup> T cells from previously WNV-infected mice (50+ days post infection) mice into FoxP3-DTR mice that received 2 injections of diphtheria one day apart to deplete endogenous Tregs (Figure 30A). Fontenot *et al* and others have shown that in the absence of Tregs, wasting disease and colitis develop with noticeable weight loss beginning 5-10 days after either depletion of Tregs<sup>138</sup> or introduction of effector T cells to RAG<sup>-/-</sup> mice in the absence of Tregs<sup>4</sup>. As such, weight loss was monitored for 14 days post transfer and mice euthanized shortly after to minimize potential suffering from the effects of Treg depletion. We found that despite the addition of memory time point CKO-derived CD8<sup>+</sup> T cells, recipient mice did not show signs of accelerated or exacerbated weight loss as compared to FoxP3-DTR mice that received DT alone (Figure 30B). Initially it appeared that CKO-derived CD8<sup>+</sup> T cell recipients were losing weight more quickly than DT alone controls, but this trend quickly dissipated and weight loss stabilized between groups (Figure 30B). This initial weight loss could be an indication that the donor T cells were indeed self-reactive, and that perhaps a higher dose of DT or a longer injection schedule would have revealed increased and consistent weight loss. However, in conjunction with the lack of increased CD5 expression in CKO-derived CD8<sup>+</sup> T cells (Figure 28) and the failure of these cells to outcompete WT controls in a

lymphopenic setting (Figure 29), it is unlikely that CD8<sup>+</sup> T cells generated in  $\beta$ 1 integrin Treg CKO mice are productively self-reactive.

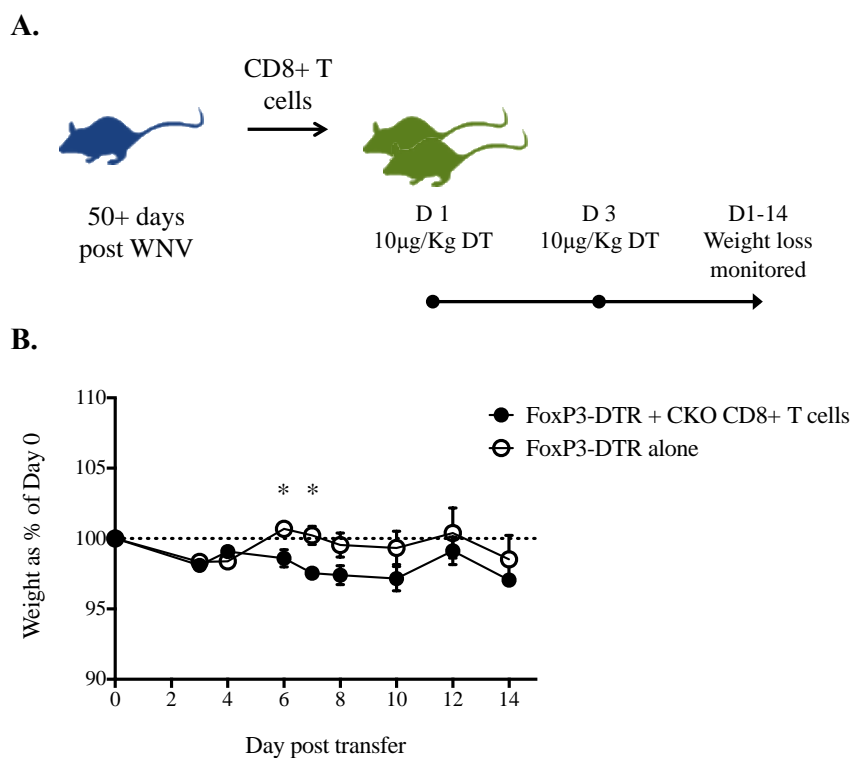


Figure 30. Weight loss after Treg depletion is not accelerated or exacerbated, despite the addition of CKO-derived CD8<sup>+</sup> T cells.

### 3.2.8

#### *Discussion*

VLA-4 is a well-characterized integrin with putative trans-migratory function when expressed by a variety of leukocytes. However, recent work has shown that it is dispensable for access of the CNS by at least two T cell subsets, T<sub>H</sub>17 cells<sup>139</sup> and Tregs<sup>111</sup>. In addition, most investigations of VLA-4 function have focused on  $\alpha$ 4 integrin through loss-of-function studies, however the contributions of the secondary component of VLA-4,  $\beta$ 1 integrin, especially as they pertain to Treg function remain unknown. As such we first characterized the expression profile of  $\beta$ 1<sup>+/-</sup> integrin Tregs and found that there was considerable overlap between  $\beta$ 1<sup>+</sup> Tregs and the

activated phenotype (Figure 17) of eTregs (Figure 16) at steady state. To determine whether  $\beta 1$  integrin expression carried a function consequence for Tregs or instead a surrogate marker for eTregs, we utilized a FoxP3 driven  $\beta 1$  conditional knockout mouse model (Figure 18). Characterization of Tregs in these mice revealed that Treg specific deletion of  $\beta 1$  led to an activation profile in these cells that surpassed that of eTregs (Figure 20 and Figure 21), including increased CD44, Ly6C and CTLA-4 expression but interestingly diverged from eTregs in decreased CD73 expression.

To further develop our understanding of the consequences of Treg specific  $\beta 1$  integrin deletion, we next assessed the expression of  $\beta 7$  integrin, an integrin that competes with  $\beta 1$  integrin to bind with  $\alpha 4$  integrin. Others have shown that CD4-specific deletion of  $\beta 1$  integrin led to concomitant increased expression of  $\beta 7$  integrin but that the reverse did not lead to increased  $\beta 1$  integrin expression, suggesting that  $\beta 1$  integrin serves a regulatory function for the gut-homing molecule  $\alpha 4\beta 7$ <sup>116</sup>. Using flow cytometry we found that CKO Tregs showed significant up regulation of  $\beta 7$  integrin and that it coincided with increased Treg frequency in the gut-draining mesenteric lymph nodes (Figure 22). Furthermore, dendritic cells associated with the mesenteric lymph nodes showed elevated expression of the co-stimulatory molecules CD80/CD86 suggesting a deficiency in Treg suppressive function in spite of increased levels of CTLA-4 (Figure 22). These alterations led us to investigate the potential effects of Treg-specific  $\beta 1$  integrin on other cell types, in particular CD8<sup>+</sup> T cells as Tregs have been shown to play a role in both modulating the effects of CD8<sup>+</sup> T cells<sup>120</sup> and in the development of memory after infection<sup>140</sup>. We found that similar to Tregs, CKO-derived CD8<sup>+</sup> T cells also had an activated profile as assessed through the expression of activation markers including CD44 and migration markers such as CXCR3 and CD103 (Figure 23 and Figure 24).

We then probed the ability of CKO-derived CD8<sup>+</sup> T cells to respond to WNV infection and develop a recall-able memory response.  $\beta$ 1 integrin CKO mice succumbed to primary WNV infection at the same rate as WT controls (Figure 25A) and the frequency of WNV-specific CD8 T cells were comparable at the peak of infection and at an early memory time point (Figure 25B), however the SLEC/MPEC ratio was heavily weighted towards short-lived effector cells indicating that despite being able to generate a sufficient quantity of the WNV-specific CD8<sup>+</sup> T cells, the quality of these cells might be compromised in the CKO (Figure 25C). To test this hypothesis, we transferred CD8<sup>+</sup> T cells from CKOs or WT controls at a memory time point post WNV infection into naive mice and infected recipients, thereby testing the recall ability of the donor CD8<sup>+</sup> T cells (Figure 26A). We assessed the expansion of the CD8<sup>+</sup> T cell compartment at d8 post-secondary infection as well as the contribution of the donor cells. We found that although the frequency of CD8<sup>+</sup> T cells was similar between WT and CKO-derived CD8<sup>+</sup> T cell recipients, the donor cells from CKO mice had expanded to a much greater degree (Figure 26B), however the proportion of WNV-specific cells was greatly diminished within the CKO-derived donor population (Figure 26B).

Together, the above findings led us to hypothesize that  $\beta$ 1 integrin may be playing a role in mediating the interactions between Tregs and DCs at steady state (Figure 27). Previous studies have shown that  $\beta$ 1 integrin concentrates at the periphery of the immune synapse during T cell:APC interactions<sup>129</sup> and given the function of other p-SMAC associated integrins<sup>131</sup> we further hypothesized that Tregs may be stabilizing the contact between these cells. We speculate that inadequate Treg suppression of incidentally activated DCs as a result of the instability caused by  $\beta$ 1 integrin deletion could lead to the enrichment of self-reactive CD8<sup>+</sup> T cells. To begin to test this hypothesis, we used three approaches; first we assessed CD5 expression<sup>135</sup>, a

surface protein associated with increased TCR affinity for self-antigens. We found that CD5 expression was comparable between CKO-derived and WT CD8<sup>+</sup> T cells (Figure 28). Secondly, we utilized a radiation-induced lymphopenia mouse model to test the proliferation capacity of CKO-derived CD8<sup>+</sup> T cells vs. WT in recipient mice and found that CKO-derived CD8<sup>+</sup> T cells did not have a competitive advantage over WT cells in this environment (Figure 29). Finally, to induce a recall response from self-reactive memory CD8<sup>+</sup> T cells that might have developed during the inflammatory setting of WNV infection and exacerbate or accelerate the development of autoimmunity, we transferred memory time point CKO-derived CD8<sup>+</sup> T cells into Treg deleted mice (Figure 30A). Despite the addition of CKO-derived CD8<sup>+</sup> T cells, recipient FoxP3-DTR mice did not show increased or early weight loss as compared to DT alone controls (Figure 30B). Together these three experiments indicate that although CD8<sup>+</sup> T cells in  $\beta$ 1 integrin CKO mice display elevated levels of activation and migration markers at steady state and appear to expand to a stimulus exclusive of the WNV-immunodominant peptide when transferred into newly infected WT mice (Figure 26B), CKO-derived CD8<sup>+</sup> T cells are unlikely to be enriched for self-reactivity. In conclusion, it is clear that Treg specific deletion of  $\beta$ 1 integrin leads to dramatic phenotypic changes in DCs, CD8<sup>+</sup> T cells and the Tregs themselves, elucidating functional consequence of these changes remains challenging. As such, further investigation of these populations in  $\beta$ 1 integrin CKO mice is warranted.

### 3.2.9

#### *Limitations and unanswered questions*

*In vivo* mouse models of cell-specific gene deletion provide a powerful tool to investigate the system wide function of a protein of interest. This reductive approach initially appears simple in that any effects can be attributed to the selected deletion, however upon closer inspection the true complexity of the model is revealed. In our model, the nearly complete deletion of  $\beta$ 1 integrin on

a single cell population, Tregs, results in a catalog of extensive expression changes in a variety of cells. As such, it is particularly important that the limitations and caveats of this model be thoroughly analyzed.

### 3.2.9.1 $\beta 1$ integrin expression and suppressive function

Through flow cytometric analyses of  $\beta 1$  integrin +/- Tregs we found that  $\beta 1^+$  Tregs made up roughly 1/3 of the Treg population at steady state and that this Treg subpopulation shared many phenotypic characteristics with eTregs (Figure 16). Upon deletion of  $\beta 1$  integrin expression in Tregs, the activated profile of these cells within the CKO mouse is enhanced (Figure 19 and Figure 20) however, the functional consequence of these phenotypic alterations remains to be determined. As such, we propose to test the ability of  $\beta 1^+$  and  $\beta 1^-$  integrin Tregs culled from WT mice at steady state to suppress CD8<sup>+</sup> T cells by sorting Tregs by  $\beta 1$  expression and then using classical *in vitro* and *in vivo* Treg suppression assays<sup>141</sup>. Given the activated profile of  $\beta 1^+$  Tregs, we expect these Tregs to be more effective suppressors of CD8<sup>+</sup> T cell proliferation (as measured via quantification of proliferation dye dilution) than their  $\beta 1^-$  Treg counterparts. Other distinguishing features including increased cellular turnover and a decreased dependence on IL-2 differentiate eTregs from other Treg subsets such as cTregs<sup>23</sup>. We intend to further examine the potential overlap of eTregs and  $\beta 1^+$  Tregs by comparing these features through Annexin-V and Ki67 staining and through the quantification of  $\beta 1^{\pm}$  Treg proliferation in response to IL-2 supplementation or blockade.

### 3.2.9.2 Effects of $\beta 7$ integrin overexpression

One of the lingering questions regarding the functional consequences of Treg specific  $\beta 1$  integrin deletion remains whether the effects on DCs and CD8<sup>+</sup> T cells detailed above are attributable to the deletion of  $\beta 1$  integrin or instead could be caused by the overexpression of  $\beta 7$

integrin that it elicits. In addition to retinoic acid-sensitive receptors such as the chemokine receptor CCR9<sup>142</sup> and colon-specific targeting receptors such as GPR15<sup>143</sup>, up-regulation of  $(\alpha4/\alphaE)\beta7$  can result from gut “imprinting” if a cell is activated by DCs in mesenteric LNs or Peyer’s patches (PP)<sup>144</sup>. Shimizu *et al*<sup>116</sup> and our data (Figure 22) indicate that  $\beta1$  integrin expression may be regulating the expression of  $\beta7$  integrin. Hence, deletion of  $\beta1$  integrin results in concomitant  $\beta7$  integrin expression, presumably independent of interactions of gut-associated DCs. One consequence of  $\beta7$  integrin overexpression in Tregs appears to be increased migration (or expansion) in the mLN (Figure 22) however disentangling what other effects these “pre-imprinted” Tregs may have is more complex. These potential effects are further complicated by the intricate and manifold interactions between leukocytes, the resident microbiota and dietary metabolites in the intestine.

Intestinal DCs are especially capable of producing the vitamin A metabolite, (all-trans) retinoic acid (RA) and in conjunction with  $\alpha\beta8$  expression can activate latent TGF $\beta$ <sup>145,146</sup>. In conjunction, RA and TGF $\beta$  have been shown to induce the development of pTregs from activated naïve CD4<sup>+</sup>FoxP3<sup>-</sup> T cells<sup>147</sup>. Speculating, we can envision a scenario in which the added presence of  $\beta7$  integrin overexpressing Tregs in the mLN could delay or block access of potential pTregs to DCs, perhaps resulting in subtle alterations in the maintenance of oral tolerance or disruptions in the regulation of the intestinal microbiota. Of note is the intriguing finding that despite increased expression of CTLA-4 in  $\beta1$  integrin-deleted Tregs, CD73 expression is decreased (Figure 20). As previously stated, one suppressive mechanism utilized by Tregs is the modification of pro-inflammatory ATP into immune-suppressive adenosine through surface expression of CD39 and CD73<sup>88</sup>. In addition, autocrine signaling of adenosine in Tregs can lead to the up regulation of CD39 and CD73 in a positive feedback loop<sup>148</sup>. Therefore the

down regulation of CD73 on  $\beta$ 1 integrin-null Tregs may be an indication that levels of pro-inflammatory ATP supersede those of adenosine, which begs the question of whether CKO Tregs have an inherent inability to suppress inflammation.

To begin to address many of these questions, we plan to better characterize the different Treg populations that reside in different intestinal compartments<sup>149</sup>. Ideally, differentiating between peripherally- or thymically-derived Tregs would allow us to quantify the contributions of each of Treg subset however, consistent identifying markers for these populations have yet to be established<sup>150</sup>. Even so, determining if there are excesses or deficits of Tregs, effector cells (i.e.  $T_H17$  cells) or DC frequencies in the PPs vs. the colon for example could provide insight into the migration or stability of different populations within these tissues.

Although  $\beta$ 1 integrin CKOs do not display any overt signs of autoimmunity or spontaneous colitis at steady state, subtle deficits in the development of oral tolerance might go undetected in uniform food antigen environment of an SPF-mouse colony. As such, we propose an experiment in which a novel food antigen such as the chicken egg protein ovalbumin (OVA) could be introduced to a subset of CKO and WT mice which would subsequently be challenged through the introduction of OVA under the skin<sup>153</sup>. Measuring cytokine production as well as quantifying OVA-specific T cell responses in the blood and lymphoid tissues using readily available tetramers would allow us to determine if  $\beta$ 1 integrin-deficient Tregs retain the ability to aid in the establishment of oral tolerance<sup>54</sup>. The gut is a highly complex and interconnected organ and so investigating the role of a single protein within that system poses many challenges, however with further testing and characterization of our CKO model, we hope to begin to understand the implications of Treg specific- $\beta$ 1 integrin expression within the broader context of mucosal immunity.

### 3.2.9.3 Virtual Memory or Innate Memory CD8+ T cells

CKO-derived CD8+ T cells express both higher levels of activation markers at steady state (Figure 23 and Figure 24) and undergo seemingly non-pathogen-specific expansion in response to infection (Figure 26B). We initially hypothesized that instability in the interactions between Tregs and activated DCs might lead to ineffective control of incidentally activated self-reactive CD8+ T cells leading to enrichment of this population (Figure 27). However, this hypothesis does not seem to bear out as we were unsuccessful in our attempts to elicit accelerated proliferation or cytotoxic behavior in CKO-derived CD8+ T cells in lymphopenic or Treg-deficient settings respectively (Figure 29 and Figure 30). Additionally, two other hypotheses proved unfruitful.

While preparing gut tissue samples we discovered that the  $\beta 1$  integrin CKO mice were infected with a protozoan not included in our SPF-pathogen list. Although this discovery was disheartening, we initially considered the possibility that the activated steady state profile of CD8+ T cells within the CKO model might be due to an immune response to the protozoa. (*See Appendix A for details on the identification of this parasite and the treatment course we pursued*). However, stimulation of CKO-derived CD8+ T cells with a closely related protozoa<sup>154</sup> (*Tritrichomonas mobilensis*) that had been purified and heat-inactivated did not yield increased cytokine production as compared to negative controls (data not shown), suggesting that CKO-derived CD8+ T cells are unlikely to be specific for *T. mobilensis* and by extension the closely related *T. muris*. (We were unsuccessful in our attempts to selectively purify *T. muris* from the feces of infected CKO mice and instead acquired *T. mobilensis* through ATCC to ensure reagent quality).

Additionally, we considered that because Tregs can increase the avidity of a developing CD8+ T cell response by competing for access to APCs<sup>51</sup>, perhaps CKO-derived CD8+ T cells

exposed to secondary WNV infect might be proliferating (Figure 26B) in response to subdominant peptides. However, stimulation of CKO-derived CD8<sup>+</sup> T cells harvested at a primary WNV infection memory time point with heat inactivated whole WNV failed to yield significant differences in cytokine production as compared to WT controls (data not shown). These data suggest that CKO-derived CD8<sup>+</sup> T cells are unlikely to be responding to subdominant WNV peptides however this possibility cannot be ruled out as perhaps the compromised Tregs in the CKOs have altered the capacity of their corresponding CD8<sup>+</sup> T cells to respond to TCR stimulation, despite comparable cytokine production after the application of an anti-CD3/anti-CD28 polyclonal stimulus.

Given these results, we propose that the steady state activated phenotype CD8<sup>+</sup> T cells in  $\beta$ 1 integrin CKO mice may represent expansion of a population of CD8<sup>+</sup> T cells termed “virtual memory” CD8<sup>+</sup> T cells (VM) or unconventional memory CD8<sup>+</sup> T cells. Although investigations of this cell type are in their infancy, VM CD8<sup>+</sup> T cells have been defined as foreign peptide-specific memory phenotype CD8<sup>+</sup> T cells that arise and are maintained in mice that remain naïve<sup>155</sup>. In addition to expressing a TCR specific for foreign antigens, VM CD8<sup>+</sup> T cells are phenotypically described as CD44<sup>hi</sup>, CXCR3<sup>hi</sup>, Ly6C<sup>hi</sup>, CD122<sup>hi</sup> (the common IL-15/2R $\beta$  chain) and CD49<sup>dlo</sup> (coincidentally, the CD designation for  $\alpha$ 4 integrin)<sup>156,157,158</sup>. There is considerable overlap between this VM profile and the expression profile identified in CKO-CD8<sup>+</sup> T cells at steady state (Figure 23 and Figure 24). As such, we will further assess CKO-derived CD8<sup>+</sup> T cells for expression of CD122, CD49d as well as the transcription factors Tbet and Eomes as they have also been found to be up regulated in tandem depending on the origin of the VM CD8<sup>+</sup> T cells<sup>156</sup>.

Functionally, VM CD8<sup>+</sup> T cells have been shown to preferentially differentiate into SLECs during an infection<sup>157</sup>; a pattern reflected in our data (Figure 25C). These cells subsequently develop a central memory phenotype as the infection resolves<sup>157</sup>, a characteristic change that we intend to investigate in our own model. Furthermore, VM CD8<sup>+</sup> T cells have been proposed as a “bridging” cell between the innate and adaptive responses because of their ability to rapidly produce IFN $\gamma$  in response to the presence of the pro-inflammatory cytokines IL-12 and IL-18 in the absence of their cognate antigen<sup>155</sup>. If we found a similar capacity in CKO-derived CD8<sup>+</sup> T cells, it might help explain the seemingly non-specific CD8<sup>+</sup> T cell expansion we found after secondary WNV infection (Figure 26B). We intend to directly test the ability of CKO-derived CD8<sup>+</sup> T cells to produce IFN $\gamma$  in response to IL-12 and IL-18 by culturing isolated CD8<sup>+</sup> T cells from  $\beta$ 1 integrin CKO mice or WT controls in the presence of IL-12 and IL-18 or (an unrelated cytokine such as IL-6) and then measuring the amount of IFN $\gamma$  produced by ELISA at various time points. In addition, IL-4<sup>159</sup> and IL-15<sup>160</sup> have been implicated as drivers of the development and expansion of the VM CD8<sup>+</sup> T cell pool and we further plan to assess the effect of these cytokines in culture with CKO-derived CD8<sup>+</sup> T cells.

In conjunction with flow cytometric assessment of the defining markers of VM CD8<sup>+</sup> T cells we hope that these assays will allow us to further our understanding of the Treg-specific  $\beta$ 1 integrin deletion mediated changes that develop in CD8<sup>+</sup> T cells in these mice. However, considerably more work will have to be done to discover the connections between the alterations in  $\beta$ 1-null Tregs, increased trafficking to the gut, and the potential expansion of the VM CD8<sup>+</sup> T cell pool that we have described in this CKO mouse model.

## Chapter 4. MATERIALS AND METHODS

### 4.1 AIM I: MAVS IS DISPENSABLE FOR TREG FUNCTION DURING WNV INFECTION

#### *Ethics Statement*

Mouse experiments were approved by the University of Washington Institutional Animal Care and Use Committee (IACUC protocol #4327-01 and 4158-01) and the Fred Hutchinson Cancer Research Center (IACUC protocol #1810). The Office of Laboratory Animal Welfare of the National Institutes of Health (NIH) has approved the University of Washington (#A3464-01) and the Fred Hutchinson Cancer Research Center (#A3226-01), and this study was carried out in strict compliance with the Public Health Service (PHS) Policy on Humane Care and Use of Laboratory Animals.

#### 4.1.1 *West Nile Virus*

West Nile virus TX-2002-HC (WN-TX) was generously provided by Dr. Jason Netland (University of Washington) and propagated as previously described<sup>85,86</sup>. Working stocks were generated from supernatants collected from infected Vero cell lines, and stored at -80°C.

#### 4.1.2 *Mice*

MAVS-deleted mice were bred and maintained under specific pathogen-free conditions in the University of Washington South Lake Union 3.1 animal facility. FoxP3<sup>DTR</sup><sup>87</sup> and FoxP3<sup>GFP</sup><sup>88</sup> mice (kindly provided by Dr. Alexander Rudensky, Memorial Sloan-Kettering Cancer Center) were bred under specific pathogen-free conditions onsite in the Fred Hutchinson Cancer Research Center animal facility. Ly5.1 FoxP3<sup>DTR</sup> mixed bone marrow chimeric mice were

transported to the animal facility at the University of Washington for all West Nile virus infection studies. Wild-type C57BL/6J control mice were purchased through The Jackson Laboratory (Bar Harbor, ME USA) and housed in the University of Washington animal facility.

#### 4.1.3 *90%/10% Mixed bone marrow chimeras*

One day prior to bone marrow transplant, recipient FoxP3-DTR Ly5.1 mice were irradiated (900 Rads). On the day of transplant, FoxP3-DTR Ly5.1, WT Ly5.2 (C57BL/6) and MAVS<sup>-/-</sup> Ly5.2 mice were euthanized and femurs and tibias from both hind legs collected from each mouse. Bones were irrigated with 1X PBS and bone marrow was homogenized through 100µm cell strainers. Red blood cells were lysed using ACK lysis buffer (3mL for 3 mins per 2 mice) and then re-filtered through 100µm cell strainers to remove dead cell debris. Bone marrow cell suspensions were enumerated using a hemocytometer after trypan blue staining. Appropriate dilutions were calculated to ensure a 90% FoxP3-DTR Ly5.1 + 10% WT Ly5.2 or MAVS<sup>-/-</sup> Ly5.2 bone marrow mixture was achieved (Figure 31A). Cell preparations were re-suspended in 200 µL sterile HBS buffer and introduced intravenously through the tail vein of recipient FoxP3-DTR Ly5.1 mice. Recipient mice were provided with antibiotic (Baytril ®, Bayer Corp) supplemented water and recovery food gel for 2 weeks post transplant. Mice were then allowed to recover for a total of 12 weeks prior to use in any experiments (Figure 31B).

#### 4.1.4 *90%/10% Mixed bone marrow chimeras – Diphtheria toxin administration*

Four to five days prior to infection with WNV, mixed bone marrow chimeras were intraperitoneally injected with 10 µg/Kg of diphtheria toxin (Calbiochem, Merck KGaA, Darmstadt, Germany). Chimeras were then bled via intra-orbital sinus puncture to ensure that

either MAVS<sup>-/-</sup> or WT-B6 Tregs had reconstituted the depleted Treg compartment (Figure 31C). Roughly 8-12 hours later mice were infected with WNV as described below with a continuing schedule of 5 µg/Kg intraperitoneal DT administration every other day thereafter throughout the course of infection in order to maintain ablation of endogenous DTR-expressing Tregs.

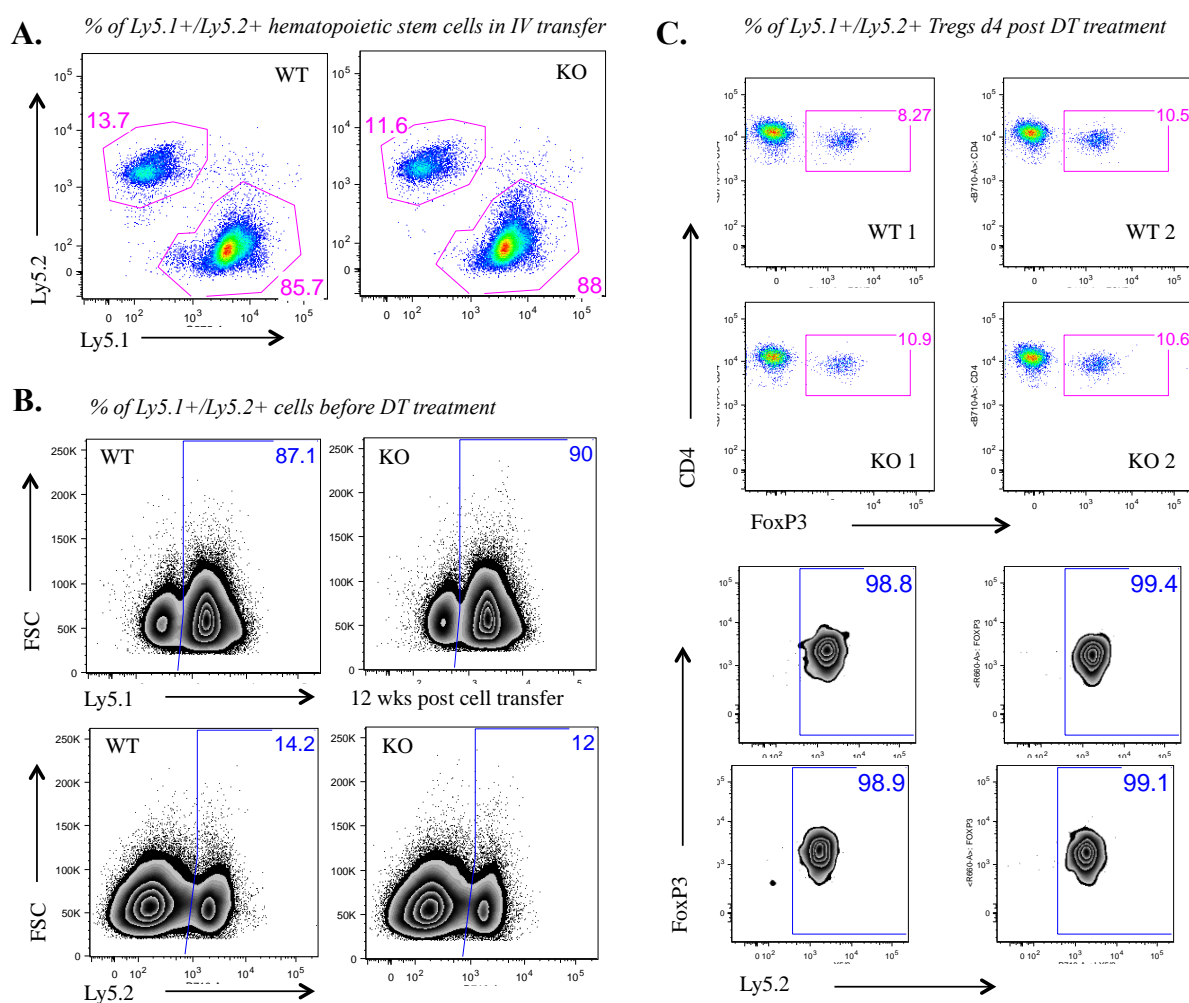


Figure 31. Donor Tregs (Ly5.2+) supplant endogenous Tregs 4 days after initiation of DT treatment.

#### 4.1.5

#### *In vivo West Nile Virus infection*

Age-matched MAVS<sup>-/-</sup> or mixed bone chimeras and WT controls were infected through subcutaneous injection of the left foot pad with 1000 PFU West Nile virus TX-2002-HC delivered in

a 40  $\mu$ l dilution of sterile 1X PBS.

#### 4.1.6 *TGF $\beta$ , IL-6 and IL-17 ELISAs*

Whole blood was collected from WNV infected MAVS<sup>-/-</sup> and WT control mice 6 days post infection. Blood was allowed to coagulate at room temperature for >1 hour and then centrifuged at RT, 3000 rpm for 10 mins. Supernatant serum layer was then carefully transferred to a new tube and stored at -80°C prior to ELISA assays. On day of ELISA, samples were allowed to thaw at 4°C and then UV irradiated for 30 mins in BSL2+ conditions to inactivate WNV. TGF $\beta$  concentration was measured as per manufacturer's protocol in Mouse TGF-beta1 Platinum ELISA kit (Affymetrix, eBioscience, Inc. CA, USA). Samples were diluted 1:500 as per kit instructions and spectrophotometric data collected at 1<sup>o</sup> wavelength = 450nm and 2<sup>o</sup> wavelength = 620nm. IL-6 concentration was measured as per protocol included in Mouse IL-6 ELISA Ready-Set-Go!<sup>®</sup> kit (eBioscience, Inc). Samples were diluted 1:10 and analyzed at 1<sup>o</sup> wavelength = 450nm and 2<sup>o</sup> wavelength = 570nm. Finally, IL-17 concentration was measured as per protocol included in Mouse IL-17A (homodimer) ELISA Ready-SET-Go!<sup>®</sup> kit (eBioscience, Inc). In addition, detection antibody with overlaid sample or standard was incubated overnight to increase assay sensitivity. Samples were diluted 1:5 and analyzed at 1<sup>o</sup> wavelength = 450nm and 2<sup>o</sup> wavelength = 570nm.

#### 4.1.7 *In vitro Treg suppression assay*

MAVS<sup>-/-</sup> or WT mice on a B6 background were euthanized, spleens harvested and homogenized through a 100 $\mu$ m cell strainer to create a single cell suspension. Cell suspension was enriched for Tregs using a mouse CD4+CD25+ magnetic bead-based column regulatory T cell isolation kit (Cat: 130-091-041) as per manufacturer's instructions (MACS Miltenyi Biotec, Germany). Flow

through was stained with CFSE (eBioscience, Inc, San Diego, CA) and used as Tconv population. Briefly, spleens from WT mice were homogenized to form a single cell suspension, RBCs lysed using in-house ACK lysis buffer (3mL for 3 mins per sample), and remaining splenocytes irradiated. Irradiated splenocytes served as antigen presenting cells. Decreasing concentrations of Tconv to enriched Tregs were cultured with  $5 \times 10^4$ -irradiated splenocytes supplemented with  $1 \mu\text{g}/\text{well}$  anti-CD3 antibody. Samples were incubated for 80 hours at  $37^\circ\text{C}$  and CFSE dilution was measured through flow cytometry. Detailed assay protocol is as described in Chapter 2, Section 3.2 Variations of Basic Protocol: Antigen Presenting Cell Activation<sup>89</sup>.

#### 4.1.8 *In vitro proliferation assay*

Spleens were harvested from MAVS<sup>-/-</sup> or WT mice and homogenized through a  $100 \mu\text{m}$  cell strainer to create a single cell suspension. RBCs were lysed using ACK lysis buffer and Tregs isolated using the EasySep™ Mouse CD4+CD25+ Regulatory T Cell Isolation Kit (STEMCELL Technologies Inc, Vancouver, BC, Canada) as per manufacturer's instructions. Tregs were subsequently labeled with CFSE (eBioscience, Inc, San Diego, CA). For DC isolation, spleens were collected from WT mice, minced in a cell culture well and incubated in a DMEM/collagenase D/DNAse I (Roche) media solution with mechanical agitation for 30 mins at  $37^\circ\text{C}$ . The digestive solution was inactivated after incubation by re-suspending the sample in HBSS/0.5M EDTA and re-incubating the minced tissue at  $37^\circ\text{C}$  for 5 mins. The digested tissue was then homogenized through a  $100 \mu\text{m}$  cell strainer and RBCs lysed using ACK lysis buffer. Dendritic cells were then isolated using CD11c microbead magnetic column enrichment (MACS Miltenyi Biotec, Germany). Isolated DCs were incubated with heat-inactivated WNV for 1hr at  $37^\circ\text{C}$  or left "naïve". Tregs were plated at  $5 \times 10^4$  cells per well and co-cultured with  $2 \times 10^5$  DCs

(either WNV loaded or not) for 3 days at 37°C. Anti-CD3 and anti-CD28 (1:10 dilution from 1µg/mL stock) were used as a polyclonal stimulus for positive controls. After 3 days samples were stained for viability as well as T cell and DC markers and CFSE dilution analyzed via flow cytometry.

#### 4.1.9 *Flow Cytometry*

MAVS<sup>-/-</sup> and WT Treg chimeras were infected as described above. On scheduled collection days mice were euthanized in accordance with University of Washington IACUC regulations and spleens collected. Mice were then perfused through the left heart ventricle with ~10mL cold 1X PBS. Brains were then harvested into 5mL RPMI culture media supplemented with 10% fetal bovine serum (FBS), Pen/Strep, L-glutamine, HEPES buffer and sodium pyruvate. Spleens were homogenized and passed through a 100µm cell strainer to create a single cell suspension, RBCs lysed using ACK lysis buffer and cells enumerated (after trypan blue staining) using a hemocytometer. Splenocytes were then diluted to a concentration of 1x10<sup>7</sup> cells/mL using a 1X PBS/0.5% FBS solution and 100µL for a total of 1x10<sup>6</sup> cells/well per sample. Brains and collection media were poured into culture wells in a 6-well culture plate and homogenized using frosted ends of 2 microscope slides. Homogenate was then returned to original 15 mL collection conical and corresponding culture well rinsed with 600µL of collection media. Tubes containing 5.6mL of homogenate were then overlaid with 2.4mL of hypertonic Percoll density centrifugation media (1:10, 10X PBS: Percoll), (GE Healthcare Life Sciences, Pittsburgh, PA) for a final Percoll concentration of 30%. Samples were vortexed and spun at 1250 RPM for 30 mins at 4°C. After centrifugation, supernatant was aspirated and pellet re-suspended in 2mL 1X PBS/0.5% FBS solution and cells enumerated. Samples were re-suspended in 600µL and 100µl plated per well. Cells were then stained (all incubation steps were at 4°C) for viability using

LIVE/DEAD® Fixable Aqua Dead Cell Stain (ThermoFisher Scientific) at 1:1000 for 30 mins. This was followed by 10 min incubation with anti-CD16/32 (clone: 93) at 1:500. Cells were subsequently re-suspended in 50µL antibody cocktails for 15 mins. Antibody markers included CD3-BUV395 (145-2C11) CD4-BV605 (RM4-5), CD8-BV650 (53-6.7) and FoxP3-Alexa700 (FJK-16s). WNV NS4b-H2D<sup>b</sup> tetramer-APC (generated by the Immune Monitoring Lab, Fred Hutch tetramer core) was used to determine frequency of WNV-specific CD8<sup>+</sup> T cells. Additional antibodies for Treg characterization included: CD73-V450 (ebioTy/11.8), GITR-PECy7 (DTA-1), CTLA-4-APC (UC10-4B9). Cells were fixed and permeabilized for 30 mins before intracellular staining antibodies were applied. Data was collected via flow cytometry using a BD LSRII and BD FACSDiva Software. Sample analysis was performed using FlowJo software.

#### 4.1.10 *RNA extraction*

After CO<sub>2</sub> euthanasia, mice were perfused through the left heart ventricle with ~10mL cold 1X PBS. The brain cavity was accessed and the cerebellum removed and immediately placed into pre-weighed tubes containing 5mL RNAlater Stabilization Reagent (Qiagen, Valencia, CA). Samples were reweighed, weight of cerebellums alone was calculated and samples placed in -80°C freezer. Brains were thawed at 4°C, homogenized using a handheld homogenizer and total RNA extracted following protocol instructions included with the RNeasy® Lipid Tissue Mini Kit (Qiagen, Valencia, CA). RNA was eluted into RNase-free 10mM TE Buffer, pH 7.0 and RNA concentration measured using a Nanodrop 2000 UV-Vis spectrophotometer (Thermo Scientific, Waltham, MA).

#### 4.1.11 *WNV DNA standard for qRT-rtPCR*

Competent *E. coli* cells transformed with kanamycin resistant plasmids containing the WNV PCR target region were grown in kanamycin-containing media and plasmids isolated using the Qiagen Plasmid Mini kit (Qiagen, Valencia, CA). The plasmid concentration was determined using a Nanodrop 2000 UV-Vis spectrophotometer (ThermoScientific) and 10 fold standard dilution series was generated spanning a concentration of  $1 \times 10^{10}$  to  $1 \times 10^2$  plasmids/5ul.

#### 4.1.12 *qRT-rtPCR for positive strand WNV RNA*

WNV primers and probe were selected as previously described<sup>90</sup>. The fluorogenic probe was synthesized with a 5' reporter dye 6-carboxyfluorescein (6-FAM) and a 3' quencher dye 6-carboxytetramethylrhodamine (5'-TAMRA). Primers and probe were generated as custom assays from Integrated DNA Technologies (IDTDNA, Coralville, Iowa). qRT-PCR assays were performed using the SuperScript® III Platinum® One-Step Quantitative RT-PCR System (Life Technologies, Grand Island, NY). Reactions were carried out in a total volume of 20µL, containing 5µL of template RNA, 1X reaction mix, 500nM final concentration for forward and reverse primers and 250nM final concentration for probe, 0.4µL ROX dye, 0.4µL RT/Taq enzyme mix and brought up with nuclease free water. After adding the reaction mixture and template RNA to MicroAmp® Fast Optical 96-Well Reaction Plates (Applied Biosystems, Inc., Foster City CA), reverse-transcription and amplification were carried out on the ABI 7900HT Fast Real-Time PCR System (Applied Biosystems, Inc., Foster City CA) in standard mode. Cycling conditions were as follows: 50°C for 15 minutes hold (cDNA synthesis step), 95°C for 2 minutes hold, 40 cycles of 95°C for 15 seconds followed by 60°C, 1 minute.

## 4.2 AIM 2: INTEGRIN B1 EXPRESSION IS ASSOCIATED WITH TISSUE-SPECIFIC EFFECTOR FUNCTION IN TREGS

### 4.2.1 *Mice*

$Itgb1^{Flox/Flox} \times FoxP3^{eYFP-Cre-ERT2}$  mice were generously provided by Dr. Alexander Rudensky and bred and maintained in house at the Fred Hutchinson Cancer Research Center animal facility. Control mice included from  $Itgb1^{Flox/WT} \times FoxP3^{eGFP-Cre-ERT2}$ ,  $Itgb1^{WT/WT} \times FoxP3^{eGFP-Cre-ERT2}$  and various (ITGb1) WT mice on a B6 background. These controls were either bred in house or purchased through Taconic Biosciences, Inc or The Jackson Laboratory.

### 4.2.2 *Virus*

West Nile virus TX-2002-HC (WN-TX) was generously provided by Dr. Jason Netland (University of Washington) and propagated as previously described<sup>91,92</sup>. Working stocks were generated from supernatants collected from infected Vero cell lines, and stored at -80°C.

### 4.2.3 *Flow Cytometry*

Procedure is as described in 4.1.9. Briefly, tissues used for antibody staining were first mechanically disrupted to form a single cell suspension. When lymph nodes collected for DC analysis enzymatic digestion of tissue was performed as described in 4.1.8. Suspensions were then incubated with ACK lysis buffer to remove red blood cells (RBCs) and filtered and washed in PBS without the addition of FBS in preparation for viability staining. Viability dye used was either Live/Dead® Fixable Aqua Dead Cell stain kit, for 405 nm excitation (Cat #: L34957, ThermoFisher Scientific) or Fixable Viability Dye eFluor® 780 (Cat #: 65-0865, eBioscience) depending on channel availability on panels. Samples were then incubated with Fc receptor block at 4°C to improve surface retention of applied antibodies and reduce incidental antibody

uptake by Fc receptor expressing cell-types (i.e. phagocytic cells). Finally antibodies were applied in appropriate dilution concentrations determined empirically through titration.

Antibodies used were as follows:

Table 2: Antibodies used in Flow cytometric analyses

<b><i>Antibody</i></b>	<b><i>Clone</i></b>	<b><i>Panel/Function</i></b>
CD4	RM4-5	Helper T cell marker
CD44	IM7	Activation
CXCR3	CXCR3-173	Migration/activation
CCR5	7A4	Migration
CCR7	4B12	Lymph node homing
CD62L	MEL-14	Lymph node/spleen homing
CD69	H1.2F3	Activation/resident memory
NS4b Class 1 Tet		WNV specific CD8+ T cell identifier
CD103	2E7	Migration/activation
CD8	53-6.7	CTL marker
CD3*	145-2C11	Lymphocyte co-stimulation
Ki67*	SolA15	Cell cycle progression/proliferation
CD29 (ITGb1)	HMB1-1	Migration
FoxP3*	FJK-16S	Transcription factor (Treg)
GITR	DTA-1	TNF receptor associated with activation
ICOS	7E.17G9	Treg activation/suppressive capacity
CTLA-4*	UC10-4B9	Treg suppressive function
CD73*	TY/11.8	Converts AMP to adenosine/suppressive function
CD25	PC61	IL-2 receptor/activation/rudimentary Treg identifier
IFN $\gamma$ *	XMG1.2	Pro-inflammatory cytokine
IL-17*	17B7	Pro-inflammatory cytokine notably produced by T <sub>H</sub> 17 cells
PSGL-1	2PH1	Adhesion and migration
Tbet*	B410	Transcription factor (T <sub>H</sub> 1)
TNF $\alpha$ *	MP6-XT22	Pro-inflammatory cytokine
Ly6C	HK1.4	Migration/self-recognition (?) [CD4+/Tregs] <sup>93</sup>
KLRG-1	ZF1	SLEC identifier/Signifier of terminal differentiation in Tregs <sup>94</sup>
CD127	A7R34	IL-7R $\alpha$ (IL-7 promotes cell survival)/MPEC identifier <sup>95</sup>
Ly5.2 (CD45.2)	104	Congenic marker on leukocytes
Ly5.1 (CD45.1)	A20	Congenic marker on leukocytes
Integrin $\beta$ 7	FIB504	Migration (Gut homing when paired with Integrin $\alpha$ 4)
CD11c	N418	Conventional dendritic cell marker
CD11b	M1/70	Adhesion/Migration (associated with DC subsets) <sup>96</sup>
CD80 (B7-1)	16-10A1	Co-stimulatory molecule highly expressed in APCs
CD86 (B7-2)	GL1	Co-stimulatory molecule highly expressed in APCs
CD5	53-7.3	Surface protein associated with self-reactivity <sup>97</sup>
PD-1	J43	Associated with T cell activation & exhaustion <sup>98</sup>
CD122	5H4	IL-2/IL-15 receptor $\beta$ chain (VM CD8+ T cell identifier) <sup>99</sup>
CD49d (ITGa4)	R1-2	Binds to ITGb1 and ITGb7 (VM CD8+ T cell identifier) <sup>100</sup>
GATA3*	TWAJ	Transcription factor (T <sub>H</sub> 2)/(Tregs during inflammation) <sup>101</sup>
ROR $\gamma$ T*	B2D	Transcription factor (T <sub>H</sub> 17)

\*indicates intracellular protein

#### 4.2.4

#### *In vivo viral infection*

For WNV infections, age-matched ITGb1 CKO and WT controls were infected through subcutaneous injection of the left foot pad with 1000 PFU West Nile virus TX-2002-HC delivered in a 40 $\mu$ L dilution of sterile 1X PBS. For Flu infections, age-matched ITGb1 CKO and WT controls were infected through intranasal administration of 1.5 PFU Influenza A PR8 diluted in 40 $\mu$ L sterile 1X PBS. Mice were anesthetized using isoflurane prior to infection.

#### 4.2.5

#### *Memory time point CD8+ T cell adoptive transfer*

ITGb1 CKO and WT mice were infected with either WNV-Tx or Flu PR8 as described in 4.2.3 and weight loss and clinical score monitored during the course of disease. Mice were euthanized if they reached the FHCRC/UW IACUC criteria of weight loss  $\geq$  20% of initial body weight or any hind limb paralysis (WNV criteria only). Surviving mice were euthanized 30+ days post infection and spleens and easily accessed LNs (mesenteric, inguinal, iliac, superficial cervical, brachial and axillary) collected from 2-4 mice per group. Single cell suspensions were made by pushing spleens or pooled LNs (pooled per mouse) through 100 $\mu$ m strainers and washing through with sterile 1X PBS. RBCs were eliminated using ACK lysis buffer and samples washed and strained again to remove cellular debris. Samples were then pooled per group and CD8+ T cells isolated using manufacturer's instructions included with EasySep™ Mouse CD8+ T cell Isolation kit (Cat# 19853A, STEMCELL Technologies, Inc, Vancouver, BC, Canada). 1.5 – 5x10<sup>6</sup> bulk memory time point negative isolation CD8+ T cells were then infused into B6-WT recipient Ly5.1 congenically marked mice. Mice were rested overnight to allow some time for transferred CD8+ T cells to reach lymphoid tissues. Mice were then infected with either 1000 PFU WNV-Tx or 1.5 PFU Influenza A PR8 and weight and clinical score monitored until peak

of infection in the spleen (8-9 days WNV) or lung respectively (7-8 days Flu). Spleens/brains or spleens/lungs were harvested cell suspensions made and transferred Ly5.2+ CD8+ T cells analyzed via flow cytometry.

#### 4.2.6 *CD8+ T cell in vivo proliferation assay*

Ly5.1 congenically marked WT mice on a B6 background were sub-lethally irradiated (900 Rads) to eliminate hematopoietic stem cells and their progeny. This creates a lymphopenic environment while simultaneously providing pro-inflammatory stimulation for donor lymphocytes<sup>102</sup>. Roughly 24 hours later, bulk CD8+ T cells were isolated from naïve Ly5.2 congenically marked ITGb1 CKO or B6 WT controls using manufacturer's instructions included with the EasySep™ Mouse CD8+ T cell Isolation kit. CKO or WT cells were then labeled using CFSE (see 4.1.8 for details) in separate tubes to track proliferation. Resulting CFSE labeled CD8+ T cells were then combined in a 1:1 ratio ( $7.5 \times 10^5$  each for a total of  $1.5 \times 10^6$  transferred cells) and infused intravenously into irradiated naïve recipient WT mice. Mesenteric lymph nodes and spleens were harvested 3 days post labeled CD8+ T cell transfer and CFSE dilution quantified after flow cytometric analysis.

#### 4.2.7 *CD8+ T cell adoptive transfer after Treg ablation*

Ly5.1 congenically marked FoxP3-DTR mice were intra-peritoneally injected with 10µg/Kg diphtheria toxin 1 day prior to cell transfer. CD8+ T cells were isolated using magnetic microbeads (as described above) from ITGb1 CKO or WT controls previously infected with 1000 PFU WNV-Tx and allowed to reach a memory time point 50+ days after initial infection.  $4-5 \times 10^6$  isolated CD8+ T cells were infused intravenously into recipient Ly5.1+ FoxP3-DTR mice with subsequent administration of 5µg/Kg diphtheria toxin on day of CD8+ T cell transfer.

Mice were then monitored for weight loss and signs of developing autoimmunity (such as dermatitis) up to 21 days post CD8<sup>+</sup> T cell transfer.

## APPENDIX A

### **Detection and treatment strategy for *Tritrichomonas muris* in the common laboratory mouse, *Mus Musculus***

#### *Introduction*

*Tritrichomonas muris* is a triflagellate single celled protozoan that infects the intestinal tissues of mice, hamsters and other rodents. It is closely related to the more familiar *Tritrichomonas foetus*, a pathogen known to infect the reproductive organs of bovine and the intestinal tracts of cats<sup>103</sup>. *T. foetus* is of particular commercial interest as it has been shown to induce spontaneous abortion in cows that become infected<sup>104</sup>. *T. muris* however, has been listed in a variety of veterinary resources as a commensal organism<sup>105</sup> and therefore is rarely tested for during routine mouse colony maintenance screens for pathogens. Despite this categorization, Kashiwagi *et al* undertook a proteomic analysis of intestinal tissue from experimentally *T. muris* infected mice and found differential expression of 10 proteins (a subset of which were involved in the immune response) in infected mice as compared to uninfected controls<sup>106</sup>, indicating that *T. muris* infections may be less innocuous than previously concluded. In addition, because *T. muris* forms pseudocysts instead of true cysts, traditional testing of bedding and microscopy techniques can often miss its presence if fresh feces are not available.

During a routine gut tissue preparation, we discovered that a subset of our mouse colony was infected with *T. muris*. In particular, we determined that a conditional knock out (CKO), B6;129-Itgb1<sup>Flox/Flox</sup> x FoxP3<sup>eYFP-Cre-ERT2</sup>, was most affected. These mice lack expression of a single migration-associated protein (integrin  $\beta$ 1) on FoxP3-expressing regulatory T cells (Tregs). In order to continue our primary investigation of the effect of  $\beta$ 1 deletion on Tregs in this mouse model, it was critical that we remove the potential confounding effects of a *T. muris* infection.

Therefore, we developed a PCR-based detection assay in order to determine the *T. muris* infection status of the strain and subsequently developed a treatment plan that would allow for the segregation of “clean” mice to be used in future experiments. It is exceedingly important to maintain uniform adherence of the SPF conditions for all mice within an experiment. In characterization experiments where a novel gene deletion (especially those involved in the development or functioning of the immune response) is being investigated it is critical that all potentially interacting factors are accounted for, including ongoing infections that are considered commensal or otherwise.

## Results

### *T. muris* infection can potentially confound characterization of novel immune system-associated gene deletion mouse models.

The Cre/LoxP conditional knockout (CKO) mouse model has proven to be an invaluable tool in the reductive investigation of the function of individual genes in specific cells and tissues. Use of CKOs in studies of the immune system vary widely and have elucidated the inner workings of immune cells as well as their relationships with other systems within the organism<sup>161</sup>. As such, we set out to characterize the effect of integrin  $\beta 1$  deletion in a subset of lymphocytes, CD4<sup>+</sup>FoxP3<sup>+</sup> Tregs. When preparing excised small intestine from ITGb1 CKOs and WT controls for isolation and analysis of lamina propria lymphocytes, we first noticed a dramatic discoloration in the CKO derived tissue (Figure 32) and secondly detected a free-swimming organism in the tissue media under 20X magnification after addition of Trypan blue exclusion dye.

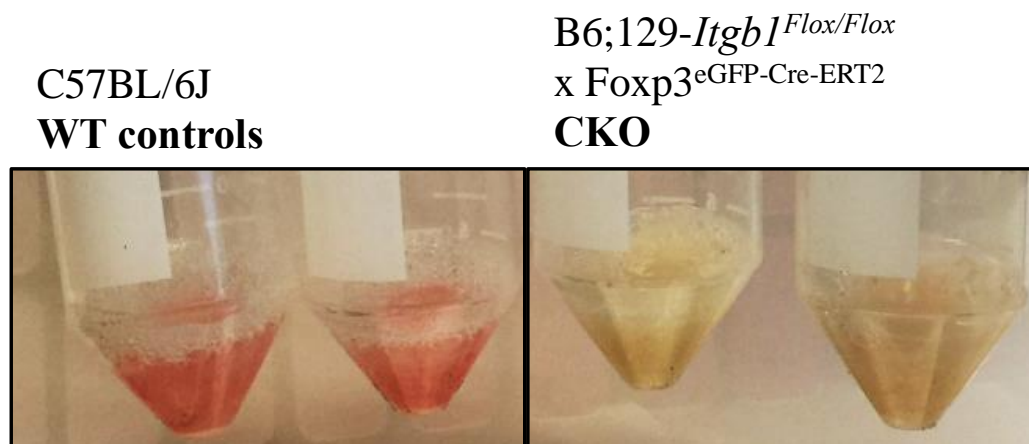


Figure 32. Small intestine collected from uninfected WT and *T. muris* infected ITGb1 CKO mice in cell culture media.

Fecal samples from ITGb1 CKOs were sent for identification of the protozoan (IDEXX Bioresearch, Columbia, MO, USA) that was confirmed to be *Tritrichomonas muris*. Although *T. muris* has been grouped with other protozoan infections associated with symptoms including weight loss, runting and diarrhea<sup>162</sup>, we did not find a statistically significant weight difference in CKOs as compared to age matched WT controls within our colony (Figure 33).

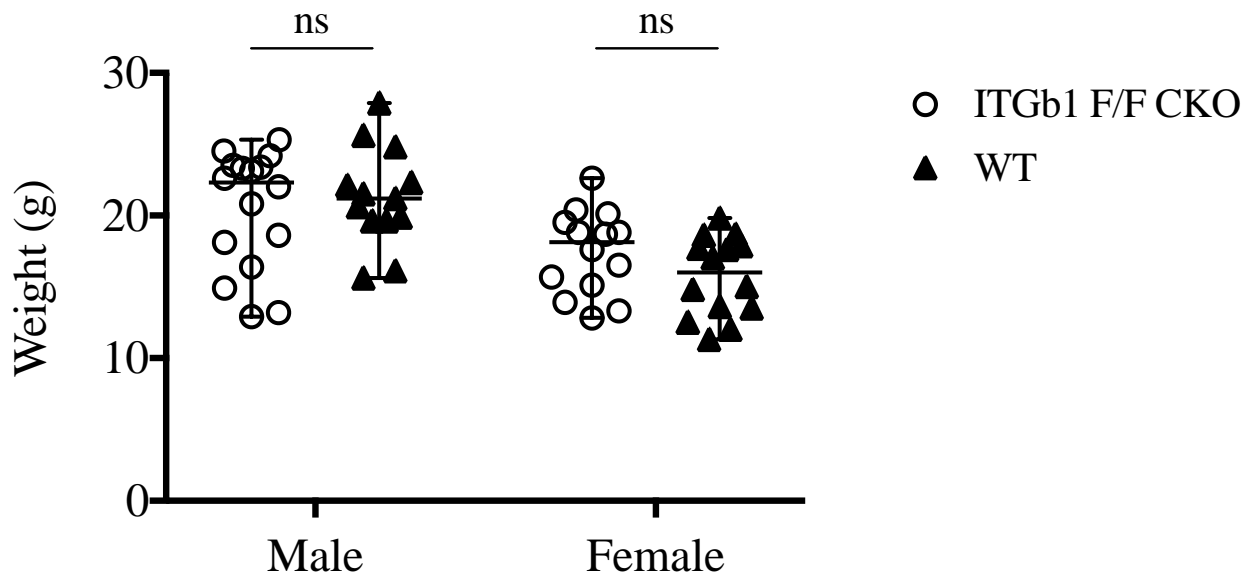


Figure 33. Weights were not significantly different between male or female CKO and WT mice despite *T. muris* infection.

To confirm infection we analyzed sections of bowel and other organs, including the spleen (not shown) through histopathology (Figure 34).

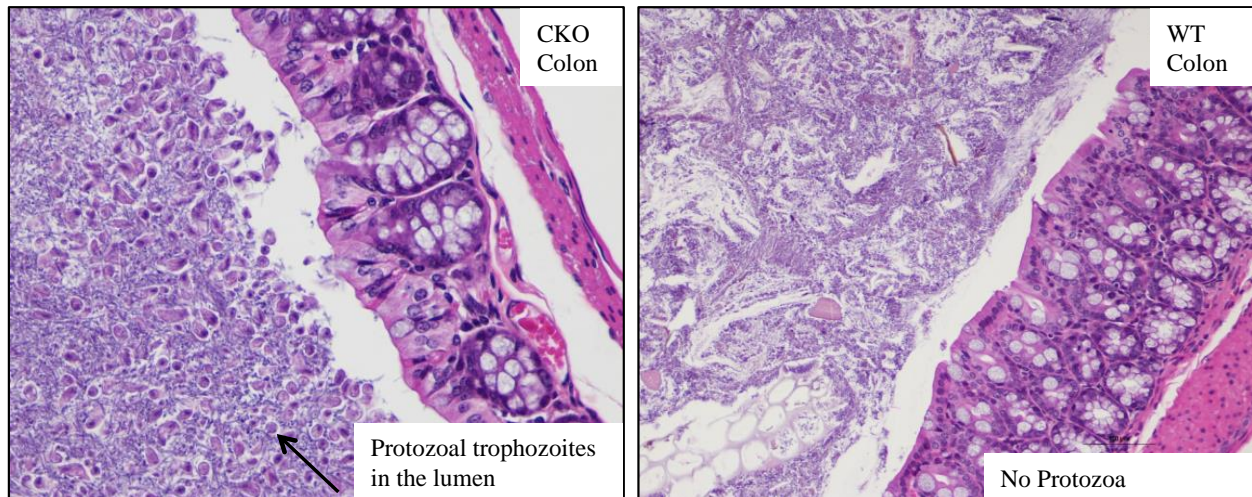


Figure 34. Protozoal trophozoites can be seen in the lumen of colon taken from infected CKO mice but is absent in WT controls.

#### ***Selection of effective *T. muris*-specific PCR primers***

As previously described, *T. muris* and *T. foetus* are closely related protozoan species, with *T. foetus* being the focus of studies of commercial interest. In order to develop the most effective PCR primers given the lack of publicly available sequence data for *T. muris*, we aligned the 18s ribosomal sequences of *T. muris* and *T. foetus* using the nucleotide blast program hosted by NCBI BLAST<sup>163</sup>, and selected primers that covered conserved exon regions shared between both species (Figure 35).

ATCAGTTTCGT-T-AA--TAATTACAAACATAAttttttt-AATTTCTATAA-CTATT--T	<i>T. foetus</i>
ATCAGTTTCGTATAAATTTAAACACAAAAATATTTTTTTAATGTATATAACCTTTAAT	<i>T. muris</i>
-ATACAAA-ATTAAACACATAATCTAAAAAATTTAGACCTTAGGCAATGGATGCTTTGGC	<i>T. foetus</i>
CATACAAACAATAAAAAACA-AAT-AAAAAATTTAGACCTTAGGCAATGGATGCTTTGGC	<i>T. muris</i>
TTTACACGATGAAGAACGTTGCATAATGCGATAAGCGGCTGGATTAGCTTTCTTTGCG	<i>T. foetus</i>
TTCATTACACGATGAAGAACGTTGCATAATGCGATAAGCGGCTGGAGTTGCTTTCTTTGCG	<i>T. muris</i>
ACAAGTTCGATCTTTGAAATGCATATTGCGCGCCGTTTTAGCTT--GCTAGAACACGCATA	<i>T. foetus</i>
ACAAGTTCGATCTTTGAAATGCATATTGCGCGCCGTCGG-GCTTCTGCTTTGACACGCATA	<i>T. muris</i>
TATGTTACAGTAACCCATATTAATTTAATACCAAATCTCTTTTTAAGCAAAAGAGCGAA	<i>T. foetus</i>
TATGGTACAGTAACCCATAATAGTTTAAAAAATAA-TCTCTTTTTACGTAAAAGAGCGAA	<i>T. muris</i>
AAACAAATATGTATT-AACAAAAGGGTTCTGTCTCATATA	<i>T. foetus</i>
AAATTTATATGTATAAACGAAAGGGTTCTGTATCATATA	<i>T. muris</i>

Figure 35. *T. foetus/T. muris* 18s ribosomal sequence alignment.

Master mix composition was based on manufacturer's recommendations included in the 2X MyTaq™ HS Red Mix purchased through Bioline USA Inc, (Taunton, MA) (Figure 36).

<b>T. Muris PCR Master Mix</b>	25 $\mu$ L reaction	<i>Forward primer</i>	GCA ATG GAT GTC TTG GCT TC
Dnase-free dH <sub>2</sub> O	9.5 $\mu$ L	<i>Reverse primer</i>	GCG CAA TAT GCA TTC AAA GA
10 $\mu$ M <i>T. muris</i> FWD primer	1 $\mu$ L		
10 $\mu$ M <i>T. muris</i> REV primer	1 $\mu$ L		
2X MyTaq™ HS Red Mix	12.5 $\mu$ L		
Extracted DNA	1 $\mu$ L		

Figure 36. Master mix composition and primer sequence for *T. muris* detection assay.

Similarly, initial denaturation, denaturation and extension temperatures and duration were based on manufacturer's recommendation. Annealing temperature, duration and cycle number were determined empirically (Figure 37).

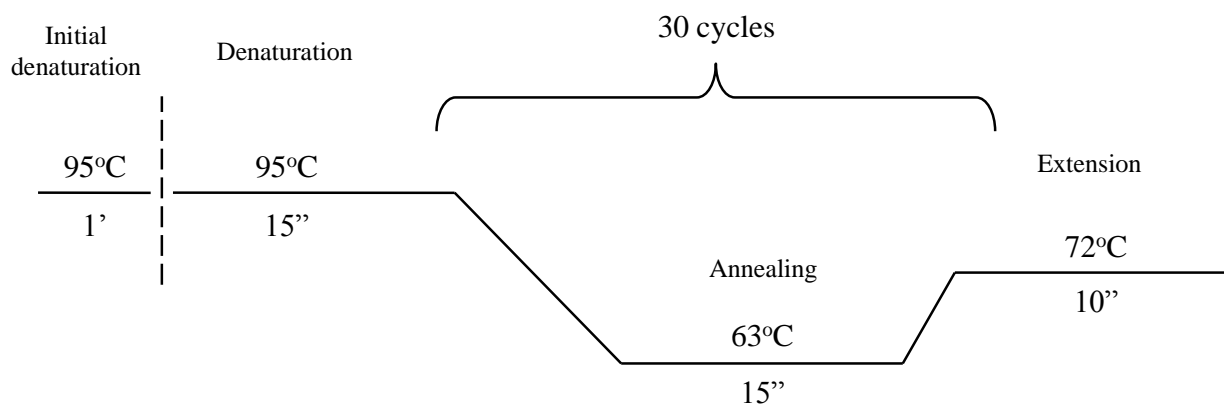


Figure 37. PCR denaturation, annealing and extension schedule for *T. muris* detection assay

### ***T. muris* infection is easily transmitted but can evade detection by sentinel mice**

Using the primers and PCR program illustrated in Figure 36 and Figure 37, we sought to determine the extent of *T. muris* infection within our ITGb1 CKO breeder population. To ensure that infection status was attributed correctly to individual mice, each mouse tested was segregated to a clean receptacle until a fresh fecal sample was produced. Fresh gloves were used to handle each individual mouse and corresponding sample. All surfaces were sterilized with Clidox® solution after collection. Mice were housed using a ventilated microisolator caging system with individual sterile water bottles. We found that every ITGb1 CKO breeder cage sampled tested positive for *T. muris* DNA (Figure 38, lanes 3-10).

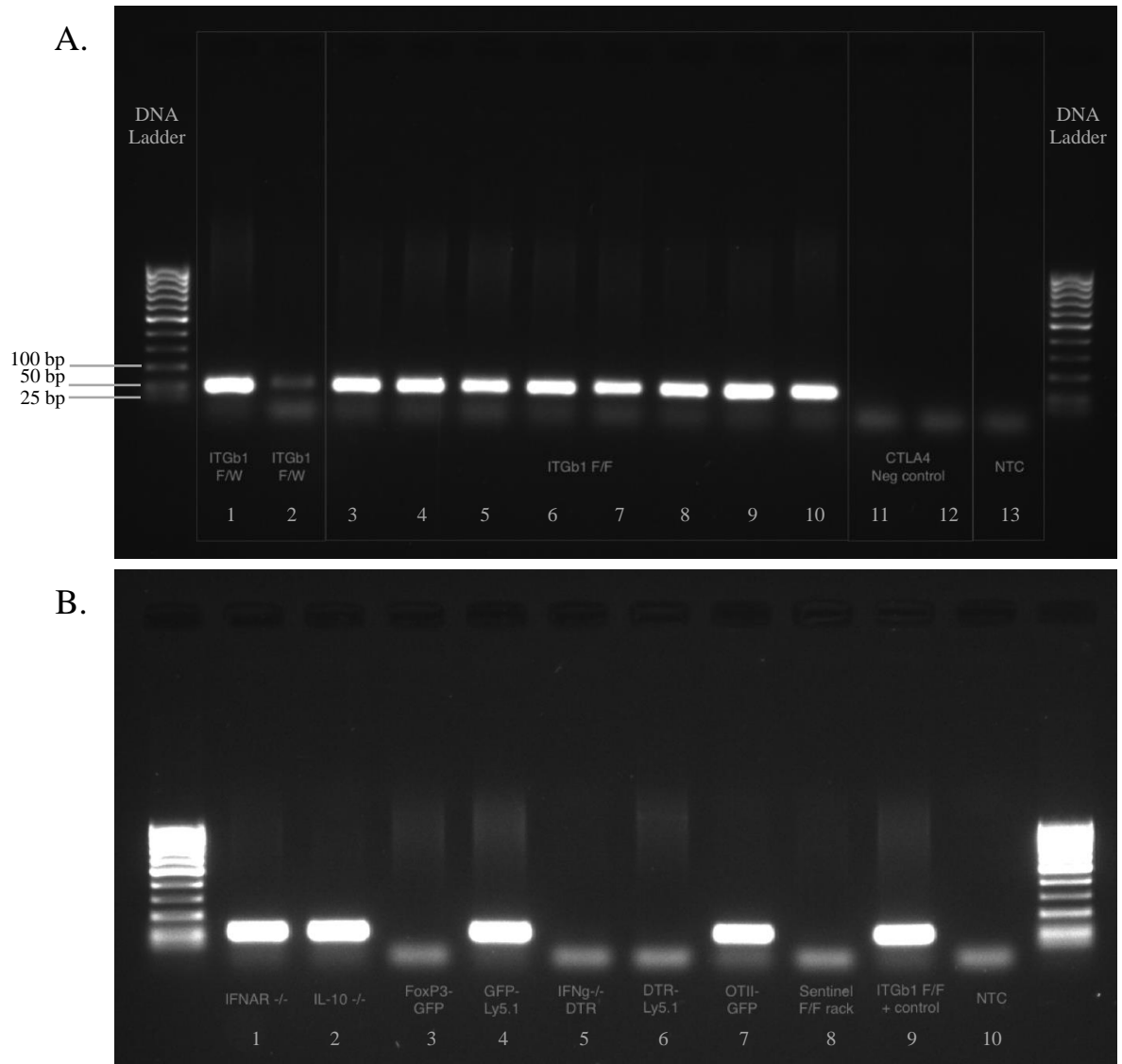


Figure 38. *T. muris* infection is easily transmitted but can evade detection by sentinel mice.

Furthermore, the CKO control mice generated to lack a flanking LoxP site and therefore have no gene deletion, also tested positive (Figure 38, lanes 1 and 2). This indiscriminate infection pattern suggests that the gene deletion in the CKO mice did not engender an immune deficit that made them especially susceptible to *T. muris* colonization. A different gene deletion strain, CTLA4 (C57BL/6 background) was previously tested commercially and so was utilized as a negative infection control (Figure 38, lanes 11 and 12). After determining that all of our

ITGb1 breeding stock was infected, we next tested a variety of other strains that were maintained on the same cage rack. We discovered that the infection had spread to other strains despite the lack of physical contact between ITGb1 CKO mice and other mice in the colony (Figure 38B, lanes 1-7). Most surprising of all was that the sentinel mice housed in the ITGb1 CKO rack consistently tested negative for *T. muris* DNA (Figure 38B, lane 8). As sentinel mice are used to detect infections that might arise in a colony and are routinely exposed to bedding from various cages housed in the same rack this finding was particularly disheartening. This “false” negative underscores the need to expose sentinels to fresh feces to most effectively surveil the colony.

Finally, it appeared that the strains that tested positive were seemingly infected at random when compared to those that escaped *T. muris* infection. However, when we visually plotted the layout of our breeder cage set up (Figure 39), we noted that breeder cages that were housed on the same side of the rack as the ITGb1 CKO strain were most likely to have tested positive for *T. muris* after fecal sampling.

1A	A	B	C	D	E	F	G	1B	A	B	C	D	E	F	G
1		XXX		XXX	000	000		1	000	XXX	ITGb1				
2	000			000		000	000	2	000		ITGb1	ITGb1			
3		000	000	000			000	3	000	XXX	ITGb1				
4	000	000	000	000	000	000	000	4			ITGb1			ITGb1	
5	000			000	000	000	000	5	000	XXX	ITGb1	XXX		ITGb1	
6	000		000	000	000			6	000		000	XXX			
7	000	000						7	000	000		XXX			
8								8	000						
9								9	XXX						
10								10	000						

Figure 39. *T. muris* spread was most evident while animals were housed in breeding racks.

This pattern appears to hold when mice were housed in different racks after weaning. The potentially increased vulnerability to infection during segregation for breeding may be a consequence of the increased mouse density in these cages. Although adult mice are housed <5 per cage, a dam and a pre-wean litter has no such limitation. This set-up potentially increases the number of individual mice shedding *T. muris* pseudocysts thereby increasing the likelihood of transmission between cages when users handle multiple cages at once.

### ***Metronidazole treatment in combination with a fostering plan can clear T. muris infection***

In determining how to proceed, we considered the time and financial investment necessary in clearing *T. muris* infection from our CKO model. One potential strategy, euthanasia of all affected cages and repurchasing the original floxed and Cre recombinase breeder pairs would be effective however, repopulating the colony would be both costly and time consuming. Furthermore because there is no live repository of floxed mice with our gene of interest it would take many months for the offspring of the cryopreserved specimens to become available. As such we decided to use metronidazole treatment in combination with a pup-fostering plan. Metronidazole serves as both an antibiotic and antiprotozoal medication often prescribed to treat human *Giardia lamblia*, *Clostridium difficile* and *Trichomonas vaginalis* infections<sup>164</sup>. Although very little has been published describing treatment strategies for *T. muris*, Roach et al showed that *T. muris* and *Tetratrichomonas microta* introduced from infected gerbils to mouse hosts were successfully treated by supplementing drinking water with metronidazole or tinidazole but not dimetridazole<sup>165</sup>. As such we purchased outbred Swiss Cr1:CD1 (ICR) CD-1® IGS breeders both for ease of differentiation of foster pups by coat color and because of anecdotal reports of CD-1 dams' efficient handling of large litter sizes. CD-1 mice were tested upon arrival and found

to be negative for fecal presence of *T. muris* DNA. CD-1 and CKO breeder pairs were subsequently set-up on different racks. After visual confirmation of the development of a mucus plug, breeder males were removed. Gestating dams were then monitored closely and metronidazole-supplemented water introduced approximately 5 days prior to birth. Upon arrival of pups in both CD-1 and CKO cages, CD-1 pups were removed from the breeder cage and replaced with the recently birthed CKO pups. Metronidazole supplementation was continued for 5 more days post pup transfer (Figure 40).

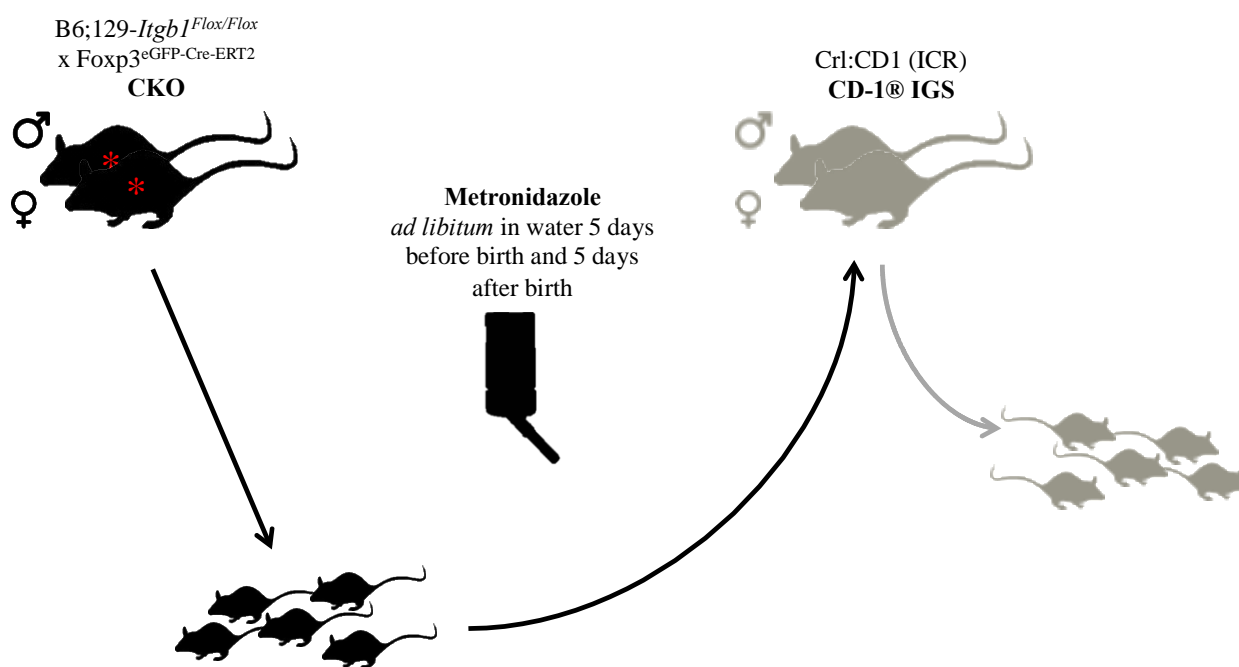


Figure 40. Schematic depicts the combination Metronidazole and fostering strategy used to clear CKO mice of *T. muris* infection.

After a total of 10 days of water supplementation, metronidazole treatment was ceased and pups remained under the care of the CD-1 foster dam until 21 days after birth. Foster pups were weaned, fecal samples collected and DNA extracted. PCR analyses of the collected fecal samples were negative for the presence of *T. muris* DNA indicating that the treatment strategy was

successful (Figure 41). Although, several studies both, mouse and human, have concluded that metronidazole does not increase the incidence of cancer in treated patients (or animals)<sup>166,167</sup> the Food and Drug Administration (FDA) has labeled metronidazole as a potential mutagen and teratogen<sup>168</sup>. As such, several rounds of backcrossing of the newly fostered *T. muris*-free CKO to WT C57Bl/6 mice were undertaken. This was both to limit potential mutagenic effects of metronidazole treatment and mitigate the effects of genetic bottlenecking as a result of the necessarily small number of pups fostered. Subsequent litters were genotyped to confirm retention of both the LoxP and Cre recombinase inserts.

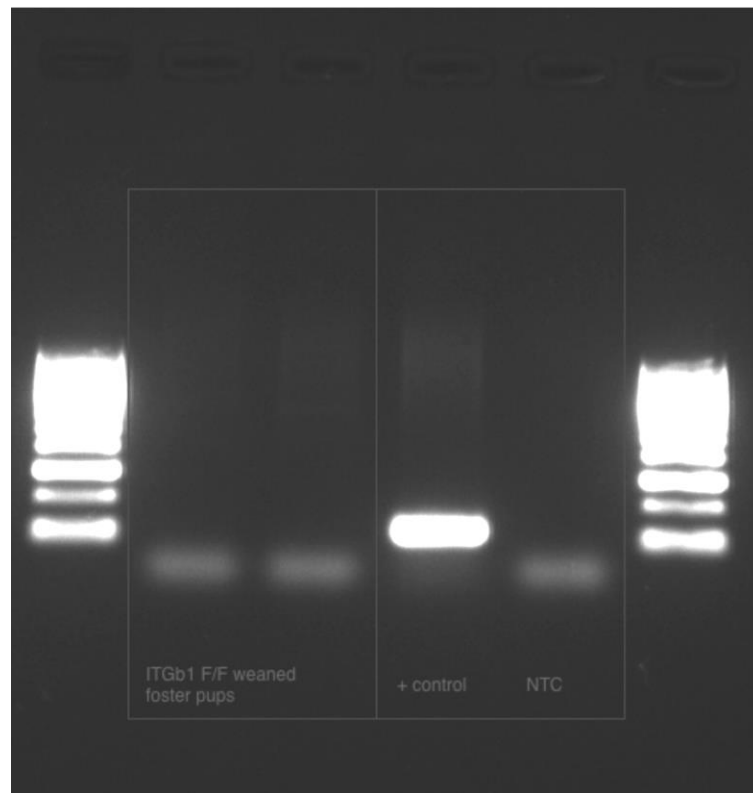


Figure 41. CKO foster pup fecal samples are free of *T. muris* DNA after metronidazole treatment.

### ***Concluding Remarks***

Maintaining a uniform specific pathogen-free (SPF) colony is critical in the generation of reliable and replicable data. This is especially true in studies investigating the effect of gene deletions in cells of the immune system. A confounding variable such as an ongoing infection can lead to the misguided characterization of misleading phenotypes. Here we report an instance of protozoan *Tritrichomonas muris* (*T. muris*) infection of regulatory T cell (Treg)-specific integrin  $\beta 1$  deleted mice in an SPF facility that was not detected through the use of sentinel mice. Although *T. muris* has historically been considered to be a commensal organism, we have found that this characterization may need to be reassessed. This may be especially necessary in instances of asymmetric infection where wild-type controls remain uninfected. We utilized concomitant treatment of infected pregnant dams and foster dams with metronidazole as well as collection and extraction of fresh fecal DNA followed by PCR detection of *T. muris* to successfully restore the original SPF status of the colony.

## BIBLIOGRAPHY

1. Pradeu T, Vivier E. The discontinuity theory of immunity. *Science Immunology*. *Science Immunology*; 2016 Jul 14;1(1):aag0479–9.
2. Eberl G. Immunity by equilibrium. *Nature Reviews Immunology*. 2016 Aug;16(8):524–32.
3. Gershon RK, Kondo K. Tolerance to Sheep Red Cells: Breakage with Thymocytes and Horse Red Cells. *Science*. American Association for the Advancement of Science; 1972 Mar 3;175(4025):996–7.
4. Fontenot JD, Gavin MA, Rudensky AY. Foxp3 programs the development and function of CD4+CD25+ regulatory T cells. *Nat. Immunol*. Nature Publishing Group; 2003 Apr 1;4(4):330–6.
5. Hori S, Nomura T, Sakaguchi S. Control of Regulatory T Cell Development by the Transcription Factor Foxp3. *Science*. American Association for the Advancement of Science; 2003 Feb 14;299(5609):1057–61.
6. Kim JM, Rasmussen JP, Rudensky AY. Regulatory T cells prevent catastrophic autoimmunity throughout the lifespan of mice. *Nat. Immunol*. 2007 Feb;8(2):191–7.
7. Abbas AK, Benoist C, Bluestone JA, Campbell DJ, Ghosh S, Hori S, et al. Regulatory T cells: recommendations to simplify the nomenclature. *Nat. Immunol*. Nature Research; 2013 Apr 1;14(4):307–8.
8. Lee H-M, Bautista JL, Hsieh C-S. Thymic and peripheral differentiation of regulatory T cells. *Advances in Immunology*. 2011;112:25–71.
9. Leventhal DS, Gilmore DC, Berger JM, Nishi S, Lee V, Malchow S, et al. Dendritic Cells Coordinate the Development and Homeostasis of Organ-Specific Regulatory T Cells. *Immunity*. 2016 Apr 19;44(4):847–59. PMID: PMC4842258
10. Rubtsov YP, Nieuwehuis RE, Josefowicz S, Li L, Darce J, Mathis D, et al. Stability of the Regulatory T Cell Lineage in Vivo. *Science*. American Association for the Advancement of Science; 2010 Sep 24;329(5999):1667–71.
11. Zhou X, Bailey-Bucktrout SL, Jeker LT, Penaranda C, Martínez-Llordella M, Ashby M, et al. Instability of the transcription factor Foxp3 leads to the generation of pathogenic memory T cells in vivo. *Nat. Immunol*. 2009 Jul 26;10(9):1000–7.
12. Bettini ML, Pan F, Bettini M, Finkelstein D, Rehg JE, Floess S, et al. Loss of Epigenetic Modification Driven by the Foxp3 Transcription Factor Leads to Regulatory T Cell Insufficiency. *Immunity*. 2012 May;36(5):717–30.
13. Verhagen J, Burton BR, Britton GJ, Shepard ER, Anderton SM, Wraith DC.

- Modification of the FoxP3 Transcription Factor Principally Affects Inducible T Regulatory Cells in a Model of Experimental Autoimmune Encephalomyelitis. *PLoS ONE*. Public Library of Science; 2013 Apr 8;8(4):e61334.
14. Mancebo C. The 2016 Barbara Deeb Lecture. 2016 Aug p. 1–1.
  15. Hori S. Lineage stability and phenotypic plasticity of Foxp3+ regulatory T cells. *Immunol. Rev.* 2014 May 1;259(1):159–72.
  16. Shevach EM, Thornton AM. tTregs, pTregs, and iTregs: similarities and differences. *Immunol. Rev.* 2014 May;259(1):88–102. PMID: PMC3982187
  17. Hoeppli RE, Wu D, Cook L, Levings MK. The environment of regulatory T cell biology: cytokines, metabolites, and the microbiome. *Front Immunol. Frontiers*; 2015;6:61. PMID: PMC4332351
  18. Yadav M, Bluestone JA, Stephan S. Peripherally Induced Tregs – Role in Immune Homeostasis and Autoimmunity. *Front Immunol. Frontiers*; 2013 Aug 7;4.
  19. Thornton AM, Korty PE, Tran DQ, Wohlfert EA, Murray PE, Belkaid Y, et al. Expression of Helios, an Ikaros Transcription Factor Family Member, Differentiates Thymic-Derived from Peripherally Induced Foxp3+ T Regulatory Cells. *The Journal of Immunology*. American Association of Immunologists; 2010 Apr 1;184(7):3433–41.
  20. Yadav M, Louvet C, Davini D, Gardner JM, Martínez-Llordella M, Bailey-Bucktrout S, et al. Neuropilin-1 distinguishes natural and inducible regulatory T cells among regulatory T cell subsets in vivo. *J Exp Med*. Rockefeller Univ Press; 2012 Sep 24;209(10):1713–22.
  21. Szurek E, Cebula A, Wojciech L, Pietrzak M, Rempala G, Kisielow P, et al. Differences in Expression Level of Helios and Neuropilin-1 Do Not Distinguish Thymus-Derived from Extrathymically-Induced CD4 + Foxp3 + Regulatory T Cells. *PLoS ONE*. Public Library of Science; 2015 Oct 23;10(10):e0141161.
  22. Singh K, Hjort M, Thorvaldson L, Sandler S. Concomitant analysis of Helios and Neuropilin-1 as a marker to detect thymic derived regulatory T cells in naïve mice. *Sci Rep*. Nature Publishing Group; 2015 Jan 14;5:7767.
  23. Smigiel KS, Richards E, Srivastava S, Thomas KR, Dudda JC, Klonowski KD, et al. CCR7 provides localized access to IL-2 and defines homeostatically distinct regulatory T cell subsets. *J Exp Med*. 2014 Jan 13;211(1):121–36. PMID: PMC3892972
  24. Sallusto F, Lenig D, Förster R, Lipp M, Lanzavecchia A. Two subsets of memory T lymphocytes with distinct homing potentials and effector functions. *Nature*. Nature Publishing Group; 1999 Oct 14;401(6754):708–12.
  25. Cheng G, Yuan X, Tsai MS, Podack ER, Yu A, Malek TR. IL-2 receptor signaling is essential for the development of Klrp1+ terminally differentiated T regulatory cells. *J*

Immunol. 2012 Aug 15;189(4):1780–91. PMID: PMC3411868

26. Toomer KH, Yuan X, Yang J, Dee MJ, Yu A, Malek TR. Developmental Progression and Interrelationship of Central and Effector Regulatory T Cell Subsets. *The Journal of Immunology*. American Association of Immunologists; 2016 May 1;196(9):3665–76.
27. Qureshi OS, Zheng Y, Nakamura K, Attridge K, Manzotti C, Schmidt EM, et al. Trans-Endocytosis of CD80 and CD86: A Molecular Basis for the Cell-Extrinsic Function of CTLA-4. *Science*. American Association for the Advancement of Science; 2011 Apr 29;332(6029):600–3. PMID: PMC3198051
28. Francois V, Shehade H, Acolty V, Preyat N, Delrée P, Moser M, et al. Intestinal immunopathology is associated with decreased CD73-generated adenosine during lethal infection. *Mucosal Immunol*. Nature Publishing Group; 2015 Jul 1;8(4):773–84.
29. Rubtsov YP, Rasmussen JP, Chi EY, Fontenot J, Castelli L, Ye X, et al. Regulatory T cell-derived interleukin-10 limits inflammation at environmental interfaces. *Immunity*. 2008 Apr;28(4):546–58.
30. Li MO, Wan YY, Flavell RA. T cell-produced transforming growth factor-beta1 controls T cell tolerance and regulates Th1- and Th17-cell differentiation. *Immunity*. 2007 May;26(5):579–91.
31. Collison LW, Workman CJ, Kuo TT, Boyd K, Wang Y, Vignali KM, et al. The inhibitory cytokine IL-35 contributes to regulatory T-cell function. *Nature*. 2007 Nov 22;450(7169):566–9.
32. Yuan X, Cheng G, Malek TR. The importance of regulatory T-cell heterogeneity in maintaining self-tolerance. *Immunol. Rev.* 2014 May;259(1):103–14. PMID: PMC3983566
33. Koch MA, Tucker-Heard G, Perdue NR, Killebrew JR, Urdahl KB, Campbell DJ. The transcription factor T-bet controls regulatory T cell homeostasis and function during type 1 inflammation. *Nat. Immunol*. Nature Publishing Group; 2009 Jun 1;10(6):595–602.
34. Chaudhry A, Rudra D, Treuting P, Samstein RM, Liang Y, Kas A, et al. CD4+ Regulatory T Cells Control TH17 Responses in a Stat3-Dependent Manner. *Science*. American Association for the Advancement of Science; 2009 Nov 13;326(5955):986–91.
35. Zheng Y, Chaudhry A, Kas A, deRoos P, Kim JM, Chu T-T, et al. Regulatory T-cell suppressor program co-opts transcription factor IRF4 to control TH2 responses. *Nature*. Nature Publishing Group; 2009 Mar 19;458(7236):351–6.
36. Shafiani S, Dinh C, Ertelt JM, Moguche AO, Siddiqui I, Smigiel KS, et al. Pathogen-Specific Treg Cells Expand Early during Mycobacterium tuberculosis Infection but Are Later Eliminated in Response to Interleukin-12. *Immunity*. 2013 Jun;38(6):1261–70.

37. Shafiani S, Tucker-Heard G, Kariyone A, Takatsu K, Urdahl KB. Pathogen-specific regulatory T cells delay the arrival of effector T cells in the lung during early tuberculosis. *J Exp Med*. Rockefeller Univ Press; 2010 Jul 5;207(7):1409–20.
38. Urdahl KB, Shafiani S, Ernst JD. Initiation and regulation of T-cell responses in tuberculosis. *Mucosal Immunol*. Nature Publishing Group; 2011 May 1;4(3):288–93.
39. Filippi CM, Estes EA, Oldham JE, Herrath von MG. Immunoregulatory mechanisms triggered by viral infections protect from type 1 diabetes in mice. *J. Clin. Invest*. American Society for Clinical Investigation; 2009 Jun 1;119(6):1515–23.
40. Diana J, Brezar V, Beaudoin L, Dalod M, Mellor A, Tafuri A, et al. Viral infection prevents diabetes by inducing regulatory T cells through NKT cell–plasmacytoid dendritic cell interplay. *J Exp Med*. Rockefeller Univ Press; 2011 Apr 11;208(4):729–45.
41. MacDonald AS, Araujo MI, Pearce EJ. Immunology of Parasitic Helminth Infections. *Infect. Immun*. American Society for Microbiology; 2002 Feb 1;70(2):427–33.
42. Ehrlich A, Castilho TM, Goldsmith-Pestana K, Chae W-J, Bothwell ALM, Sparwasser T, et al. The Immunotherapeutic Role of Regulatory T Cells in *Leishmania (Viannia) panamensis* Infection. *The Journal of Immunology*. American Association of Immunologists; 2014 Sep 15;193(6):2961–70.
43. Belkaid Y. Regulatory T cells and infection: a dangerous necessity. *Nature Reviews Immunology*. 2007 Nov;7(11):875–88.
44. Veiga-Parga T, Suryawanshi A, Mulik S, Giménez F, Sharma S, Sparwasser T, et al. On the Role of Regulatory T Cells during Viral-Induced Inflammatory Lesions. *The Journal of Immunology*. American Association of Immunologists; 2012 Dec 15;189(12):5924–33.
45. Haeryfar SMM, DiPaolo RJ, Tschärke DC, Bennink JR, Yewdell JW. Regulatory T cells suppress CD8+ T cell responses induced by direct priming and cross-priming and moderate immunodominance disparities. *The Journal of Immunology*. 2005 Mar 15;174(6):3344–51.
46. Lanteri MC, O’Brien KM, Purtha WE, Cameron MJ, Lund JM, Owen RE, et al. Tregs control the development of symptomatic West Nile virus infection in humans and mice. *J. Clin. Invest*. American Society for Clinical Investigation; 2009 Nov 2;119(11):3266–77. PMID: PMC2769173
47. Lund JM, Hsing L, Pham TT, Rudensky AY. Coordination of Early Protective Immunity to Viral Infection by Regulatory T Cells. *Science*. American Association for the Advancement of Science; 2008 May 30;320(5880):1220–4.
48. Soerens AG, Da Costa A, Lund JM. Regulatory T cells are essential to promote proper CD4 T-cell priming upon mucosal infection. *Mucosal Immunol*. 2016 Mar 23.

49. Belkaid Y, Piccirillo CA, Mendez S, Shevach EM, Sacks DL. CD4<sup>+</sup>CD25<sup>+</sup> regulatory T cells control *Leishmania* major persistence and immunity. *Nature*. Nature Publishing Group; 2002 Dec 5;420(6915):502–7.
50. Fernandez MA, Yu U, Zhang G, White R, Sparwasser T, Alexander SI, et al. Treg depletion attenuates the severity of skin disease from ganglionic spread after HSV-2 flank infection. *Virology*. 2013 Dec;447(1-2):9–20.
51. Pace L, Tempez A, Arnold-Schrauf C, Lemaitre F, Bousso P, Fetler L, et al. Regulatory T cells increase the avidity of primary CD8<sup>+</sup> T cell responses and promote memory. *Science*. American Association for the Advancement of Science; 2012 Oct 26;338(6106):532–6.
52. Zacccone P, Burton O, Miller N, Jones FM, Dunne DW, Cooke A. *Schistosoma mansoni* egg antigens induce Treg that participate in diabetes prevention in NOD mice. *European Journal of Immunology*. WILEY- VCH Verlag; 2009 Apr 1;39(4):1098–107.
53. Jiang TT, Chaturvedi V, Ertelt JM, Kinder JM, Clark DR, Valent AM, et al. Regulatory T Cells: New Keys for Further Unlocking the Enigma of Fetal Tolerance and Pregnancy Complications. *The Journal of Immunology*. American Association of Immunologists; 2014 Jun 1;192(11):4949–56.
54. Pabst O, Mowat AM. Oral tolerance to food protein. *Mucosal Immunol*. Nature Publishing Group; 2012 May 1;5(3):232–9.
55. Honda K, Littman DR. The Microbiome in Infectious Disease and Inflammation. <http://dx.doi.org/10.1146/annurev-immunol-020711-074937>. *Annual Reviews*; 2012 Mar 26;30(1):759–95.
56. Belkaid Y, Tamoutounour S. The influence of skin microorganisms on cutaneous immunity. *Nature Reviews Immunology*. Nature Research; 2016 Jun 1;16(6):353–66.
57. Mougiakakos D, Choudhury A, Lladser A, Kiessling R, Johansson CC. Regulatory T Cells in Cancer. Elsevier; 2010. p. 57–117.
58. Petersen LR, Brault AC, Nasci RS. West Nile Virus: Review of the Literature. *JAMA*. American Medical Association; 2013 Jul 17;310(3):308–15.
59. Petersen LR, Carson PJ, Biggerstaff BJ, CUSTER B, BORCHARDT SM, BUSCH MP. Estimated cumulative incidence of West Nile virus infection in US adults, 1999–2010. *Epidemiology and Infection*. Cambridge University Press; 2013 Mar 1;141(03):591–5.
60. Suthar MS, Diamond MS, Gale M. West Nile virus infection and immunity. *Nat. Rev. Microbiol*. 2013 Feb;11(2):115–28.
61. Murray K, Walker C, Herrington E, Lewis JA, McCormick J, Beasley DWC, et al. Persistent infection with West Nile virus years after initial infection. *J Infect Dis*. Oxford University Press; 2010 Jan 1;201(1):2–4. PMID: PMC2791189

62. Omalu BI, Shakir AA, Wang G, Lipkin WI, Wiley CA. Fatal fulminant pan-meningo-polioencephalitis due to West Nile virus. *Brain Pathol.* 2003 Oct;13(4):465–72.
63. Sitati EM, Diamond MS. CD4+ T-cell responses are required for clearance of West Nile virus from the central nervous system. *J. Virol.* 2006 Dec;80(24):12060–9. PMID: PMC1676257
64. Austin SK, Dowd KA. B cell response and mechanisms of antibody protection to West Nile virus. *Viruses.* 2014;6(3):1015–36. PMID: PMC3970136
65. Lim JK, Obara CJ, Rivollier A, Pletnev AG, Kelsall BL, Murphy PM. Chemokine receptor Ccr2 is critical for monocyte accumulation and survival in West Nile virus encephalitis. *J. Immunol.* 2011 Jan 1;186(1):471–8. PMID: PMC3402345
66. Wang Y, Lobigs M, Lee E, Mullbacher A. CD8 T Cells Mediate Recovery and Immunopathology in West Nile Virus Encephalitis. *J. Virol.* 2003;77(24):13323–34.
67. James EA, Gates TJ, LaFond RE, Yamamoto S, Ni C, Mai D, et al. Neuroinvasive West Nile Infection Elicits Elevated and Atypically Polarized T Cell Responses That Promote a Pathogenic Outcome. *PLoS Pathog.* 2016 Jan;12(1):e1005375. PMID: PMC4721872
68. Graham JB, Da Costa A, Lund JM. Regulatory T cells shape the resident memory T cell response to virus infection in the tissues. *J. Immunol. American Association of Immunologists;* 2014 Jan 15;192(2):683–90. PMID: PMC3894741
69. Jensen S, Thomsen AR. Sensing of RNA viruses: a review of innate immune receptors involved in recognizing RNA virus invasion. *J. Virol. American Society for Microbiology;* 2012 Mar;86(6):2900–10. PMID: PMC3302314
70. Suthar MS, Ma DY, Thomas S, Lund JM, Zhang N, Daffis S, et al. IPS-1 Is Essential for the Control of West Nile Virus Infection and Immunity. *PLoS Pathog.* 2010;6(2):e1000757.
71. Vijay R, Zhao J, Gale M. MAVS expressed by hematopoietic cells is critical for control of West Nile virus infection and pathogenesis. Sandri-Goldin RM, editor. *Journal of ...* 2016;90(16):7098–108.
72. Michallet M-C, Rota G, Maslowski K, Guarda G. Innate receptors for adaptive immunity. *Curr. Opin. Microbiol.* 2013 Jun;16(3):296–302.
73. Bendigs S, Salzer U, Lipford GB, Wagner H, Heeg K. CpG-oligodeoxynucleotides co-stimulate primary T cells in the absence of antigen-presenting cells. *European Journal of Immunology.* 1999 Apr;29(4):1209–18.
74. Caron G, Duluc D, Frémaux I, Jeannin P, David C, Gascan H, et al. Direct Stimulation of Human T Cells via TLR5 and TLR7/8: Flagellin and R-848 Up-Regulate Proliferation and IFN- $\gamma$  Production by Memory CD4+ T Cells. *The Journal of Immunology. American Association of Immunologists;* 2005 Aug 1;175(3):1551–7.

75. Gelman AE, LaRosa DF, Zhang J, Walsh PT, Choi Y, Sunyer JO, et al. The adaptor molecule MyD88 activates PI-3 kinase signaling in CD4+ T cells and enables CpG oligodeoxynucleotide-mediated costimulation. *Immunity*. 2006 Nov;25(5):783–93. PMID: PMC2840381
76. Gelman AE, Zhang J, Choi Y, Turka LA. Toll-Like Receptor Ligands Directly Promote Activated CD4+ T Cell Survival. *The Journal of Immunology*. American Association of Immunologists; 2004 May 15;172(10):6065–73. PMID: PMC2833313
77. Imanishi T, Hara H, Suzuki S, Suzuki N, Akira S, Saito T. Cutting Edge: TLR2 Directly Triggers Th1 Effector Functions. *The Journal of Immunology*. American Association of Immunologists; 2007 Jun 1;178(11):6715–9.
78. Komai-Koma M, Jones L, Ogg GS, Xu D, Liew FY. TLR2 is expressed on activated T cells as a costimulatory receptor. *Proc. Natl. Acad. Sci. U.S.A.* 2004 Mar 2;101(9):3029–34. PMID: PMC365739
79. Reynolds JM, Dong C. Toll-like receptor regulation of effector T lymphocyte function. *Trends in Immunology*. 2013 Oct;34(10):511–9.
80. Peng G, Guo Z, Kiniwa Y, Voo KS, Peng W, Fu T, et al. Toll-like receptor 8-mediated reversal of CD4+ regulatory T cell function. *Science*. 2005 Aug 26;309(5739):1380–4.
81. Nyirenda MH, Sanvito L, Darlington PJ, O'Brien K, Zhang G-X, Constantinescu CS, et al. TLR2 Stimulation Drives Human Naive and Effector Regulatory T Cells into a Th17-Like Phenotype with Reduced Suppressive Function. *The Journal of Immunology*. American Association of Immunologists; 2011 Sep 1;187(5):2278–90.
82. Caramalho I, Lopes-Carvalho T, Ostler D, Zelenay S, Haury M, Demengeot J. Regulatory T Cells Selectively Express Toll-like Receptors and Are Activated by Lipopolysaccharide. *J Exp Med*. Rockefeller Univ Press; 2003 Feb 17;197(4):403–11.
83. Anz D, Koelzer VH, Moder S, Thaler R, Schwerd T, Lahl K, et al. Immunostimulatory RNA Blocks Suppression by Regulatory T Cells. *The Journal of Immunology*. American Association of Immunologists; 2010 Jan 15;184(2):939–46.
84. Li X-D, Chiu Y-H, Ismail AS, Behrendt CL, Wight-Carter M, Hooper LV, et al. Mitochondrial antiviral signaling protein (MAVS) monitors commensal bacteria and induces an immune response that prevents experimental colitis. *Proc. Natl. Acad. Sci. U.S.A.* 2011 Oct 18;108(42):17390–5. PMID: PMC3198352
85. Wan YY, Flavell RA. Regulatory T-cell functions are subverted and converted owing to attenuated Foxp3 expression. *Nature*. 2007 Feb 15;445(7129):766–70.
86. Chauhan SK, Saban DR, Lee HK, Dana R. Levels of Foxp3 in Regulatory T Cells Reflect Their Functional Status in Transplantation. *The Journal of Immunology*. American Association of Immunologists; 2009 Jan 1;182(1):148–53.

87. Xu L, Kitani A, Fuss I, Strober W. Cutting Edge: Regulatory T Cells Induce CD4+CD25–Foxp3– T Cells or Are Self-Induced to Become Th17 Cells in the Absence of Exogenous TGF- $\beta$ . *The Journal of Immunology*. American Association of Immunologists; 2007 Jun 1;178(11):6725–9.
88. Yang XO, Nurieva R, Martinez GJ, Kang HS, Chung Y, Pappu BP, et al. Molecular Antagonism and Plasticity of Regulatory and Inflammatory T Cell Programs. *Immunity*. 2008 Jul;29(1):44–56. PMID: PMC2630532
89. Omalu BI, Shakir AA, Wang G, Lipkin WI, Wiley CA. Fatal fulminant pan-meningo-polioencephalitis due to West Nile virus. *Brain Pathol*. 2003 Oct;13(4):465–72.
90. Vignali DAA, Collison LW, Workman CJ. How regulatory T cells work. *Nature Reviews Immunology*. Nature Publishing Group; 2008 Jul 1;8(7):523–32.
91. Shrestha B, Diamond MS. Role of CD8+ T cells in control of West Nile virus infection. *J. Virol*. American Society for Microbiology; 2004 Aug;78(15):8312–21. PMID: PMC446114
92. Campbell DJ, Koch MA. Phenotypical and functional specialization of FOXP3+ regulatory T cells. *Nature Reviews Immunology*. 2011 Feb;11(2):119–30. PMID: PMC3289970
93. Nish SA, Schenten D, Wunderlich FT, Pope SD, Gao Y, Hoshi N, et al. T cell-intrinsic role of IL-6 signaling in primary and memory responses. *Elife*. 2014;3:e01949. PMID: PMC4046568
94. Zheng SG, Wang J, Horwitz DA. Cutting edge: Foxp3+CD4+CD25+ regulatory T cells induced by IL-2 and TGF-beta are resistant to Th17 conversion by IL-6. *The Journal of Immunology*. 2008 Jun 1;180(11):7112–6.
95. Goodman WA, Levine AD, Massari JV, Sugiyama H, McCormick TS, Cooper KD. IL-6 signaling in psoriasis prevents immune suppression by regulatory T cells. *J. Immunol*. American Association of Immunologists; 2009 Sep 1;183(5):3170–6. PMID: PMC2903207
96. Lanteri MC, Heitman JW, Owen RE, Busch T, Geftter N, Kiely N, et al. Comprehensive analysis of west nile virus-specific T cell responses in humans. *J Infect Dis*. Oxford University Press; 2008 May 1;197(9):1296–306.
97. Hsieh C-S, Liang Y, Tzwnik AJ, Self SG, Liggitt D, Rudensky AY. Recognition of the Peripheral Self by Naturally Arising CD25+ CD4+ T Cell Receptors. *Immunity*. 2004 Aug;21(2):267–77.
98. Suffia IJ, Reckling SK, Piccirillo CA, Goldszmid RS, Belkaid Y. Infected site-restricted Foxp3+ natural regulatory T cells are specific for microbial antigens. *J Exp Med*. 2006 Mar 20;203(3):777–88. PMID: PMC2118233

99. Srivastava S, Koch MA, Pepper M, Campbell DJ. Type I interferons directly inhibit regulatory T cells to allow optimal antiviral T cell responses during acute LCMV infection. *J Exp Med*. Rockefeller Univ Press; 2014 May 5;211(5):961–74.
100. Lee SE, Li X, Kim JCK, Lee J, Navajas JMG, Hong SH, et al. Type I Interferons Maintain Foxp3 Expression and T-Regulatory Cell Functions Under Inflammatory Conditions in Mice. *Gastroenterology*. 2012;143(1):145–54.
101. Fredericksen BL, Keller BC, Fornek J, Katze MG, Gale M. Establishment and maintenance of the innate antiviral response to West Nile Virus involves both RIG-I and MDA5 signaling through IPS-1. *J. Virol*. 2008 Jan;82(2):609–16. PMID: PMC2224571
102. Kato H, Takeuchi O, Sato S, Yoneyama M, Yamamoto M, Matsui K, et al. Differential roles of MDA5 and RIG-I helicases in the recognition of RNA viruses. *Nature*. 2006 May 4;441(7089):101–5.
103. Loo Y-M, Fornek J, Crochet N, Bajwa G, Perwitasari O, Martinez-Sobrido L, et al. Distinct RIG-I and MDA5 Signaling by RNA Viruses in Innate Immunity. *J. Virol*. American Society for Microbiology; 2008 Jan 1;82(1):335–45.
104. Pribila JT, Quale AC, Mueller KL, Shimizu Y. Integrins and T cell-mediated immunity. *Annu. Rev. Immunol*. 2004;22:157–80.
105. Srichai MB, Zent R. Integrin Structure and Function. *Cell-Extracellular Matrix Interactions in Cancer*. 2009. p. 19–41.
106. Vestweber D. How leukocytes cross the vascular endothelium. *Nature Reviews Immunology*. 2015 Nov;15(11):692–704.
107. Chataway J, Miller DH. Natalizumab therapy for multiple sclerosis. *Neurotherapeutics*. 2013 Jan;10(1):19–28. PMID: PMC3557363
108. Yednock TA, Cannon C, Fritz LC, Sanchez-Madrid F, Steinman L, Karin N. Prevention of experimental autoimmune encephalomyelitis by antibodies against  $\alpha 4\beta 1$  integrin. *Nature*. 1992;356(6364):63–6.
109. Griffith JW, Luster AD. Targeting cells in motion: Migrating toward improved therapies. *European Journal of Immunology*. 2013 Jun 1;43(6):1430–5.
110. Rothhammer V, Heink S, Petermann F, Srivastava R, Claussen MC, Hemmer B, et al. Th17 lymphocytes traffic to the central nervous system independently of  $\alpha 4$  integrin expression during EAE. *J Exp Med*. 2011 Nov 21;208(12):2465–76. PMID: PMC3256959
111. Kleinewietfeld M, Hafler DA. Regulatory T cells in autoimmune neuroinflammation. *Immunol. Rev*. 2014 May 1;259(1):231–44.

112. Stenner M-P, Waschbisch A, Buck D, Doerck S, Einsele H, Toyka KV, et al. Effects of natalizumab treatment on Foxp3+ T regulatory cells. Unutmaz D, editor. PLoS ONE. Public Library of Science; 2008;3(10):e3319. PMID: PMC2553177
113. Glatigny S, Duhén R, Arbelaez C, Kumari S, Bettelli E. Integrin alpha L controls the homing of regulatory T cells during CNS autoimmunity in the absence of integrin alpha 4. *Sci Rep*. 2015;5:7834. PMID: PMC4296287
114. OHNO S, WOLF U, ATKIN NB. EVOLUTION FROM FISH TO MAMMALS BY GENE DUPLICATION. *Hereditas*. Blackwell Publishing Ltd; 1968 Feb 1;59(1):169–87.
115. Espinosa-Cantú A, Ascencio D, Barona-Gómez F, DeLuna A. Gene duplication and the evolution of moonlighting proteins. *Frontiers in Genetics*. 2015;6.
116. Cervantes-Barragán L, Firner S, Bechmann I, Waisman A, Lahl K, Sparwasser T, et al. Regulatory T Cells Selectively Preserve Immune Privilege of Self-Antigens during Viral Central Nervous System Infection. *The Journal of Immunology*. 2012 Mar 9;188(8):3678–85.
117. DeNucci CC, Shimizu Y.  $\beta$ 1 integrin is critical for the maintenance of antigen-specific CD4 T cells in the bone marrow but not long-term immunological memory. *The Journal of Immunology*. American Association of Immunologists; 2011 Apr 1;186(7):4019–26. PMID: PMC3062718
118. DeNucci CC, Pagán AJ, Mitchell JS, Shimizu Y. Control of alpha4beta7 integrin expression and CD4 T cell homing by the beta1 integrin subunit. *The Journal of Immunology*. 2010 Mar 1;184(5):2458–67. PMID: PMC2824783
119. Habtezion A, Nguyen LP, Hadeiba H, Butcher EC. Leukocyte Trafficking to the Small Intestine and Colon. *Gastroenterology*. 2016 Feb;150(2):340–54. PMID: PMC4758453
120. Fiorino G, Gilardi D, Danese S. The clinical potential of etrolizumab in ulcerative colitis: hypes and hopes. *Therap Adv Gastroenterol*. 2016 Jul;9(4):503–12. PMID: PMC4913345
121. Wyant T, Fedyk E, Abhyankar B. An Overview of the Mechanism of Action of the Monoclonal Antibody Vedolizumab. *J Crohns Colitis*. 2016 Jun 1.
122. McNally A, Hill GR, Sparwasser T, Thomas R, Steptoe RJ. CD4+CD25+ regulatory T cells control CD8+ T-cell effector differentiation by modulating IL-2 homeostasis. *Proc Natl. Acad. Sci. U.S.A.* 2011 May 3;108(18):7529–34. PMID: PMC3088596
123. Liu Z, Gerner MY, Van Panhuys N, Levine AG, Rudensky AY, Germain RN. Immune homeostasis enforced by co-localized effector and regulatory T cells. *Nature*. *Nature Research*; 2015 Dec 10;528(7581):225–30. PMID: PMC4702500
124. Beura LK, Hamilton SE, Bi K, Schenkel JM, Odumade OA, Casey KA, et al.

- Normalizing the environment recapitulates adult human immune traits in laboratory mice. *Nature. Nature Research*; 2016 Apr 28;532(7600):512–6.
125. Martin B, Auffray C, Delpoux A, Pommier A, Durand A, Charvet C, et al. Highly self-reactive naive CD4 T cells are prone to differentiate into regulatory T cells. *Nat Commun.* 2013;4:2209.
  126. Walunas TL, Bruce DS, Dustin L, Loh DY. Ly-6C is a marker of memory CD8+ T cells. ... of *Immunology.* 1995.
  127. Ichii H, Sakamoto A, Hatano M, Okada S. Role for Bcl-6 in the generation and maintenance of memory CD8+ T cells. *Nature.* 2002;3(6):558–63.
  128. Brien JD, Uhrlaub JL. Protective capacity and epitope specificity of CD8+ T cells responding to lethal West Nile virus infection. *European Journal of Immunology.* 2007;37(7):1855–63.
  129. Kaech SM, Tan JT, Wherry EJ, Konieczny BT, Surh CD, Ahmed R. Selective expression of the interleukin 7 receptor identifies effector CD8 T cells that give rise to long-lived memory cells. *Nat. Immunol.* 2003 Dec;4(12):1191–8.
  130. Sun JC, Bevan MJ. Defective CD8 T cell memory following acute infection without CD4 T cell help. *Science.* 2003;300(5617):339–42.
  131. Mittelbrunn M, Molina A, Escribese MM, Yáñez-Mó M, Escudero E, Ursa Á, et al. VLA-4 integrin concentrates at the peripheral supramolecular activation complex of the immune synapse and drives T helper 1 responses. *Proc. Natl. Acad. Sci. U.S.A. National Acad Sciences*; 2004 Jul 27;101(30):11058–63.
  132. Bachmann MF, McKall-Faienza K, Schmits R, Bouchard D, Beach J, Speiser DE, et al. Distinct Roles for LFA-1 and CD28 during Activation of Naive T Cells: Adhesion versus Costimulation. *Immunity.* 1997 Oct;7(4):549–57.
  133. Shimizu Y. LFA-1: more than just T cell Velcro. *Nat. Immunol.* 2003 Nov;4(11):1052–4.
  134. Onishi Y, Fehervari Z, Yamaguchi T, Sakaguchi S. Foxp3+ natural regulatory T cells preferentially form aggregates on dendritic cells in vitro and actively inhibit their maturation. *Proc. Natl. Acad. Sci. U.S.A. National Acad Sciences*; 2008 Jul 22;105(29):10113–8.
  135. Thauland TJ, Koguchi Y, Dustin ML, Parker DC. CD28–CD80 Interactions Control Regulatory T Cell Motility and Immunological Synapse Formation. *The Journal of Immunology. American Association of Immunologists*; 2014 Dec 15;193(12):5894–903.
  136. Hogquist KA, Jameson SC. The self-obsession of T cells: how TCR signaling thresholds affect fate “decisions” and effector function. *Nat. Immunol. Nature Research*; 2014 Sep 1;15(9):815–23.

137. Fulton RB, Hamilton SE, Xing Y, Best JA, Goldrath AW, Hogquist KA, et al. The TCR's sensitivity to self peptide-MHC dictates the ability of naive CD8(+) T cells to respond to foreign antigens. *Nat. Immunol.* 2015 Jan;16(1):107–17. PMID: PMC4270846
138. Manda K, Glasow A, Paape D, Hildebrandt G. Effects of ionizing radiation on the immune system with special emphasis on the interaction of dendritic and T cells. *Front Oncol. Frontiers*; 2012;2:102. PMID: PMC3426842
139. Pollizzi KN, Powell JD. Integrating canonical and metabolic signalling programmes in the regulation of T cell responses. *Nature Reviews Immunology.* 2014 Jun 25;14(7):435–46.
140. Boehm F, Martin M, Kesselring R, Schiechl G, Geissler EK, Schlitt H-J, et al. Deletion of Foxp3 + regulatory T cells in genetically targeted mice supports development of intestinal inflammation. *BMC Gastroenterology* 2012 12:1. *BioMed Central*; 2012 Jul 31;12(1):1.
141. Glatigny S, Duhon R, Oukka M, Bettelli E. Cutting edge: loss of  $\alpha 4$  integrin expression differentially affects the homing of Th1 and Th17 cells. *J. Immunol. American Association of Immunologists*; 2011 Dec 15;187(12):6176–9. PMID: PMC3237912
142. Laidlaw BJ, Craft JE, Kaech SM. The multifaceted role of CD4+ T cells in CD8+ T cell memory. *Nature Reviews Immunology. Nature Research*; 2016 Feb 1;16(2):102–11.
143. Collison LW, Vignali DAA. In vitro Treg suppression assays. *Methods Mol. Biol.* 2011;707:21–37. PMID: PMC3043080
144. Iwata M, Hirakiyama A, Eshima Y, Kagechika H, Kato C, Song S-Y. Retinoic Acid Imprints Gut-Homing Specificity on T Cells. *Immunity.* 2004 Oct;21(4):527–38.
145. Nguyen LP, Pan J, Dinh TT, Hadeiba H, O'Hara E III, Ebtikar A, et al. Role and species-specific expression of colon T cell homing receptor GPR15 in colitis. *Nat. Immunol. Nature Research*; 2015 Feb 1;16(2):207–13.
146. Iwata M. Retinoic acid production by intestinal dendritic cells and its role in T-cell trafficking. *Seminars in Immunology.* 2009 Feb;21(1):8–13.
147. Travis MA, Reizis B, Melton AC, Masteller E, Tang Q, Proctor JM, et al. Loss of integrin  $\alpha(v)\beta 8$  on dendritic cells causes autoimmunity and colitis in mice. *Nature.* 2007 Sep 20;449(7160):361–5. PMID: PMC2670239
148. Worthington JJ, Czajkowska BI, Melton AC, Travis MA. Intestinal Dendritic Cells Specialize to Activate Transforming Growth Factor- $\beta$  and Induce Foxp3+ Regulatory T Cells via Integrin  $\alpha v\beta 8$ . *Gastroenterology.* 2011 Nov;141(5):1802–12.
149. Sun C-M, Hall JA, Blank RB, Bouladoux N, Oukka M, Mora JR, et al. Small intestine lamina propria dendritic cells promote de novo generation of Foxp3 T reg cells via

- retinoic acid. *J Exp Med. Rockefeller Univ Press*; 2007 Aug 6;204(8):1775–85.
150. Ohta A, Kini R, Ohta A, Subramanian M, Madasu M, Sitkovsky M. The development and immunosuppressive functions of CD4<sup>+</sup> CD25<sup>+</sup> FoxP3<sup>+</sup> regulatory T cells are under influence of the adenosine-A2A adenosine receptor pathway. *Front Immunol. Frontiers*; 2012 Jul 5;3.
  151. Tanoue T, Atarashi K, Honda K. Development and maintenance of intestinal regulatory T cells. *Nature Reviews Immunology*. 2016;16(5):295–309.
  152. Verhagen J, Wraith DC. Comment on “Expression of Helios, an Ikaros Transcription Factor Family Member, Differentiates Thymic-Derived from Peripherally Induced Foxp3<sup>+</sup> T Regulatory Cells.” *The Journal of Immunology. American Association of Immunologists*; 2010 Dec 15;185(12):7129–9.
  153. Kang B, Kim K-M, Kang C-Y. Oral Tolerance by a High Dose OVA in BALB/c Mice is More Pronounced and Persistent in Th2-Mediated Immune Responses than in Th 1 Responses. *Immunobiology. Urban & Fischer*; 1999 Jun 1;200(2):264–76.
  154. Cepicka I, Hampl V, Kulda J, Flegr J. New evolutionary lineages, unexpected diversity, and host specificity in the parabasalid genus *Tetratrichomonas*. *Mol. Phylogenet. Evol.* 2006 May;39(2):542–51.
  155. Haluszczak C, Akue AD, Hamilton SE, Johnson LDS, Pujanauski L, Teodorovic L, et al. The antigen-specific CD8<sup>+</sup> T cell repertoire in unimmunized mice includes memory phenotype cells bearing markers of homeostatic expansion. *J Exp Med. Rockefeller Univ Press*; 2009 Feb 16;206(2):435–48. PMID: PMC2646575
  156. Jameson SC, Lee YJ, Hogquist KA. Innate memory T cells. *Advances in Immunology. Elsevier*; 2015;126:173–213.
  157. Lee J-Y, Hamilton SE, Akue AD, Hogquist KA, Jameson SC. Virtual memory CD8 T cells display unique functional properties. *Proc. Natl. Acad. Sci. U.S.A. National Acad Sciences*; 2013 Aug 13;110(33):13498–503.
  158. Kaer L. Innate and virtual memory T cells in man. *European Journal of Immunology*. 2015 Jul 1;45(7):1916–20.
  159. Kurzweil V, LaRoche A, Oliver PM. Increased peripheral IL-4 leads to an expanded virtual memory CD8<sup>+</sup> population. *J. Immunol. American Association of Immunologists*; 2014 Jun 15;192(12):5643–51. PMID: PMC4097049
  160. White JT, Cross EW, Burchill MA, Danhorn T, McCarter MD, Rosen HR, et al. Virtual memory T cells develop and mediate bystander protective immunity in an IL-15-dependent manner. *Nat Commun*. 2016;7:11291. PMID: PMC4844673
  161. Mak TW, Penninger JM, Ohashi PS. Knockout mice: a paradigm shift in modern immunology. *Nature Reviews Immunology*. 2001;1(1):11–9.

162. Services CRRAD. Intestinal Protozoa in Rodents | Charles River Research Animal Diagnostic Services. 2016 Aug 8;;1–2.
163. Zhang Z, Schwartz S, Wagner L, Miller W. A greedy algorithm for aligning DNA sequences. *J. Comput. Biol.* 2000 Feb;7(1-2):203–14.
164. Freeman CD, Klutman NE, Lamp KC. Metronidazole. *Drugs.* 1997;54(5):679–708.
165. Roach PD, Wallis PM, Olson ME. The use of metronidazole, tinidazole and dimetridazole in eliminating trichomonads from laboratory mice. *Laboratory Animals.* SAGE Publications; 1988 Oct 1;22(4):361–4.
166. Chacko M, Bhide SV. Carcinogenicity, perinatal carcinogenicity and teratogenicity of low dose metronidazole (MNZ) in Swiss mice. *J Cancer Res Clin Oncol.* Springer-Verlag; 1986;112(2):135–40.
167. Thapa PB, Whitlock JA, Worrell KGB, Gideon P, Mitchel EF, Roberson P, et al. Prenatal exposure to metronidazole and risk of childhood cancer. *Cancer.* John Wiley & Sons, Inc; 1998 Oct 1;83(7):1461–8.
168. Flagyl(R) [package insert]. New York, NY; 2010;;1–11.